UNIVERSITY OF THE
WITWATERSRAND,
JOHANNESBURG

The Roles of miRNA-128 and miRNA-223 in Cholesterol-Mediated Drug Resistance in Breast Cancer

by

Gabriella Bianca Henriques Palma

706599

Thesis

Submitted in fulfilment of Research by Thesis for the requirements for the degree

Philosophiae Doctor

In

Molecular and Cell Biology

in the Faculty of Science, University of the Witwatersrand, Johannesburg, South Africa

Supervisor: Professor Mandeep Kaur

April 2023

TABLE OF CONTENTS

DECLARATION

I, Gabriella Bianca Henriques Palma (706599), am a student registered for the degree of Doctor of Philosophy in Science (Molecular and Cell Biology) in the academic years 2019-2022.

I hereby declare the following:

- I am aware that plagiarism (the use of someone else's work without their permission and/or without acknowledging the original source) is wrong.
- I confirm that the work submitted for assessment for the above degree is my own unaided work except where explicitly indicated otherwise and acknowledged. In this context, I understand that the use of editing services is considered aided work and must be declared.
- I have not submitted this work before for any other degree or examination at this or any other University.
- The information used in the Thesis has not been obtained by me while employed by, or working under the aegis of, any person or organisation other than the University.
- I have followed the required conventions in referencing the thoughts and ideas of others.
- I understand that the University of the Witwatersrand may take disciplinary action against me if there is a belief that this is not my own unaided work or that I have failed to acknowledge the source of the ideas or words in my writing.

NRF Declaration

The financial assistance of the National Research Foundation (NRF) (grant number: 113442) towards this research is hereby acknowledged.

Opinions expressed and conclusions arrived at, are those of the author and are not necessarily to be contributed to the NRF.

Signature  on the 26th day of April 2023

ACKNOWLEDGEMENTS

This research would not have been possible without the support and assistance of the following people and institutions:

The deepest of thanks to my supervisor, Professor Mandeep Kaur, for her endless guidance and mentorship of this project as well as all the encouragement, advice, and motivation throughout the years. Since joining Prof Kaur's lab, I have learned countless skills and important life lessons that have made me a better researcher. For that, I am deeply appreciative of Prof.

I would also like to thank my colleagues in GH527 for all their help and support. A special acknowledgment to Dr Bernice Monchusi for laying the foundations of this project and getting it started. For every person I have had the privilege of working with in the lab, I am deeply thankful for our interactions. Every person (past and present) has really made it a great working environment and I have thoroughly enjoyed all the chats, lunches, games, and good times we've shared together. You guys have been the absolute best!

A huge thank you to my close family and friends who have supported and encouraged me to finish my research. You have been my biggest supporters and motivators (especially mom!), which has kept me going. It hasn't been the easiest of journeys, but your patience and support have gotten me through it, and for that I thank you.

A very special thanks to (almost Dr) Shanen Perumal, who has been the most helpful, supportive, and patient boyfriend throughout these years. All your advice, support, and knowledge has helped me more than you could imagine, and because of you, I am a better person. You truly are appreciated, and I am so proud of your journey too!

A special thanks to the Department of Chemistry at the University of the Witwatersrand for the synthesis of Acetyl Plumbagin, that was used in this project.

I would also like to acknowledge the University of the Witwatersrand (Postgraduate Merit Award) and the NRF for financial assistance during my study period (2019-2022). This has been a great relief from tuition fees, without which I would not have been able to further my studies.

Finally, a huge thank you to all the MCB staff members, especially Ms. Lucretia Brink, for all the help they have given me. Your help knows no bounds, and you will go above and beyond (even on weekends) to help us out. I am truly grateful for everything you have done for me.

LIST OF FIGURES

LIST OF TABLES

LIST OF SYMBOLS

α	Alpha
β	Beta
©	Copyright
℃	Degrees Celsius
κ	Kappa
μ	Micro
μg	Micrograms
μL	Microlitres
μM	Micromolar
®	Registered
™	Trademark

LIST OF ABBREVIATIONS

5-FU	5- Fluorouracil
ABCA1	ATP-binding cassette subfamily C member 1
ABCB1	ATP-binding cassette subfamily B member 1
ABCC5	ATP-binding cassette subfamily C member 5
ABCG1	ATP-binding cassette subfamily G member 1
ACAT1	Acetyl-coenzyme A acetyltransferase 1
Ago2	Argonaute protein 2
AIs	Aromatase inhibitors
ANOVA	Analysis of variance
AP	Acetyl Plumbagin
APOA1	Apolipoprotein A1
ATCC	American Type Culture Collection
BC	Breast cancer
BCA	Bicinchoninic acid
bp	Base pair
BRCA1/2	Breast cancer gene 1/2
BSA	Bovine serum albumin
Cav-1	Caveolin-1
cDNA	Complementary DNA
CEs	Cholesteryl esters
CETP	Cholesteryl ester transfer protein
CLL	Chronic lymphocytic leukaemia
CO_2	Carbon dioxide
C_q	Quantification cycle
CT-B	Cholera toxin subunit B
C_t	Threshold cycle
CTCF	Corrected total cell fluorescence
DAPI	4',6-diamidino-2-phenylindole
DC FBS	Dextran charcoal stripped foetal bovine serum
dH_2O	Distilled water
DMEM	Dulbecco’s Modified Eagle’s Medium

DNA	Deoxyribonucleic acid
ds	Double-stranded
E_2	Estradiol
ECACC	European Collection of Authenticated Cell Cultures
ECM	Extracellular matrix
EDTA	Ethylenediaminetetraacetic acid
EGFR	Epidermal growth factor receptor
ELISA	Enzyme-linked immunosorbent assay
EMT	Epithelial-to-mesenchymal transition
ER	Estrogen receptor
ER+	Estrogen receptor- positive
ERα	Estrogen receptor- α
ERK	Extracellular signal-regulated kinases
ERRα	Estrogen-related receptor α
ESR1	Estrogen receptor- 1
EtBr	Ethidium bromide
FBS	Foetal bovine serum
Fig.	Figure
g	Grams
g	Relative centrifugal force
GAPDH	Glyceraldehyde 3-phosphate dehydrogenase
GSLs	Glycosphingolipids
GlcCer	Glucosylceramide
HCl	Hydrochloric acid
HDL	High-density lipoprotein
HEK293	Human embryonic kidney 293
HER2	Human epidermal growth factor receptor 2
HMG-CoA	Hydroxy-methyl glutaryl-coenzyme A
HMGCR	3-hydroxy-3-methylglutaryl-CoA reductase
HMGCS1	3-hydroxy-3-methylglutaryl-CoA synthase 1
HRP	Horseradish peroxidase
h	Hours

IGF	Insulin-like growth factor
IGF1R	Insulin-like growth factor receptor
INSIG1/2	Insulin induced gene 1/2
kDa	Kilodaltons
LCAT	Lecithin–cholesterol acyltransferase
LDL	Low-density lipoprotein
LDLR	Low-density lipoprotein receptor
LTED	Long-term estrogen deprived
LXR	Liver X receptor
MAPK	Mitogen-activated protein kinase
MβCD	Methyl-β-cyclodextrin
MCF-7	Michigan Cancer Foundation-7
MDA-MB-231	M.D. Anderson-Metastatic-Breast-231
MDR	Multidrug resistance
mg	Milligrams
miRNA	MicroRNA
min	Minutes
miRISC	miRNA-induced silencing complex
mL	Millilitres
MOMP	Mitochondrial outer membrane potential
mRNA	Messenger RNA
mTOR	Mammalian target of rapamycin
mTORC1	Mammalian target of rapamycin complex 1
MTT	3-(4,5-Dimethylthiazol-z-yl)-2,5diphenyltetrazolium bromide
NCBI	National Center for Biotechnology Information
NF-κB	Nuclear factor kappa B subunit 1
nm	Nanometres
nM	Nanomolar
NPs	Nanoparticles
NSCLC	Non-small cell lung cancer
NTC	No template control
OD	Optical density

PAP	Poly(A) polymerase
PBS	Phosphate buffered saline
PCR	Polymerase chain reaction
PCSK9	Proprotein convertase subtilisin/kextin type- 9
pg	Picograms
PI3K	Phosphoinositide 3-kinase
PIP3	Phosphatidylinositol (3,4,5)-trisphosphate
PL	Plumbagin
PR	Progesterone receptor
Pre-miRNA	Precursor miRNA
Pri-miRNA	Primary miRNA
P-S	Penicillin-streptomycin
PTEN	Phosphatase and tensin homolog
PVDF	Polyvinylidene fluoride
qPCR	Real-time polymerase chain reaction
RCT	Reverse cholesterol transport
RIPA	Radio-immunoprecipitation assay
RISC	RNA-induced silencing complex
RNA	Ribonucleic acid
RNU6	RNA, U6 small nuclear 1
rpm	Revolutions per minute
rRNA	Ribosomal RNA
RT	Room temperature
RT-qPCR	Quantitative reverse transcription polymerase chain reaction
s	Seconds
SCAP	SREBP cleavage-activating protein
S.D	Standard deviation
SDS	Sodium dodecyl sulfate
SDS-PAGE	Sodium dodecyl sulfate polyacrylamide gel electrophoresis
SERMs	Selective estrogen receptor response modulators
siRNA	Small interfering RNA
SR-B1	Scavenger receptor, class B type 1

SREBF1/2	Sterol regulatory element-binding transcription factor 1/2
SREBP1/2	Sterol regulatory element-binding protein
ss	Single-stranded
TAM	Tamoxifen
TAM-R	Tamoxifen-resistant
TBE	Tris-borate-EDTA
TBST	Tris-buffered saline with Tween-20
TE	Tris-EDTA
TGFβ	Transforming growth factor-β
T_m	Melting temperature
TNBC	Triple negative breast cancer
TP53	Tumour protein p53
TRBP	Transactivation-responsive RNA binding protein
UGCG	UDP-glucose ceramide glucosyltransferase
UTR	Untranslated region
V	Volts
VLDL	Very low-density lipoprotein
XCFF	Xylene cyanol FF

ABSTRACT

Breast cancer (BC) is the most prevalent cancer in women, with 70% of BC cases being hormone responsive (estrogen receptor positive (ER+)). This ER+ BC subtype relies on estrogen for enhanced cell proliferation and survival. The main therapeutic strategy to prevent hormone responsive BC recurrence is with the use of endocrine therapy such as Tamoxifen (TAM). Despite the success in reducing mortality rates of BC patients with the use of adjuvant TAM and chemotherapy, cancer drug resistance remains a significant challenge. A major contributor to this resistance is the dysregulation of cholesterol homeostasis in these cells. BC cells have elevated intracellular cholesterol levels, which is associated with cancer progression. In our previous research, we observed that the use of a cholesterol depleting agent, Acetyl Plumbagin (AP) in combination with TAM, led to the induction of cell death via cholesterol depletion. These results therefore warranted further investigation into the molecular mechanisms in which TAM + AP are involved in. MicroRNAs (miRNAs) regulate cholesterol-related and cancer drug resistance pathways, and the aberrant expression of these miRNAs are often associated with increased cancer proliferation and resistance. It was therefore predicted that manipulating the expression of these target miRNAs could lead to a reduction in BC related drug resistance via cholesterol depletion. Thus, we aimed at investigating the roles of miRNA-128 and miRNA-223 in cholesterol-mediated TAM resistance. Three BC cell lines (MCF-7 (estrogen-dependent), MDA-MB-231 (estrogen-independent), and Long-Term Estrogen Deprived (LTED)) were treated with a combination of 1 μM TAM and 10 μM AP following transfection with a miR-128 inhibitor or a miR-223 mimic. Cell viability and cholesterol levels were assessed following treatments. In addition, gene and protein expression levels involved in cancer drug resistance and cholesterol homeostasis were also assessed. It was found that the combination treatment with altered miRNA expression led to reduced cell viability and proliferation due to a reduction in free cholesterol, cholesteryl esters, and lipid rafts in all three BC cell lines. Moreover, miR-128 inhibition lowered the expression of genes involved in cholesterol synthesis and transport (*HMGCR, HMGCS1*, *SREBF1/2*, *CETP, LCAT*, and *LDLR*), drug resistance (*ABCC5* and *UGCG*), and cell signalling (*ESR1*, *EGFR*, and *IGF1R*) in MCF-7 cells. Whereas overexpression of miR-223 led to decreased expression in *EGFR, ESR1*, *ABCC5, CETP, LCAT, LDLR, HMGCR, SREBF1*, and *SREBF2*, with increased expression in *ABCG1*, *PTEN*, and *TP53* in MDA-MB-231 cells. Therefore, the current study demonstrated that miR-128 and miR-223 could be potential targets in reducing TAM resistance through the depletion of excess cholesterol.

1. INTRODUCTION

1.1 Prevalence of cancer and breast cancer occurrence

Cancer is the second leading cause of global mortality, where 19 million new cases are reported yearly and 9.9 million deaths were reported in 2020 (WHO, 2020). Breast cancer (BC) is the most prevalent cancer in women and is the second most commonly occurring malignancy worldwide, comprising 24.5% of all cancers (WHO, 2020). There have been more than 2.2 million BC cases reported worldwide with 684 996 deaths in 2020 (WHO, 2020). BC is ranked second in cancer mortalities in South African women, behind cervical cancer (WHO, 2020). In South Africa alone, 15 491 new BC cases and 4 664 deaths have been reported in 2020 (WHO, 2020). It is estimated that there will be an increase to 26 million new cancer cases by 2030 (WHO, 2020). This indicates a significant increase in cancer-related deaths, highlighting the urgent need for novel chemotherapeutic strategies to improve current cancer treatment.

1.2 BC characteristics

BC is a malignant tumour that begins to develop in various ducts and tissues in the breast (American Cancer Society, 2018). BC is caused by genetic, hormonal, and environmental factors. It is often an accumulation of mutations resulting in oncogene formation or tumour suppressor gene silencing as well as changes in the nucleotide sequence of genomic DNA. However, the greatest risk factor for BC is a mutation in the tumour suppressor genes, breast cancer gene 1 (*BRCA1*) or *BRCA2* (Roy *et al.,* 2011) The hallmarks that govern the transformation of normal cells to malignant cells include: unlimited proliferative potential, evasion of apoptosis, sustained angiogenesis, self-sufficiency in growth signals, insensitivity to anti-growth signals, deregulating cellular energetics, avoiding immune destruction, tumour-promoting inflammation, tissue invasion and metastasis, and genome instability and mutation (Hanahan, 2022). BC is an aggressive tumour due to its highly metastatic and invasive potential as well as its inherent resistance to treatment. It has remarkable abilities to evade apoptosis, which classifies it as a difficult cancer to treat (Hanahan and Weinberg, 2000).

Apoptosis is a process of programmed cell death which leads to physiological and morphological changes in the cell (Hanahan and Weinberg, 2000). Apoptosis functions via two pathways, which include the intrinsic (responds to intracellular stresses) and extrinsic (responds to extracellular stresses) pathways (Fig. 1.1). Both of these pathways induce apoptosis via the activation of caspases 9 and 8 respectively through the degradation of proteins (Putcha *et al.,* 2002). These pathways are suppressed in BC, which leads to the up-regulation

of several proliferative pathways leading to uncontrolled proliferation. These pathways are up-regulated through the interaction between steroid hormones, such as estrogen and cell surface receptors, leading to a more resistant and aggressive tumour. BC uses anti-apoptotic regulatory molecules from the Bcl-2 family which inhibits and controls apoptosis by the regulation of mitochondrial outer membrane potential (MOMP), which is involved in the intrinsic pathway. These BC characteristics make it difficult to treat and emphasises the importance of novel treatments.

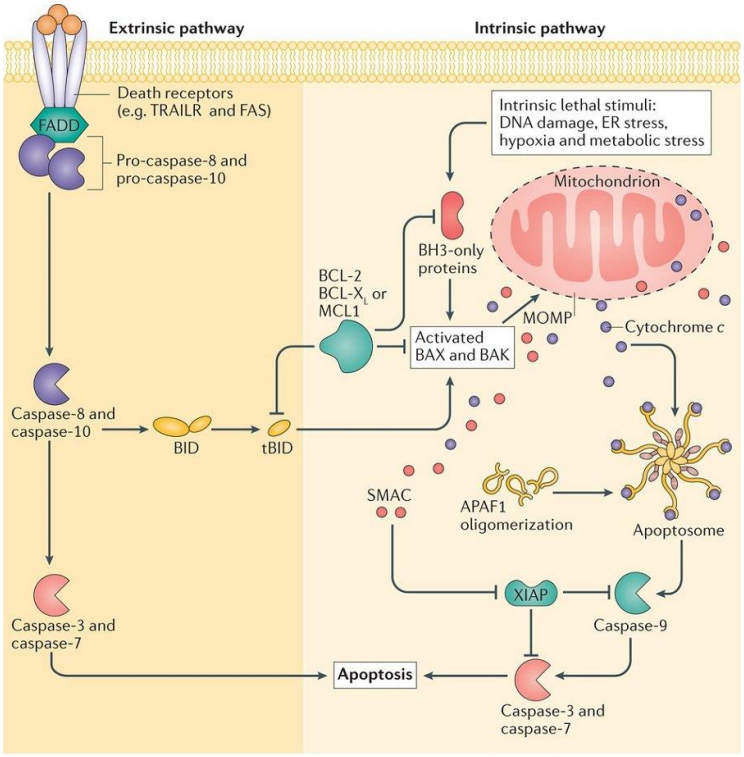

Figure 1.1: The extrinsic and intrinsic pathways involved in apoptosis

Apoptosis occurs through these pathways which includes the activation of several caspases. In the extrinsic pathway, a signal is received from outside of the cell instructing it to undergo programmed cell death. The intrinsic pathway is triggered by internal stress or damage to the cell which then undergoes apoptosis (Lowe and Lin, 2000). Source: [(Biologydictionary.net, 2018) Accessed: 10.11.22]

1.3 Hormone induced BC

Steroid hormones such as estrogen and progesterone are essential for normal breast cell growth and development (Anderson and Clarke, 2004). These hormones are synthesised from cholesterol and are fat-soluble, making it easier to pass through the cell membrane, thereby

binding to nuclear steroid hormone receptors bringing about a change in the cell (Heffner and Schust, 2010). BC is linked to the dysregulated expression of these endogenous steroid hormones (Esau *et al.*, 2016). The three main hormones associated with BC include estrogen, progesterone, and human epidermal growth factor. BC is therefore classified based on the presence of these three receptors, namely: estrogen receptor (ER), progesterone receptor (PR), and human epidermal growth factor receptor 2 (HER2) or those that lack these three receptors, termed triple negative BC (TNBC) (Baek and Nelson, 2016). There are four molecular subtypes of BC. These include luminal A, luminal B, HER2-enriched, and TNBC. Of all BC cases reported, approximately 70% of these cases are luminal A and B, where they are classified as ER positive (ER+), PR positive (PR+), and HER2+/-. The ER+ BC subtype has the best prognosis as endocrine therapy and aromatase inhibitors (AIs) are often used (Kohler *et al.*, 2015). Approximately 15% of BC cases are HER2+, where ER and PR are not expressed. This subtype has faster cell growth than luminal subtypes and targeted therapy includes Herceptin monoclonal antibody treatment. TNBC tumours are the most aggressive subtype of BC but are less commonly observed, with reports of 13% of all BC cases. This subtype often occurs in younger and African women, and available treatment options include chemotherapy and surgery. ER+ BC cells rely on the estrogen hormone and ER-mediated pathways to promote cell proliferation, survival, and migration. In contrast, TNBC cells rely on ER-independent pathways, such as the insulin-like growth factor (IGF) pathway to promote cell proliferation, migration, invasion, and survival (Davison *et al.*, 2011).

Estrogen is a key driver in BC proliferation and functions by binding to the ER, which promotes the dimerisation and conformational change of the ER. This change subsequently leads to transcriptional co-activator recruitment for further gene expression (Rosenfeld and Glass, 2001). The aberrant expression of ER in BC cells exerts proliferative, metastatic, and survival effects (Clemons and Goss, 2001). Estrogen directly initiates tumour development by activating oncogenes involved in nucleic acid synthesis and indirectly promotes tumour development by stimulating several transcription factors involved in abnormal cell proliferation (Clemons and Goss, 2001). Therefore, abnormal expression of estrogen and the ER are regularly associated with BC cases. Hormone receptors are therefore important prognostic and predictive factors for potential endocrine strategies (Cianfrocca and Goldstein, 2004).

The ER is a transcription factor required for cell growth in ER+ BC cells (Viedma-Rodríguez *et al.*, 2014). After passing through the plasma membrane, estrogen binds to nuclear bound ER

which undergoes conformational changes (phosphorylation and dimerisation). Following these changes, the ER binds to the estrogen response elements. These genes are involved in cell proliferation and survival (Viedma-Rodríguez *et al.*, 2014). ER phosphorylation occurs via the action of membrane receptor tyrosine kinases such as epidermal growth factor receptor (EGFR) and insulin-like growth factor receptor 1 (IGF1R) (Viedma-Rodríguez *et al.*, 2014). A link between these growth factor receptors and ER signalling pathways has been well established. These growth factor receptors activate the phosphoinositide 3-kinase (PI3K)/Akt and mitogen-activated protein kinase (MAPK) signalling pathways which down-regulate ER expression. ER has been found not only in the nucleus but also in the membrane and cytoplasm, working through non-genomic pathways such as the PI3K/Akt and MAPK pathways (Viedma-Rodríguez *et al.*, 2014). In conclusion, ER activity and signalling are modulated by several pathways which could contribute to ER-targeted treatment.

1.4 Current BC treatments

There have been many interventions and chemotherapeutic approaches developed to treat BC cases. However, many approaches fail due to the aggressive and resistant nature of BC cells. The most common forms of treatment of BC include surgery, radiation, chemotherapy and hormone or endocrine therapies (American Cancer Society, 2018). Although these therapies are effective, they are invasive and can lead to several complications. Therefore, the preferred treatment for BC is endocrine therapy, as many BC cases are induced by hormones.

Endocrine therapy, works by lowering estrogen levels circulating in the body by targeting and blocking the activation of the ER signalling pathway thereby reducing BC cell proliferation (Wong and Chen, 2012). Endocrine therapy is used as an adjuvant therapy often after surgery to reduce the recurrence of ER+ BC tumours. The main forms of endocrine therapy include selective estrogen receptor modulators (SERMs) followed by the use of AIs, as well as selective ER down-regulators, luteinizing hormone-releasing hormone agent, and prophylactic ovary removal. On the contrary, endocrine therapy is ineffective in the treatment of TNBC due to the lack of the therapeutic target receptors, ER, PR, and HER2 (Sun *et al.*, 2016). As a result, chemotherapy and surgery are the only options available for the treatment of TNBC.

The most common endocrine therapy is the use of SERMs which blocks the effects of estrogen's ability to stimulate BC cell growth. SERMs serve as estrogen antagonists by competing with estrogen to bind to the ER and ultimately block estrogen from binding to the ER. Examples of SERMs include Tamoxifen (TAM), Raloxifene and Toremifene. Other anti-

estrogen drugs such as Fulvestrant act in similar ways to SERMs; however, they have no estrogen agonist effects and are often used to treat advanced BC in post-menopausal women (Kohler *et al.,* 2015). Although there are currently many endocrine treatments on the market, the gold-standard drug, TAM, has been used for more than 40 years as the primary source of treatment for ER+ BC.

TAM is initially metabolised in the liver by a family of cytochrome P450 enzymes (CYP26 and CYP3A4 isoforms) into active metabolites called N-desmethyl- 4-1 hydroxy Tamoxifen (endoxifen) and 4-hydroxy-Tamoxifen (afimoxifene), whereby both metabolites competitively bind to the ERs of BC cells (Fig. 1.2) (Lu *et al.,* 2012). The active metabolites are internalised and bind to the estrogen response elements in the nucleus, thus reducing gene expression through the recruitment of co-repressors (Hodges *et al.,* 2003). Consequently, this prevents the activity of various transcription factors that promote cellular replication (Osborne, 1998). The inhibition of ER activity using TAM is important in managing and reducing ER+ BC recurrence (Cuzick *et al.,* 2010; Lin *et al.,* 2015). Interestingly, TAM lowers circulating cholesterol in the body and has been used for hypercholesterolemia (Ali *et al.,* 2016). Recent studies have shown that TAM also possesses ER-independent anti-tumour activity which enhances TNBC chemosensitivity by the reversal of their epithelial-to-mesenchymal transition (EMT) properties (Wang *et al.,* 2017). Another study revealed the reduced expression of IGF1R after neoadjuvant chemotherapy was associated with improved response in TNBC patients (de Groot *et al.,* 2016). While there are few treatment options for TNBC, there are no readily available specific targeted therapies. This highlights the urgent need for the identification and implementation of novel biomarkers and therapies to aid in the treatment of TNBC.

Death rates have decreased by 25% since 1990 from BC due to improved use of neoadjuvant TAM therapy (Karami-Tehrani and Salami, 2003; Parton *et al.,* 2001). Therefore, TAM is important in managing and reducing ER+ BC recurrence by inhibiting ER activity. Although an improvement in survival rates has been observed, these patients often acquire resistance to treatment after prolonged use after initial response. Additionally, after metastatic relapse, the disease is not curable even with other available therapies such as AIs, and consequently many patients die. Currently, there are no available therapies for this aggressive stage of BC after relapse and therefore an aggressive form of chemotherapy is required (Karami-Tehrani and Salami, 2003). Thus, further research is essential to help minimise the side effects of TAM by reducing its toxicity and inherent resistance.

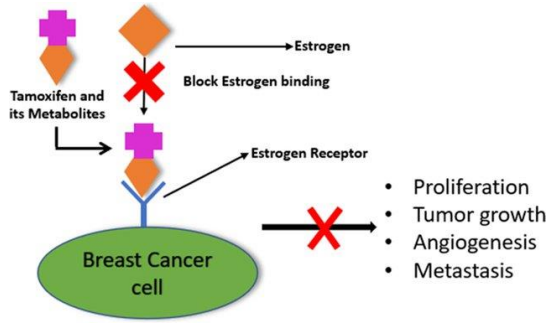

Figure 1.2: The mode of action of TAM in a cancer cell

TAM competes with estrogen to bind to the ER. Co-repressors are subsequently recruited resulting in the prevention of BC cell proliferation and survival. Source: [(Ravindranath et al., 2022). Accessed: 10.11.2022]

1.5 Cancer-related drug resistance

Although TAM has been used as the first-line adjuvant endocrine therapy for ER+ BC for several years, about 25% of patients develop resistance to this therapy resulting in aggressive, metastatic tumours (Wang *et al.,* 2018). There are two forms of drug resistance: acquired resistance and *de novo* resistance. *De novo* resistance occurs when patients do not respond to treatment initially and acquired resistance occurs when patients who respond to treatment initially, acquire resistance over prolonged use of the treatment. Different mechanisms associated with cancer drug resistance include: multidrug resistance (MDR), apoptotic pathway inhibition, drug metabolism changes, epigenetics, and enhanced DNA repair mechanisms (Mansoori *et al.,* 2017). Similarly, cholesterol has also been implicated in BC drug resistance (Hutchinson *et al.,* 2018). There have been several investigations to elucidate the mechanisms involved in acquired TAM resistance and how to overcome this resistance.

Several mechanisms of acquired TAM resistance in BC have been proposed. These include: the deregulation of the ER signalling pathway; loss of ER expression and function; differential metabolic activation of TAM; mutations and/or post-translational modifications of the ER; alterations in ER and growth factor-mediated signalling pathways; up-regulation of growth factor receptors (HER2, EGFR, IGF1R); pharmacological mechanisms; alterations in signalling that control cell cycle, proliferation, and survival; inhibition of apoptosis; stress response; alterations in microRNA (miRNA) expression; PI3K/Akt/mammalian target of rapamycin (mTOR) pathway activation; inactivation of phosphatase and tensin homolog (PTEN); induction of nuclear factor kappa B subunit 1 (NF-κB) signalling; and the presence of BC stem cells (Ali *et al.*, 2016; Chang, 2012; Musgrove and Sutherland, 2009; Viedma-

Rodríguez *et al.*, 2014). Furthermore, the alteration of expression of Bad, c-Myc, and Bcl-2 are also associated with TAM resistance (Ali *et al.*, 2016; Riggins *et al.*, 2007). Studies suggest that in the presence of TAM, BC cells use alternative growth regulatory pathways (Ali *et al.*, 2016; Knowlden *et al.*, 2003). The MAPK pathway is one of the key mediators of cell proliferation (Fig. 1.3). Increased MAPK signalling is associated with reduced survival in ER+ BC patients (Chang, 2012; Knowlden *et al.*, 2003). Furthermore, increased MAPK activity has been demonstrated in BC cells that have undergone long-term estrogen deprivation (LTED) as well as in TAM-resistant (TAM-R) BC cell lines (Knowlden *et al.*, 2003; Shim *et al.*, 2000). Therefore, understanding the link between several signalling pathways and TAM resistance in BC is crucial.

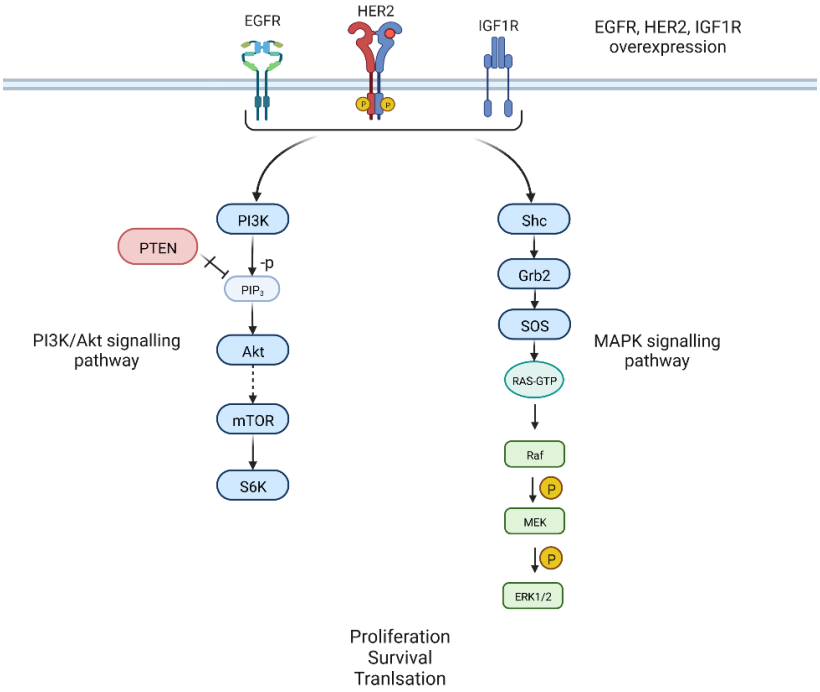

Figure 1.3: Up-regulation of growth factor-mediated signalling pathways in BC

The up-regulation of growth factor receptors (HER2, EGFR, and IGF1R) have been implicated in acquired TAM resistance in BC cells. The overexpression of these receptors activates the PI3K/Akt and MAPK signalling pathways which leads to increased BC cell survival, proliferation, and translation leading to increased TAM resistance in BC. Source: [Image created with BioRender.com]

The loss of ER expression and function is one of the major hallmarks associated with *de novo* TAM resistance. There have been several mechanisms proposed to explain the loss of ER expression and its effect in TAM resistance in ER+ BC cells over time (Fig. 1.4). These

mechanisms include ER gene mutations leading to loss of ER expression; and PI3K/Akt and MAPK signalling activation, which induces ER phosphorylation altering the response of ER to TAM (Chang, 2012; Viedma-Rodríguez *et al.*, 2014). Therefore, as mentioned previously, a combination of mechanisms owes to TAM resistance in BC cells and several of these key pathways and regulators involved in TAM resistance have been highlighted below.

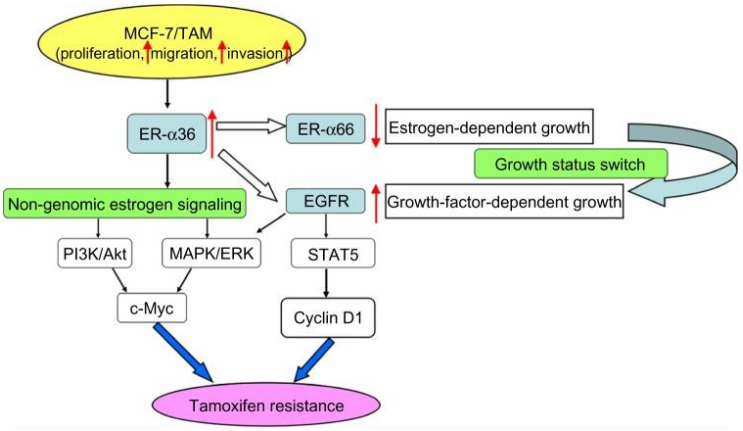

Figure 1.4: Mechanisms associated with TAM resistance

Several non-genomic and genomic signalling pathways are involved in TAM resistance in ER+ BC cells. These pathways are involved in cell survival, proliferation, migration, invasion, and stress response. Source: [(Su et al., 2014). Accessed: 10.11.22]

An important growth factor kinase receptor associated with TAM resistance is IGF1R which is dependent on ER and functions in stimulating cell growth. Phosphorylated IGF1R which interacts with EGFR and membrane bound ER is up-regulated in TAM-R tumours (Viedma-Rodríguez *et al.*, 2014). Overexpression of EGFR and HER2 in ER+ BC cells leads to increased downstream PI3K/Akt activity (Fig. 1.3) (Riggins *et al.*, 2007; Su *et al.*, 2014). The IGF1R signalling pathway is important in several functions such as cell proliferation, programmed cell death and controlling ER expression. IGF1R is a receptor tyrosine kinase, where IGF1/2 bind and activate this receptor. Following activation, the PI3K and RAS/MAPK pathways are activated (Fagan *et al.*, 2012). BC cells may evade apoptosis induced by TAM via the activation of Akt, which is mediated by IGF (Viedma-Rodríguez *et al.*, 2014). IGF1R expression is ER-dependent but can also be activated in TAM-R tumours therefore, studies have found that the inhibition of IGF1R reduced TAM-R BC cell growth (Massarweh *et al.*, 2008; Viedma-Rodríguez *et al.*, 2014) and could be a possible therapeutic approach in reducing acquired TAM resistance.

Resistance to endocrine therapies arises through several distinct mechanisms as highlighted above. For this reason, many strategies for overcoming this resistance have been in the spotlight. One such strategy is the use of combination treatments which targets multiple pathways at once, thereby delaying the onset of acquired resistance in tumours. Combination treatments can also be used to re-sensitise tumours to chemotherapeutic agents for which they are resistant (Riggins *et al.,* 2007). Treatments that inhibit the above growth factor receptors such as EGFR, IGF1R, PI3K or MAPK in combination with endocrine therapy, can block pro-proliferative activities of the ER activated by these growth factor receptors (Riggins *et al.,* 2007). There are many mechanisms related to TAM resistance, which are mainly controlled by ER and growth factor signalling crosstalk, ER expression, cell cycle regulators, deregulation in expression of pro- and anti-apoptotic proteins, and miRNAs. It is therefore pertinent to deeply understand the mechanisms related to TAM resistance, for the development of novel approaches that benefit BC patients.

The treatment of ER+ BC in post-menopausal women is often achieved by estrogen deprivation or blocking estrogen-related pathways. This is accomplished through ovarian ablation, TAM treatment to block ER action, and direct inhibition of estrogen production by the use of AIs (Wong and Chen, 2012). While the use of the above treatments is effective at first, acquired resistance towards treatment occurs at later times. Therefore, it is also necessary to develop a novel therapeutic approach in reducing cancer-related resistance in ER+ BC cells that have been deprived of estrogen for long periods of time (LTED). Studying LTED cells is important to elucidate the mechanisms present in post-menopausal women that have low circulating estrogen levels. LTED cells are usually unaffected by TAM treatment and are therefore inherently resistant to TAM by employing alternative growth factor receptor signalling pathways to activate ER (Santen *et al.,* 2008; Santen *et al.,* 2005).

1.6 LTED BC cells

LTED cells are ER+ BC cells that have undergone long-term estrogen deprivation (i.e. >180 days) and are therefore termed resistant LTED cells. Initial ER+ BC treatment includes SERMs and reduction of estrogen secretion by surgical removal of the ovaries (oophorectomy) (Jeng *et al.,* 1998). Patients initially respond well to these treatments which last approximately 12-18 months (Yue *et al.,* 2003). Among patients with relapsing disease, 50% experience further tumour regression through secondary therapies via further inhibition of circulating estrogen through the use of AIs (Yue *et al.,* 2003). Therefore, is it suggested that LTED BC cells can adapt to low estrogen levels and re-grow in these conditions, whilst being resistant to treatment.

After LTED, ER+ BC cells demonstrate increased sensitivity to estrogen and this could possibly explain the re-growth and resistance observed in these LTED cells (Masamura *et al.,* 1995; Yue *et al.,* 2003). Understanding the mechanisms involved in LTED adaptation and resistance will help improve current endocrine treatments for hormone-dependent ER+ BC and assist in the development of new chemotherapeutic drugs.

In vitro studies have revealed that BC cells that have been deprived of estrogen for long periods of time, pass through three phases. These phases include: a quiescent phase where cell proliferation is decreased and ER expression is low, a hypersensitive phase where cell growth is stimulated by exogenous estrogen, and an independent phase in which exogenous estrogen has no effect on cell growth and there is a 2-4 fold increase in ER binding sites (Martin *et al.,* 2003). The exact mechanisms underlying these adaptive phases are not well understood; however, increased secretion of growth factors plays a major role (Jeng *et al.,* 1998). Therefore, the identification of the pathways responsible for cancer-related drug resistance is crucial for developing novel anticancer strategies.

Previous *in vitro* investigations suggested that LTED cells adapt to low levels of estrogen to allow for maximum cell growth (Shim *et al.,* 2000). When residual estradiol (E_2) is completely removed or antagonised by anti-estrogens, LTED cells are adapted to grow with the addition of exogenous E_2 (Santen *et al.,* 2003; Shim *et al.,* 2000). These cells respond to much lower E_2 concentrations than MCF-7 cells, which demonstrates hypersensitivity (Shim *et al.,* 2000). In pre-menopausal women with ER+ BC, tumours initially require a range of 50-600 pg/mL of E_2 for growth. However, the removal of ovarian estrogens leads to the adaptation of low E_2 levels and tumours then only require 10-20 pg/mL of E_2 for growth. A further reduction of E_2 levels using AIs to 1-2 pg/mL causes additional tumour regression (Shim *et al.,* 2000). This evidence suggests that adaptive hypersensitivity is observed in LTED cells (Shim *et al.,* 2000). Although there is evidence for hypersensitivity, the precise mechanism of adaptation and hypersensitivity to E_2 in LTED cells is unknown and therefore several investigations have taken place to elucidate potential adaptive mechanisms.

ER+ BC cells have numerous receptors for hormones and growth factors. These cells produce many growth factors which are modulated by E_2 and anti-estrogens like TAM. It was therefore predicted that LTED of ER+ BC cells causes an increased secretion of growth factors or increased growth factor receptor production (Katzenellenbogen *et al.,* 1987; Martin *et al.,* 2003; Masamura *et al.,* 1995; Shim *et al.,* 2000) and crosstalk between growth factor and

estrogen-stimulated signalling pathways (Jeng *et al.,* 1998). This suggests that the high proliferation rate of LTED cells cannot be further increased by exogenous E_2. It also suggests that TAM or other anti-estrogens inhibiting cell growth function via decreasing growth factor production.

In ER+ BC cells, estrogen and ER-mediated signalling pathways are responsible for cell growth. However, during LTED or acquired TAM resistance, the estrogen-induced ER pathway is deactivated, resulting in ER activation through alternative mechanisms (Wong and Chen, 2012). *In vitro* studies have stipulated that the interaction between ER-mediated functions and the activation of the MAPK signalling pathway is responsible for the adaptive mechanisms observed in LTED cells (Fig. 1.5) (Jeng *et al.,* 1998; Santen *et al.,* 2003; Shim *et al.,* 2000; Yue *et al.,* 2003; Zheng *et al.,* 2007). The first stage of resistance occurs when estrogen-mediated ER signalling is blocked, and TAM functions as a weak estrogen, driving cell growth. Over time, cell growth becomes more estrogen-independent and relies on several growth factor signalling pathways. Finally, resistant cells no longer respond to TAM effects and the cells have reached total estrogen-independence (Wong and Chen, 2012).

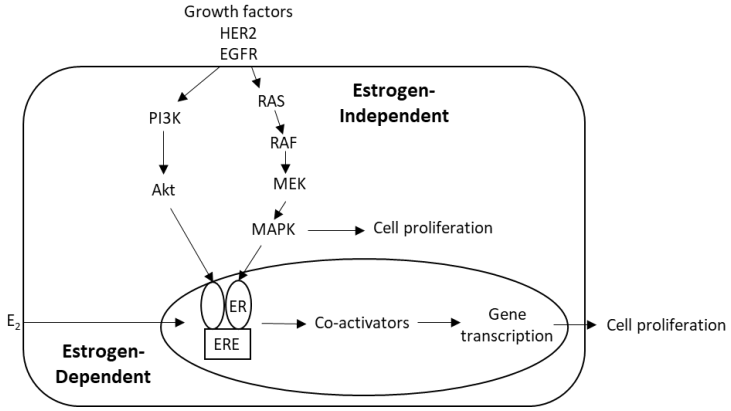

Figure 1.5: Mechanisms involved in E_2 hypersensitivity and adaptation of LTED cells

BC cell proliferation occurs in an estrogen-dependent pathway where E_2 enters the cell and binds to the ER, promoting the dimerisation and conformational change of the ER, subsequently leading to transcriptional co-activator recruitment for further gene expression, promoting cell proliferation. LTED cells adapt to low levels of estrogen through estrogen-independent pathways, which involve increased growth factor receptor secretion and signalling. Activated downstream kinases (MAPK and Akt) phosphorylate the ER recruiting co-activators leading to the activation of further growth factor signalling pathways, for

increased cell proliferation and survival of LTED cells in low levels of estrogen. Source: [Figure adapted from (Jeng et al., 2000). Accessed: 10.11.22]

In addition to enhanced growth factor receptor signalling pathways, resistant ER+ LTED BC cells have a significant increase in expression of genes in the cholesterol biosynthesis pathway which may be linked to the resistance of endocrine or TAM therapy (Simigdala *et al.,* 2016). Therefore, the up-regulation of the cholesterol biosynthesis pathway has been identified to play a role as a resistance mechanism in ER+ LTED BC cells (Simigdala *et al.,* 2016) and requires further investigation.

1.7 Cholesterol accumulation linked to BC proliferation

Cholesterol is an important sterol in the human body as it is a main component of lipid rafts, which maintains cell stability and shape, and mediates cell membrane proteins, receptor transportation, proliferation, membrane biogenesis, and signal transduction (Silvius, 2003). Cholesterol acts as a hormone precursor to produce various steroid hormones, including estrogen (promotes ER+ BC progression), vitamin D and bile acids (Gu *et al.,* 2019). In recent years, the role of cholesterol in cancer cell growth has become prominent. Cholesterol is linked to cancer progression mainly by increased cholesterol synthesis and excess cholesterol accumulation in lipid rafts for sufficient proliferative abilities (Antalis and Buhman, 2012; Clendening and Penn, 2012; Gu *et al.,* 2019; Nelson *et al.,* 2014). Interestingly, BC cells are found to be approximately 6-8 times richer in cholesterol than normal cells (Llaverias *et al.,* 2011; Simigdala *et al.,* 2016). Cholesterol has also been linked to BC drug resistance due to the accumulation of cholesterol which leads to evasion of apoptosis, continuous proliferation, and drug resistance (Gu *et al.,* 2019). Cancer cells have elevated levels of cholesterol-rich lipid rafts which contain several signalling proteins and receptors regulating pro-oncogenic and apoptotic pathways (Antalis and Buhman, 2012). This is done by an increased influx of glucose into proliferating cells and can also be done through the glycolytic pathway. Decreasing plasma cholesterol levels disrupts lipid raft formation thereby inhibiting BC development. Lowering the levels of cholesterol-rich lipid rafts could be a novel therapeutic strategy in BC treatment as this process induces chemosensitivity to certain drugs such as TAM thus inducing apoptosis.

1.8 Cellular cholesterol homeostasis

Cholesterol biosynthesis is a natural process that occurs through the mevalonate pathway (Fig. 1.6) (Silvente-Poirot and Poirot, 2014). Briefly, Acetyl-CoA, which is produced during glycolysis, acts as a precursor molecule for cholesterol synthesis. In the first step of the

mevalonate pathway, two Acetyl-CoA molecules are condensed via 3-hydroxy-3-methylglutaryl-CoA synthase 1 (HMGCS1) to yield acetoacetyl-CoA (Martín *et al.*, 2014). Following this, a second condensation step occurs, forming hydroxy-methyl glutaryl-coenzyme A (HMG-CoA). The rate-limiting step of the pathway occurs when HMG-CoA gets reduced to mevalonate by 3-hydroxy-3-methylglutaryl-CoA reductase (HMGCR). Thereafter, mevalonate is converted to isopentenyl pyrophosphate, and then squalene, which undergoes several reactions to ultimately form cholesterol (Martín *et al.*, 2014).

Cholesterol is a lipid molecule that is encapsulated in a water-soluble protein coat, called a lipoprotein (Didichenko *et al.*, 2016). Lipoproteins are complex amphiphilic molecules that act as carriers for the transport of cholesteryl esters (CEs) and free cholesterol (Tosi and Tugnoli, 2005). There are four principal classes of lipoproteins. These include: chylomicrons, high-density lipoproteins (HDLs), low-density lipoproteins (LDLs), and very low-density lipoproteins (VLDLs) (Cruz *et al.*, 2013). Intracellularly, cholesterol is taken up by the cell through the binding of LDL to the LDL receptor (LDLR). LDLs transport cholesterol from the liver, which is the site of synthesis to peripheral tissues (Cruz *et al.*, 2013). Endosomes are then formed due to internalisation of LDL. Lysosomal degradation releases cholesterol into the cytosol of cells, where it is used for various purposes or exported directly out of the cell via HDL and excreted by the liver. HDLs maintain cholesterol homeostasis by eliminating excess cholesterol from cells through the reverse cholesterol transport (RCT) pathway or by directly transporting cholesterol to the liver (Cruz *et al.*, 2013). In the process of RCT, HDLs shuttle CEs to the LDLs and then to the liver where it is ultimately converted to bile salts (Tosi and Tugnoli, 2005). CEs are a form of esterified cholesterol, which allow for more efficient transport of free cholesterol by lipoproteins to the liver and thus aids in the maintenance of cholesterol homeostasis (Tosi and Tugnoli, 2005).

Many proteins are involved in aiding intra- and extracellular cholesterol homeostasis (Fig. 1.7). In the endoplasmic reticulum, intracellular free cholesterol is converted to CEs by acetyl-CoA acyltransferase (ACAT1) for storage or promotion of cholesterol synthesis through sterol regulatory element-binding proteins (SREBPs) (Chang *et al.*, 1997; Nelson *et al.*, 2014). When proprotein convertase subtilisin-like kexin type 9 (PCSK9) is bound to LDLR, it triggers LDLR degradation, thereby reducing surface LDLR and increasing cholesterol levels intracellularly (Horton *et al.*, 2007). On the contrary, HDLs remove cholesterol from cells to the liver to be excreted. This is achieved by either an increase in cholesterol efflux (through membrane transporters) or by the conversion of lecithin–cholesterol acyltransferase (LCAT) into HDLs

(Tosi and Tugnoli, 2005). This is achieved when free cholesterol is converted into CEs for a more effective mode of transport of cholesterol by LCAT, later forming into HDLs. Thereafter, HDLs transport CEs directly to the liver through scavenger receptor, class B type 1 (SR-B1). CEs are shuttled from HDLs to LDLs through cholesteryl ester transfer protein (CETP), and are delivered to the liver for cholesterol homeostasis (Esau *et al.*, 2016). Extracellularly, cholesterol is delivered to cells via LDLs and binds to LDLR which is internalised and forms lysosomes that dissociate the interaction between LDL and LDLR. The free cholesterol is then incorporated into the plasma membrane for stability and the LDLRs are recycled back to the surface (Chang *et al.*, 1997).

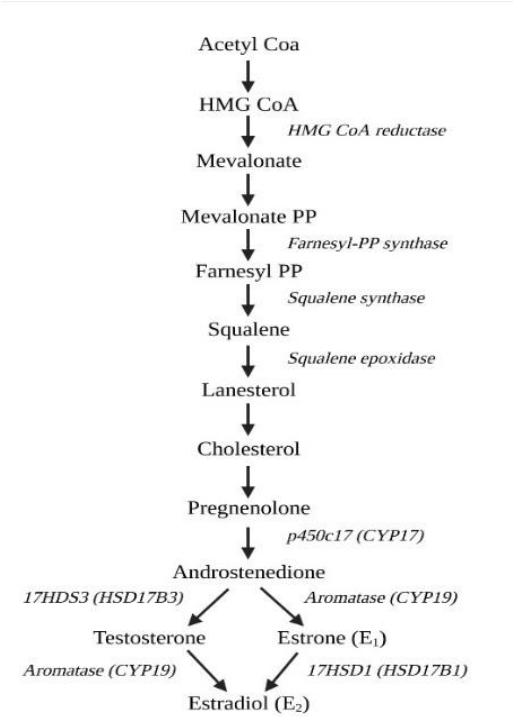

Figure 1.6: The cholesterol biosynthesis pathway

Acetyl-CoA is a precursor molecule for cholesterol biosynthesis. It is ultimately converted to HMG-CoA, which is later reduced into mevalonate via HMGCR. Mevalonate is phosphorylated into phosphomevalonate (mevalonate PP). Thereafter, a series of phosphorylation events result in the synthesis of isopentenyl PP, geranyl PP, farnesyl PP, squalene, and lanesterol, which is finally converted into cholesterol. Cholesterol is the precursor of several steroid hormones such as progesterone, testosterone and estrone, which are ultimately converted into E_2. Source: [Image created with BioRender.com. Adapted from: (Buhaescu and Izzedine, 2007; Gu et al., 2019; Payne and Hales, 2004)]

Cholesterol accumulation in BC cells occurs via hyper-activation of the PI3K/Akt/mTOR pathway which activates *SREBP2*. This esterifies and compartmentalises cholesterol into lipid droplets allowing for fatty acid uptake. This finally leads to increased cancer cell proliferation (Peck and Schulze, 2014). *SREBP* is an essential regulator of cholesterol homeostasis as it regulates genes involved in cholesterol biosynthesis. These genes include *HMGCS1* and *HMGCR*, mevalonate kinase, and *LDLR* (Guan *et al.,* 2019). Under normal conditions, *SREBP1/2* is associated with SREBP cleavage-activating protein (SCAP), and insulin induced gene 1/2 (*INSIG1*/2) in the endoplasmic reticulum (Afonso *et al.,* 2018). In conditions of reduced cholesterol levels, the SREBP-SCAP complex dissociates from INSIG which degrades and localises to the Golgi body (Afonso *et al.,* 2018). SREBP is then cleaved, therefore enabling it to enter the nucleus undergoing nuclear translocation and promote the expression of cholesterol uptake and biosynthesis genes. The nuclear translocation of *SREBP1* transcriptionally activates unsaturated fatty acid and triglyceride biosynthesis which regulates tumour growth through membrane biosynthesis (Kondo *et al.*, 2017). On the other hand, the nuclear translocation of *SREBP2* preferentially increases cholesterol biosynthesis (Horton *et al.,* 1998), thereby promoting cancer progression due to alterations in cancer metabolism (Kondo *et al.*, 2017). In addition, *SREBP* binds to the promoter region of ATP binding cassette subfamily B member 1 (*ABCB1*) to prevent its expression, consequently inhibiting cholesterol efflux (Afonso *et al.,* 2018). On the contrary, under conditions of excess cholesterol, the INSIG-SCAP-SREBP complex remains in the endoplasmic reticulum, where the SREBP-SCAP complex is unable to move to the Golgi body, which prevents lipogenesis and cholesterol uptake is prevented (Nazih and Bard, 2020).

There are several factors contributing to elevated cholesterol levels in cancer cells. A study revealed cholesterol levels were increased in TNBC (MDA-MB-231 cells) due to high LDLR expression, which is associated with reduced recurrence-free survival in BC patients (Gallagher *et al.,* 2017). Increased LDLR expression plays a role in increased cellular cholesterol uptake, which leads to TNBC cell migration and metastasis (Nazih and Bard, 2020). Additionally, cholesterol has recently been identified as a ligand for the estrogen-related receptor α (ERRα), suggesting that there is a link between cholesterol biogenesis and mitochondrial biogenesis particularly in tumour cells (Chimento *et al.,* 2019). Cholesterol binds to the ERRα, allowing for the recruitment of co-activators, which increases ERRα transcriptional activity, thereby inducing BC tumour growth (Chimento *et al.,* 2019). Moreover, PI3K expression is elevated in resistant ER+ LTED cells which demonstrates cholesterol accumulation in BC cells

(Simigdala *et al.*, 2016). In addition, several other proteins, enzymes, and gene regulatory elements help maintain cholesterol homeostasis. Therefore, targeting these molecules or using cholesterol depleting compounds can be an alternative therapeutic approach in lowering excess cholesterol in BC. Studying the molecular mechanisms involved in cholesterol accumulation and how it affects resistance in BC cells is also important.

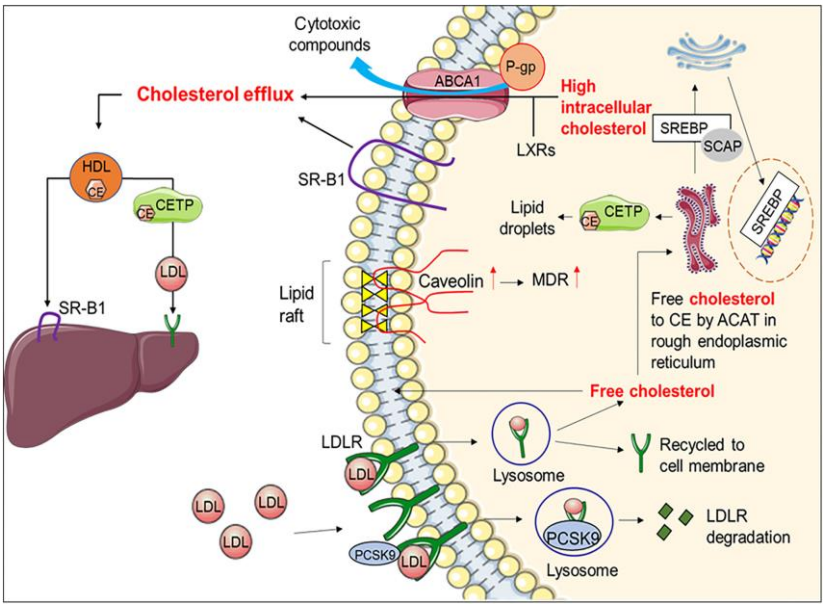

Figure 1.7: Cholesterol homeostasis

A summary of the cholesterol transport system in maintaining intra- and extracellular cholesterol homeostasis. Cholesterol is transported by LDLs to the cell surface by binding to LDLR, forming a lysosome that is then internalised and degraded into free cholesterol in the presence of PCSK9. In the absence of PCSK9, LDLRs are recycled to the membrane. The free cholesterol is then incorporated into the plasma membrane for cell stability or is converted into CEs in the rough endoplasmic reticulum by ACAT1. CEs are transported to storage droplets by CETP. Intracellular CE levels determine SREBP activity. In low CE conditions, SREBP is activated in the Golgi body by SCAP, signalling cholesterol biosynthesis. In high CE conditions, SREBP activity is inhibited, and membrane cholesterol transporters (ABCA1 and SR-B1) are activated leading to cholesterol efflux. Source: [(Gu et al., 2019). Accessed: 10.11.22]

1.9 Targeting cholesterol for BC treatment

It was demonstrated that ER+ LTED BC cells have increased ER expression and increased lipogenesis (Simigdala *et al.*, 2016). Therefore, increased lipogenesis may be associated with acquired resistance in ER+ LTED BC cells (Simigdala *et al.*, 2016). Thus, targeting cholesterol

and its associated pathways to reduce cancer-related drug resistance could be a possible anticancer therapeutic strategy.

Currently, there are two methods in targeting cholesterol as a possible anticancer therapy for BC. The first approach involves the blocking of cholesterol synthesis using statins (Garcia-Bermudez *et al.,* 2019; Vallianou *et al.*, 2014; Van Wyhe *et al.,* 2017) and the second treatment involves the depletion of accumulated membrane cholesterol by the use of cholesterol depleting agents (Mohammad *et al.,* 2014; Simigdala *et al.,* 2016; Yamaguchi *et al.,* 2015). A detailed viewpoint on the advantages and disadvantages of the above two approaches has been discussed (Gu *et al.,* 2019).

Statins, also known as HMGCR inhibitors, are the most common lipid-lowering drugs. Statins are cholesterol synthesis inhibitory drugs and there has been extensive research on the use of these drugs. Statins can be hydrophilic (rosuvastatin and pravastatin) and lipophilic (fluvastatin, lovastatin, simvastatin, and atorvastatin) (Chimento *et al.,* 2019). Statins inhibit HMGCR which plays a major role in cholesterol synthesis (Mostaghel *et al.,* 2012). This inhibition impedes the mevalonate pathway as the conversion of acetyl-CoA to HMG-CoA does not occur. Consequently, cholesterol levels decrease thus being an effective treatment in atherosclerosis and coronary heart disease (Stancu and Sima, 2001). There have been numerous debates regarding the use of statins in cancer treatments. Several studies have concluded that statins can act as anticancer therapies (Campbell *et al.,* 2006; Chan *et al.,* 2003), whereas other studies have made contradictory conclusions suggesting that statins actually promote cancer cell growth (Boudreau *et al.,* 2010; Duncan *et al.,* 2005). Studies have failed to establish a significant link between statins and chemo-prevention of BC as reviewed by Gu and colleagues, 2019. Therefore, it is important to further expand on the knowledge of statin use as a therapeutic approach in cancer treatment.

The second approach in targeting cholesterol as a possible therapy for BC is the use of cholesterol depleting agents. Recently, studies have revealed that the administration of cholesterol depleting compounds such as, Methyl-β-cyclodextrin (MβCD) and Acetyl Plumbagin (AP) has been shown to be effective in promoting BC cell death (Esau *et al.,* 2016; Gu *et al.,* 2019; Sagar *et al.,* 2014). These agents deplete excess cholesterol or deplete cholesterol in the lipid rafts thereby disrupting cell membrane rigidity and permeability. For these reasons, these compounds have been extensively researched in recent years as an alternative method in the treatment of BC and cholesterol-related diseases. The depletion of

excess cholesterol within BC cell membranes induces apoptosis and chemosensitivity to current endocrine treatments, such as TAM (Esau *et al.,* 2016; Mandal and Rahman, 2014; Mohammad *et al.,* 2014; Yamaguchi *et al.,* 2015). MβCD increases TAM's efficacy by increasing membrane permeability for drug passage due to disrupted lipid raft integrity (Mohammad *et al.,* 2014). In recent years, studies have shown that lipid raft disruption in TNBC cell lines using MβCD resulted in reduced proliferation, migration, and invasion as well as induced apoptosis (Badana *et al.,* 2018; Raghu *et al.,* 2010). These findings highlight the advantages of using cholesterol depleting agents over statins in the treatment of BC as they have been found to have several anticancer properties.

The cholesterol depleting agent, AP has recently emerged to have a promising effect on BC cells. AP is a derivative of Plumbagin (PL) (5-hydroxy-2-methyl-1,4-naphthoquinone), which is a naturally occurring yellow pigment found in the plants of the Plumaginaceae, Ancestrocladaceae and Dioncophyllaceae families (Manu *et al.,* 2011). It is a naphthoquinone derived from the roots of the *Plumbago zeylanica* plant (Jamal *et al.,* 2014). PL has many pharmacological properties and has shown pro-apoptotic and anti-proliferative activities in various cancer cells (Manu *et al.,* 2011). It is especially well known for its anticancer activities as it has many inhibitory effects on various cancer signalling pathways; however, the exact molecular interactions of these pathways have not yet been elucidated (Jamal *et al.,* 2014).

PL has been reported as a 'lead' molecule in developing novel anticancer agents (Sagar *et al.,* 2014). However, novel derivatives of PL to enhance its activity and reduce toxicity have been developed in order to maximise therapeutic potential (Sagar *et al.,* 2014). The addition of an acetyl group at the 5-C position, which produces AP (Fig. 1.8) has been shown to reduce the toxicity of PL towards normal cells and induces apoptosis in ER+ BC cell lines (Sagar *et al.,* 2014).

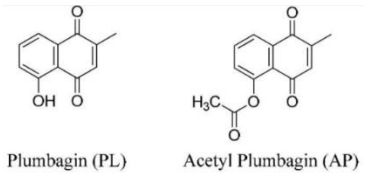

Figure 1.8: The molecular structures of PL and AP

The addition of an acetyl group at the 5-C position of PL significantly increases cytotoxicity in cancer cells while reducing toxicity in normal cells. Source: [(Sagar et al., 2014) Accessed: 10.11.22]

AP has the potential to reduce toxicity and increase efficacy of known endocrine treatments such as TAM. It may enhance the usage of these drugs at lower concentrations with increased cancer killing effects. Preliminary data has shown that when AP is used in combination with chemotherapeutic drugs such as 5-Fluorouracil (5-FU), Paclitaxel and TAM, viability of normal cells is unaffected while simultaneously significantly reducing the viability of cancer cells (Fig. 1.9) (previous unpublished work of Professor Kaur). Another important observation found that AP is a cholesterol depleting agent and could function by altering cholesterol-related mechanisms (Esau *et al.,* 2016). Although the exact mechanisms of AP have not yet been established, the depletion of cholesterol using AP resulted in a significant increase in mitochondrial-mediated apoptosis (Esau *et al.,* 2016; Henriques Palma and Kaur, 2022), demonstrating AP's ability to induce apoptosis by depleting cellular cholesterol. This indicates that AP could act as a novel lead molecule for further drug development targeting cholesterol accumulation in BC. It also has the potential to overcome the resistance associated with TAM.

It can be postulated that cholesterol depletion from BC cell membranes disrupts lipid rafts, which increases membrane permeability for chemotherapeutic drug passage (Mohammad *et al.,* 2014). Therefore, the use of a cholesterol depleting agent (AP) in combination with an endocrine treatment (TAM) can be an effective strategy in combating cholesterol-rich BC. This therapeutic combination strategy also has the potential to increase drug efficacy and reduce cancer-related drug resistance. However, this is a novel concept which requires the basic understanding of the role of AP in combination with TAM and the molecular mechanisms involved. miRNAs regulate numerous genes that have been implicated in cancer, and the aberrant expression of certain miRNAs has been linked to tumorigenesis and drug resistance (Encarnación-Medina *et al.,* 2019). As a link between miRNA dysregulation and BC drug resistance has been established, it may prove advantageous if novel BC therapeutics employ specific miRNAs.

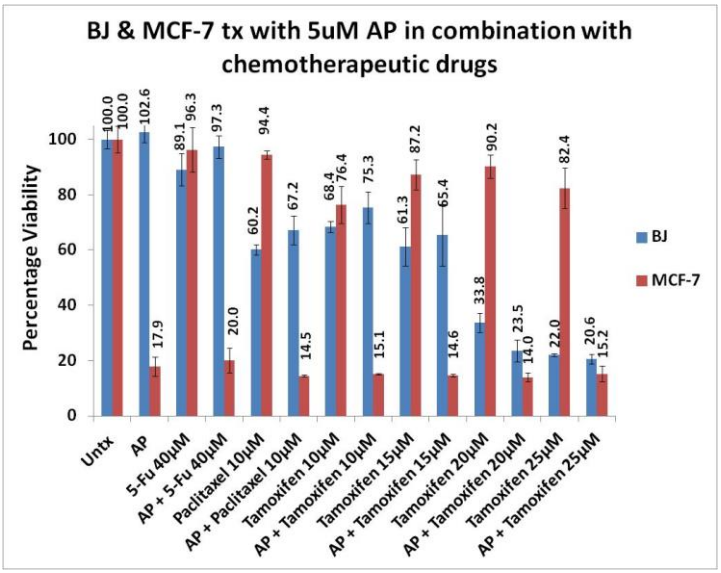

Figure 1.9: The effect of AP on viability of normal and BC cells

When AP is combined with a range of concentrations of various chemotherapeutic drugs, such as TAM, 5-FU and Paclitaxel, the viability of normal cells is unaffected whereas the viability of BC cells is decreased. BJ: normal skin fibroblast cell line used as a control, Untx: untreated control, 5-FU: *5-Fluorouracil, AP: Acetyl Plumbagin. Source: [Previous unpublished work of Professor Kaur]*

1.10 The role of miRNAs

Over the past several years, miRNAs have been proven to be master regulators in several cholesterol-related mechanisms in the cell. miRNAs are small, single-stranded, non-coding RNA transcripts that are 19-24 nucleotides long (Fig. 1.10). They play important roles in cell activity at the transcriptional level (Schwarzenbach *et al.,* 2015). miRNAs regulate over 30% of protein-coding genes, indicating the importance of these molecules in almost all biological cellular processes (He *et al.,* 2016). Furthermore, miRNAs also play vital roles in tumourigenesis and cancer development, as they can act as either oncogenes or tumour suppressors (He *et al.,* 2016).

The biogenesis of miRNAs occurs in the following way: RNA polymerase II or III initially transcribes these molecules into primary, immature transcripts (pri-miRNAs). This primary transcript contains a region of imperfect complementary sequences forming a structure called a stem-loop or a hairpin (Lynch and Wang, 2014). The stem-loop or hairpin is recognised by the Drosha-DGCR8 microprocessor complex in the nucleus, which mediates pri-miRNA cleavage at the stem of the hairpin structure (Winter *et al.,* 2009). This cleavage releases a small hairpin called the precursor miRNA (pre-miRNA) (Lynch and Wang, 2014). The pre-

miRNA 3’ overhang is recognised by the exportin-5:Ran:GTP complex. Subsequently, this complex transports the pre-miRNA through the nuclear pore complex, into the cytoplasm where it is further cleaved and processed to its mature length by a RNase III enzyme, Dicer1 (a ribonuclease) and its co-factor transactivation-responsive RNA binding protein (TRBP). This cleavage forms a mature miRNA duplex in the cytoplasm (Hata and Kashima, 2016). Dicer:TRBP recruits Argonaute (Ago2) proteins to the miRNA-induced silencing complex (miRISC) to form the ribonucleoprotein complex, miRISC/RISC (Wilson *et al.*, 2015). In the miRISC, the mature miRNA duplex unwinds, and the functional strand of the mature miRNA strand is retained, which interacts with complementary sequences located at the 3′-untranslated region (UTR) of target messenger RNAs (mRNAs) in the cell’s cytoplasm, mediating mRNA cleavage, translational repression or deadenylation (Schwarzenbach *et al.*, 2015), whereas the passenger strand is degraded (Winter *et al.*, 2009). Ultimately, this process silences gene expression due to the decrease in the production of effector proteins. Individual miRNAs often repress several targets within the same pathway thereby resulting in the amplification of their biological effects (Schwarzenbach *et al.*, 2015).

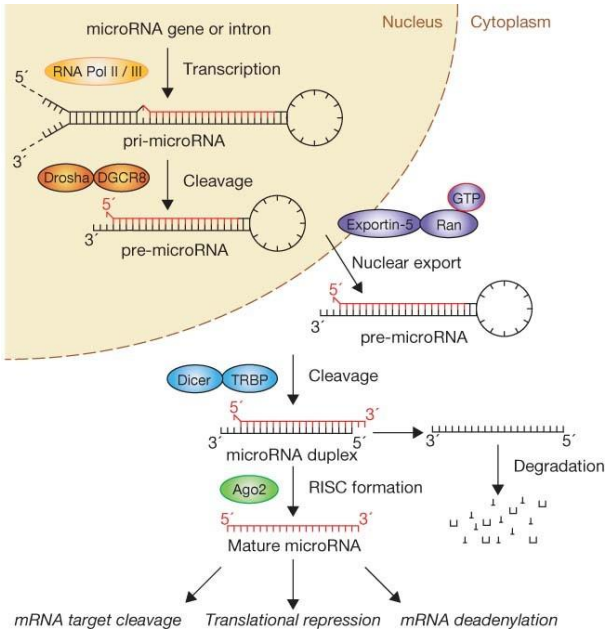

Figure 1.10: miRNA biogenesis

miRNA biogenesis involves the production of a pri-miRNA by RNA Pol II. The pri-miRNA is cleaved by Drosha:DGCR8 in the nucleus. The resulting pre-miRNA hairpin structure is exported by Exportin-5:Ran:GTP to the cytoplasm and is further cleaved by Dicer:TRBP. This produces the mature miRNA, which is a double-stranded anti-parallel RNA. This mature miRNA unwinds, and one strand is then incorporated into the miRISC by Ago2, ultimately

leading to mRNA target cleavage, translational repression, and mRNA deadenylation. Source: [(Winter et al., 2009). Accessed 10.11.22]

1.10.1 miRNAs in regulating cellular cholesterol homeostasis

Cholesterol levels are regulated through mechanisms such as cholesterol biogenesis, cholesterol internalisation, and efflux of intracellular cholesterol. Two transcription factors, sterol regulatory element binding transcription factor 1 (*SREBF1*) and liver X receptor (*LXR*) facilitate the regulation of these mechanisms. SREBFs are involved in cholesterol uptake and biogenesis, while LXRs mediate cholesterol efflux and maintain cholesterol homeostasis (Gu *et al.,* 2019). Low cholesterol levels induce SREBP (*SREBP2* and *SREBP1c*) expression, in turn up-regulating the expression of *HMGCR* and *LDLR*, resulting in increased cholesterol biosynthesis and uptake (Gu *et al.,* 2019). Whereas high cholesterol levels activate a negative feedback loop that is mediated by LXRs (*LXRα* and *LXRβ*) (Monchusi and Kaur, 2020).

It has recently emerged that miRNAs play important roles in intracellular cholesterol homeostasis. Several miRNAs regulate lipid metabolism, accumulation, and synthesis, namely miR-1, miR-19b, miR-27, miR-33, miR-96, miR-106, miR-122, miR-144, miR-145, miR-197, miR-206, miR-223, miR-302, miR-378, miR-370, miR-185, miR-128, and miR-26a/b to name a few (DiMarco and Fernandez, 2015). This suggests that targeting miRNAs involved in cholesterol regulation may be effective as an anti-BC strategy. Furthermore, understanding the role of miRNAs in cancer drug resistance is crucial.

Several miRNAs, such as miR-96, miR-182, miR-183, and miR-128 increase *SREBP2* expression (Adlakha *et al.*, 2013; Jeon *et al.,* 2013). miR-185 decreases *SREBP2* expression, therefore, further decreasing expression of *SREBP2*-responsive genes such as *LDLR*, resulting in decreased cholesterol uptake (Yang *et al.,* 2014). miR-185 was also found to be negatively regulated by *SREBP1c*. A previous study found that an increase in intracellular cholesterol activated *LXR*, which further up-regulated *SREBP1c*, leading to the increased expression of miR-185, thereby suppressing *SREBP2*. This subsequently caused a reduction in cholesterol uptake by the cell (Yang *et al.,* 2014). Cholesterol efflux from the cell is mediated by ATP-binding cassette subfamily A member 1 (*ABCA1*) and this process has been found to be regulated by several miRNAs (miR-19b, miR-26, miR-106, miR-27a/b, miR-128, miR-145, miR-302a, and miR-758) by binding to the 3' UTR of *ABCA1* (DiMarco and Fernandez, 2015). Other miRNAs (miR-223 and miR-33a-3p) indirectly regulate *ABCA1* and ATP-binding cassette subfamily G member 1 (*ABCG1*) expression by targeting their transcription factors,

which reduces cholesterol efflux to apolipoprotein A1 (APOA1) and HDL (Jeon and Osborne, 2016). These miRNAs therefore limit the availability and activation of *LXR* target genets which includes *ABCA1*, and prevent cholesterol transport to the endoplasmic reticulum, until cholesterol homeostasis has been met (Jeon and Osborne, 2016). *ABCG1* is a direct target of miR-128 (Adlakha *et al.*, 2013), thus influencing cholesterol efflux to HDL. On the other hand, miR-27 directly suppresses *ABCA1* expression, while indirectly suppressing *ABCG1* thereby reducing cholesterol efflux (DiMarco and Fernandez, 2015). miR-96 directly suppresses the expression of SR-B1, but increases HDL uptake, whereby HDL binds to SR-B1 leading to increased uptake of HDL-CEs into the cell (Ben Hassen *et al.*, 2020). miR-122 directly up-regulates the expression of lipogenic genes which elevates plasma cholesterol (DiMarco and Fernandez, 2015). Lastly, miR-144 directly suppresses the expression of *ABCA1* and plasma cholesterol where *LXR* is up-regulated, suggesting that there is a negative feedback mechanism in the cholesterol efflux process (DiMarco and Fernandez, 2015; Jeon and Osborne, 2016). Therefore, the literature highlights the complex nature of miRNA-mediated regulation in cholesterol-related processes in the cell and requires further investigation.

1.10.2 miRNAs in cancer

miRNAs are involved in a multitude of cellular processes such as cell survival, apoptosis, proliferation, angiogenesis, and differentiation. Thus, aberrant miRNA expression has been implicated in many diseases including several malignancies (Lynch and Wang, 2014), and can also contribute to cancer-related drug resistance (Sun *et al.*, 2016). Various mechanisms of miRNA dysregulation have been proven in cancer cells since it was first presented in 2002, where the deletion of miR-15 and miR-16 often causes the development of chronic lymphocytic leukaemia (CLL) (Calin *et al.*, 2002). This pointed out the tumour suppressor activities of miRNAs and has since given rise to a several studies observing the altered expression of various miRNAs in tumours. Several mechanisms leading to aberrant expression of miRNAs in the development of cancer have been postulated. These mechanisms include: single nucleotide polymorphisms in miRNAs, reduced miRNA expression due to the rearrangement of the mRNA target 3' UTR, and altered expression of enzymes involved in miRNA biogenesis, like Drosha, Dicer1, Ago2, and Exportin-5 (Acunzo *et al.*, 2015; Lin and Gregory, 2015; Monchusi and Kaur, 2020; Ryan *et al.*, 2010). miRNAs play roles in both oncogenic and tumour suppressor pathways. For example, miR-1207, miR-200c, miR-14, miR-519a, miR-210, and miR-155 have oncogenic capabilities that have been found to promote cellular proliferation and metastasis, G2 cell cycle progression, promote resistance to apoptosis, induce

angiogenesis, evade immune detection, and contribute to replicative immortality (Loh *et al.,* 2019). On the contrary, miRNAs such as miR-543, miR-124a, miR-26b, miR-34a, miR-497, and miR-296 have tumour suppressor capabilities that play roles in reducing cellular proliferation, metastasis, angiogenesis, invasion, cell cycle arrest, inducing apoptosis, and activation of replicative senescence (Loh *et al.,* 2019).

Therefore, miRNAs play intricate roles in both cancer cell progression and cell cycle arrest and targeting these processes could be an effective anti-cancer treatment; however, the onset of cancer-related drug resistance is a critical factor and novel advances are required.

1.10.3 miRNAs in cancer-related drug resistance

miRNAs play key roles in cancer stem cell formation, stem cell differentiation, and EMT, which are all implicated in drug resistance (Acunzo *et al.,* 2015). Several miRNAs are involved in drug resistance and are often up- or down-regulated depending on their functions. miRNAs such as miR-19, miR-21, and miR-221/222 are significantly up-regulated in resistant cells, whereas miR-130a and miR-298 are down-regulated, suggesting the importance of the biological role of miRNAs (Acunzo *et al.,* 2015). miRNAs affect the expression of drug molecular targets thereby increasing cancer drug resistance (Acunzo *et al.,* 2015). For example, miR-17, miR-21, miR-144, miR-214, and miR221/222 all target PTEN, which activates the PI3K/Akt signalling pathway, which evades the drug induced inhibition of EGFR (Acunzo *et al.,* 2015). This demonstrates that miRNAs are involved in cancer drug resistance in several ways such as targeting proteins and influencing the expression of other miRNAs.

miRNAs have been shown to be involved in BC drug resistance. miRNAs such as miR-101, miR-206, miR-221, and miR-222 were found to make ER+ BC cells resistant to TAM (Viedma-Rodríguez *et al.,* 2014). miRNA-mediated targeting of ERα co-factors has also been linked to reduced chemotherapeutic response (Viedma-Rodríguez *et al.,* 2014). ERα co-activators and transcriptional co-repressors are targeted by several miRNAs which are dysregulated in BC cells exhibiting drug resistance. Therefore, targeting miRNAs is a novel approach in reducing drug resistance in BC cells.

Several studies have revealed a link between cancer drug resistance and intracellular cholesterol levels. A study has shown the role of cholesterol metabolism in TAM-R BC cells (Hultsch *et al.,* 2018) and another study demonstrated the improvement in the clinical outcome for ER+ BC patients who received cholesterol-lowering drugs during adjunctive endocrine treatment (Borgquist *et al.,* 2017). The cholesterol depleting agent, MβCD was found to act

with TAM to suppress pro-survival signalling and induce apoptosis in TAM-R BC cells (Tiwary *et al.,* 2011). These studies demonstrate cholesterol-mediated drug resistance in BC cells, therefore exploring the role of miRNAs in cholesterol-mediated drug resistance could be an interesting approach in BC treatment.

1.10.4 miRNAs in cholesterol-mediated drug resistance in BC

As previously mentioned, studies have found a link between altered miRNA expression and cancer drug resistance. However, the role of miRNAs in cholesterol-mediated drug resistance is a novel concept that requires much elucidation. Few studies have reported the link between miRNAs and cholesterol metabolism as a potential anticancer approach in combating drug resistance. In this study, we chose to investigate miR-128 and miR-223, due to their roles in regulating genes mediating cholesterol export and synthesis (Adlakha *et al.,* 2013; DiMarco and Fernandez, 2015). These two miRNAs may be able to regulate several genes related to cholesterol and BC drug and could be potential therapeutic targets for BC treatment.

miR-128 has been shown to regulate genes in chemo-resistant cancers as well as cellular cholesterol homeostasis. Previous analysis performed in our laboratory revealed that the potential targets regulated by miR-128 include *RXRA, BRCA2, IGF2R, BAX, EGFR, UGCG, ABCA1, ABCG1, PRKAA1, SREBF1, SREBF2, LDLR, CSF1, SNAI2, PTGS2,* and *PTEN* (Monchusi and Kaur, 2020). Based on these findings, it can be predicted that cholesterol uptake and accumulation may play a role in promoting cancer drug resistance in BC cell lines. Therefore, targeting miR-128 may mediate this resistance in BC cell lines by lowering cellular cholesterol content.

A study revealed that miR-128 is a master regulator of chemoresistance genes in BC cells, involving the down-regulation of *Bmi-1* and ATP-binding cassette subfamily C member 5 (*ABCC5*) (Zhu *et al.,* 2011). This study also showed that miR-128 is down-regulated in chemo-resistant BC and when ectopically expressed, miR-128 increases sensitivity to doxorubicin, a chemotherapeutic agent (Zhu *et al.,* 2011), indicating that miR-128 plays roles in increased cell proliferation, self-renewal, and chemoresistance in BC cells. In contrast, miR-128 expression increased resistance to the AI, letrozole, in hormone-dependent BC cells (Masri *et al.,* 2010). In addition, when miR-128 was overexpressed, cell proliferation in TNBC was suppressed (Angius *et al.,* 2020). The role of miR-128 requires further research to elucidate its mechanism of action in its role in cancer. Nevertheless, these studies provide evidence that miR-128 is

involved in BC tumorigenesis and can be a potential marker of chemoresistance, as well as a possible target for therapy.

Studies have also revealed that miR-128 directly reduced *ABCA1*, *ABCG1*, and *LDLR* expression and increased *SREBP2* expression and its downstream genes for increased lipogenesis (Adlakha *et al.*, 2013; DiMarco and Fernandez, 2015; Wagschal *et al.*, 2015). Circulating cholesterol levels of mice overexpressing miR-128 revealed reduced plasma HDL-C levels due to reduced *ABCA1* required for HDL formation (Wagschal *et al.*, 2015). Therefore, inhibiting the expression of miR-128 may decrease intracellular cholesterol and promote cholesterol efflux. Increased LDL clearance was observed in mice inhibiting miR-128, with a significant decrease in total circulating cholesterol in these mice (Wagschal *et al.*, 2015). These studies reveal that miR-128 regulates cholesterol efflux and uptake by regulating *ABCA1* and *LDLR* expression. This suggests that the inhibition of miR-128 can be an effective therapeutic approach in the treatment of cholesterol-mediated drug resistance in BC.

It has been found that miR-223 is a tumour suppressor and plays important roles in regulating proliferation, invasion, haematopoietic development, and differentiation in various cancer cells, including human BC cells lines (Gong *et al.*, 2013). Similarly, previous analysis performed in our laboratory revealed that the potential targets regulated by miR-223 include *AR, ABCB1, ATM, CCND1, CDK2, IGF1, IGF1R, IL6, INSIG2, LDLR, TP53,* and *UGCG* (Monchusi and Kaur, 2020). These targets are involved in cancer drug resistance, lipoprotein signalling and BC. Therefore, targeting miR-223 may also mediate this resistance in BC cell lines by lowering cellular cholesterol content.

miR-223 is down-regulated in BC which leads to BC cell proliferation (Yang *et al.*, 2018). It can alter several processes in the cell such as cell survival, cell cycle, immune evasion, and metastasis (Haneklaus *et al.*, 2013). A study revealed that miR-223 had high expression in non-tumourigenic MCF-10A cells and moderate expression in MCF-7 cells (Gong *et al.*, 2013). Overexpressing this miRNA significantly inhibited MDA-MB-231 cell invasion and increased the viability of these cells. This indicates that miR-223 inhibits cell proliferation, viability, and invasion in BC cell lines (Gong *et al.*, 2013). Moreover, a study demonstrated that miR-223 regulated tumour cell migration and invasion in oesophageal carcinoma and down-regulated miR-223 expression increased the risk of CLL (Gong *et al.*, 2013). It is also down-regulated in ovarian cancers and it has also been suggested that miR-223 may be used to predict the state

of BC in patients due to specific miR-223 expression levels that indicate the grade of BC (Gong *et al.*, 2013).

The expression of miR-223 regulates cholesterol uptake, efflux, homeostasis, and biosynthesis (DiMarco and Fernandez, 2015). Studies revealed that miR-223 indirectly increased *ABCA1* and *CYP7A1* expression, consequently decreasing cholesterol synthesis. Therefore, overexpressing miR-223 may enhance cholesterol efflux and increase HDL formation, thereby reducing intracellular cholesterol (DiMarco and Fernandez, 2015; Vickers *et al.*, 2014). Overexpressing miR-223 increases *ABCA1* expression thereby increasing cholesterol efflux to APOA1 via an indirect mechanism (Vickers *et al.*, 2014). In addition, miR-223 also negatively regulates SR-B1 and *HMGCS1* expression, as well as HDL uptake which ultimately suppresses intracellular cholesterol uptake (DiMarco and Fernandez, 2015; Vickers *et al.*, 2014). The overexpression of miR-223 could also attenuate BC cell proliferation, invasion and have increased recurrence-free survival in patients (Yang *et al.*, 2018) and could therefore be a potential therapeutic strategy in TNBC treatment.

As shown above, miRNAs such as miR-128 and miR-223 play complex roles in regulating BC and cholesterol-mediated pathway genes and are involved in cancer drug resistance. However, there is limited knowledge on the roles in which miRNAs regulate cholesterol-mediated drug resistance in BC. It is therefore predicted that miRNAs (particularly miR-128 and miR-223) may act as key regulators in cholesterol-mediated drug resistance in BC cells. Thus, this study proposed to investigate the connection between miRNAs and TAM resistance through regulation of cholesterol content in BC cell line models. A cholesterol depleting agent, AP, was employed to reduce TAM resistance by disrupting miR-128 and miR-223 expression and their target genes in cholesterol-rich BC cells. Consequently, these target genes could be used as biomarkers to monitor TAM resistance in BC cells in response to endocrine treatment. These findings could contribute to a potentially novel miRNA-based treatment strategy for resistant BC, through the reduction of cholesterol accumulation, thereby reducing the global burden of BC mortality.

2. AIMS AND OBJECTIVES

2.1 Aims

- To establish the role of miRNA-128 and miRNA-223 in regulating cholesterol-mediated TAM resistance in BC.
- To understand the dynamics of miRNA regulation across cholesterol, apoptotic, and drug resistance pathways operative in BC cells.
- To identify a set of differentially expressed genes as biomarkers for monitoring drug resistance to TAM.

2.2 Objectives

To fulfil the proposed aims, the following objectives were set:

Aim 1:

- To establish and measure the expression levels of target miRNAs in MCF-7, MDA-MB-231, LTED, and HEK293 cells in response to treatment with TAM, AP, and a TAM + AP combination.
- To inhibit or induce the expression of miR-128 and miR-223 in BC cell lines using an inhibitor or mimic, respectively.
- To study miRNA-mediated effects on cell survival and death in response to compound treatments in the presence or absence of miR-128 and miR-223.

Aim 2:

- To determine the effects of miR-128 and miR-223 knockdown/overexpression on expression levels of genes involved in cancer drug resistance and lipoprotein signalling and cholesterol metabolism pathways in response to compound treatments.

Aim 3:

- To identify differentially expressed genes as biomarkers using RT-qPCR for monitoring BC cells' response to TAM.
- To confirm protein expression of selected differentially expressed genes using western blots.
- To assess the potential of AP as an adjuvant compound to enhance TAM's efficacy.

2.3 Workflow

The plan of work for this study is summarised in the workflow diagram below (Fig. 2.1). The current study was performed on three BC cell lines and one non-cancerous cell line. Cells were transfected using a miRNA inhibitor or mimic to knockdown or overexpress miR-128 and miR-223 in BC cells, respectively and was confirmed using quantitative reverse transcription polymerase chain reaction (RT-qPCR). Thereafter, cell viability assays were performed on non-transfected and transfected cells after single treatments of TAM and AP, and a TAM + AP combination. Subsequently, the cholesterol content in cells were measured using several fluorescent cholesterol stains. Furthermore, RT-qPCR and western blots were performed to determine the expression levels of various genes and proteins involved in cancer drug resistance and lipoprotein signalling pathways in cells after miRNA overexpression/knockdown and combination treatment.

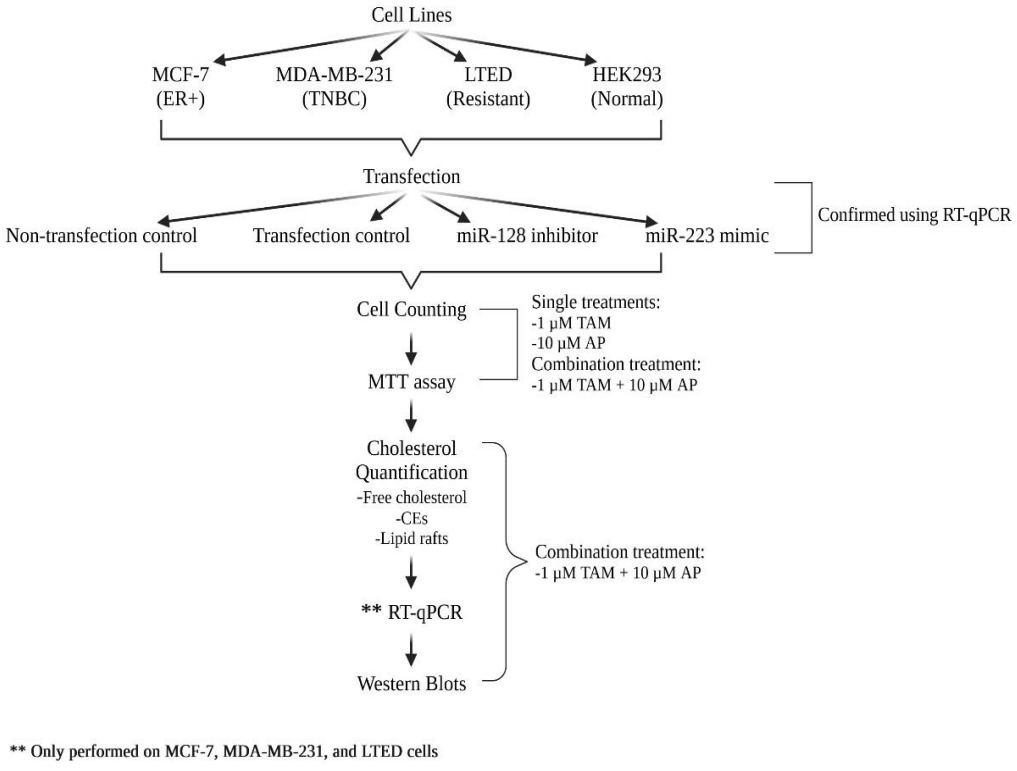

Figure 2.1: Project workflow diagram

3. MATERIALS AND METHODS

The following methods were performed on three cancerous cell lines: Michigan Cancer Foundation-7 (MCF-7), M.D. Anderson-Metastatic-Breast-231 (MDA-MB-231), long-term estrogen deprived MCF-7 (LTED) cells and one non-cancerous cell line: Human Embryonic Kidney 293 (HEK293) cells. Each experiment had three biological and three technical repeats for accurate and reproducible results unless otherwise stated. Compounds included: 1 µM of TAM (Sigma-Aldrich, UK), 10 µM of AP (synthesized as described (Sagar *et al.*, 2014)) and a combination of 1 µM TAM + 10 µM AP. PL (40 µM) (Sigma-Aldrich, UK) and MβCD (1 mM) (Sigma-Aldrich, UK) were used as positive controls. TAM and PL were dissolved in dimethyl sulfoxide (Protea Laboratory Solutions, SA) at < 0.2%. AP and MβCD were dissolved in distilled water (dH_2O). Stock solutions and working solutions were aliquoted and stored at –20 °C in the dark.

3.1 Cell Culture

The MCF-7 cell line was procured from the European Collection of Authenticated Cell Cultures (ECACC, UK). The MDA-MB-231 cell line was originally obtained from the American Type Culture Collection (ATCC, USA). The LTED cell line was derived from the MCF-7 cells. The HEK293 cell line was kindly donated by Professor Stefan Weiss, at the University of the Witwatersrand, South Africa.

All cells were routinely cultured in conditions according to Table 3.1 below, with 10% foetal bovine serum (FBS) or 5% dextran charcoal stripped FBS (DC FBS) (Biowest, UK; Celtic Molecular Diagnostics, SA), and 1% penicillin-streptomycin (P-S) (Gibco: Life Technologies, USA), and maintained at 37 °C in a humidified atmosphere of 95% air and 5% carbon dioxide (CO_2) incubator. Cells were sub-cultured when cell density reached ~70% confluency in the cell culture flask. Experimental procedures were performed on cells with this degree of confluency as cells that are too confluent (> 80%) or are in stationary phase, can cause contact inhibition resulting in morphological and cellular changes, thus results will be misleading. If cells are not confluent enough (< 50%), there will be poor cell growth without cell-to-cell contact. The growth of cells in supplemented medium is vital in order to provide nutrients to allow for cell proliferation and maintain osmolarity and pH of the cell culture micro-environment (Ackermann and Tardito, 2019). The addition of FBS allows for the adherence of cells to the culture flask and contains hormones and growth factors to allow for cell growth and

proliferation (Gstraunthaler *et al.*, 2013). The antibiotic, P-S, is essential in preventing bacterial contamination in cell culture (Ryu *et al.*, 2017).

Table 3.1: Description of cell lines used for the current study

	MCF-7	MDA-MB-231	LTED	HEK293
Full Name	Michigan Cancer Foundation-7	M.D. Anderson-Metastatic - Breast-231	Long-Term Estrogen Deprived MCF-7	Human Embryonic Kidney 293
Receptor expression	ER+ PR+ HER2-	ER- PR- HER2-	ER+ PR+ HER2-	ER- PR- HER2-
Morphology	Epithelial Polygonal	Epithelial Spindle shape	Epithelial Elongated Fibroblast-like	Epithelial Spindle shape
Disease	Adenocarcinoma Breast mammary gland Luminal-like Proliferative	Adenocarcinoma Breast mammary gland Mesenchymal-like Metastatic	Adenocarcinoma Breast mammary gland Luminal-like	Normal Embryonic kidney
Growth mode	Adherent	Adherent	Adherent	Adherent
Media	1 X Dulbecco's Modified Eagle's Medium (DMEM) (Gibco: Life Technologies, UK), 10% FBS, 1% P-S	3:1 DMEM: Ham's F-12 Nutrient Mixture (Gibco: Life Technologies, UK and Biowest, UK), 10% FBS, 1% P-S	Phenol red-free 1 X DMEM (Gibco: Life Technologies, UK), 5% DC FBS (Biowest, UK), 1% P-S	1 X DMEM, 10% FBS, 1% P-S

The LTED cell line was created by culturing cells in specific hormonal-free conditions for a minimum of 180 days to deprive the cells of estrogen (Santen *et al.*, 2005). This was accomplished because DC FBS selectively removes hormones without non-specific loss of other serum components (Sigma-Aldrich, UK).

3.1.1 Development of the LTED cell line

The LTED cell line was derived from the existing MCF-7 cell line in the laboratory. A timeline of LTED cell line development is depicted below representing the dates and phases of

development (Fig. 3.1). LTED cells required growth media free of hormones thus a change of media conditions was implemented from 10% FBS in phenol red 1 X DMEM to 5% DC FBS in phenol red-free 1 X DMEM without sodium pyruvate (LTED media). Cells were grown in this media for 30 days with a slow proliferation rate. After 60 days, cell proliferation started to increase and within 90 days, doubling time was equal to that of MCF-7 cells. Cells were grown in these conditions for 12 months and appeared to be robust.

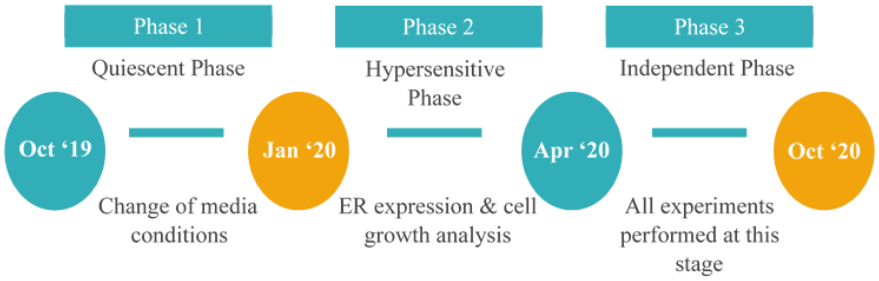

Figure 3.1: A representative timeline of LTED cell line development

3.2 Cell counting

Cell counting was performed by use of a Neubauer haemocytometer to ensure experimental accuracy and reproducibility by seeding the accurate numbers of cells in each well. Prior to cell counting, media was removed and washed once with 1 mL 1 X phosphate buffered saline (PBS) and removed. Thereafter, 2 mL of 1 X trypsin/ethylenediaminetetraacetic acid (EDTA) was added into the culture flask and incubated at 37 °C for the activation of trypsin, to allow cells to be detached from the surface of the culture flask. Trypsin is a serine protease that aids in the dissociation of adherent cells from the culture flask, through breaking down extracellular matrix (ECM) proteins (fibronectins and collagens) that are involved in cell attachment. Although trypsin is the reagent of choice for the detachment of cells, it can reduce cellular viability by damaging the ECM and cell membranes (Kurashina *et al.*, 2019); however, caution was taken to expose cells to trypsin for short periods of time. EDTA is a popular chelating or sequestering agent for divalent ions (Mg^{2+} and Ca^{2+}), which are necessary for integrin-ECM conjugation (Tsuji *et al.*, 2017). Once cells were detached, 2 mL of media was added to 2 mL of 1 X trypsin/EDTA to deactivate the action of trypsin and was placed in a 15 mL centrifuge tube. Following, a 1:1 dilution of Trypan Blue (0.4%) (Gibco: Life Technologies, USA) and the cells was prepared. This was accomplished by adding 100 µL of media containing cells to 100 µL of 0.4% Trypan Blue and mixed thoroughly. Trypan Blue is the most common dye that stains non-viable cells blue because of membrane disruption, leaving viable cells unstained due to the intact cell membrane which excludes the dye (Kwizera *et al.*, 2017). Thereafter, 10 µL

of the mixture was added onto the haemocytometer and cells were counted under a Nikon Phase Contrast Microscope.

Cellular viability was calculated as follows:

$$\%\ Cell\ Viability\ = \frac{no.of\ viable\ cells\ (unstained)}{Total\ no.of\ cells\ counted\ (viable\ and\ non-viable)} \times 100$$

Cellular viability measures the number of viable (live) cells in the culture flask that can be used in further experiments and cell viability above 95% was used for further experiments.

Cells were then seeded as follows:

$$45\ \mu L\ \times total\ no.of\ wells\ = total\ volume\ of\ media\ required\ (\boldsymbol{a})$$

$$5\ \times 10^3\ cells/well \times total\ no.of\ wells\ = total\ no.of\ cells\ required$$

$$\frac{Total\ volume\ in\ flask\ (\mu L) \times total\ no.of\ cells\ required}{Total\ no.of\ cells\ counted\ in\ flask} = volume\ of\ cells\ required\ from\ flask\ (\boldsymbol{b})$$

$$\boldsymbol{a}\ -\boldsymbol{b}\ = volume\ of\ media\ to\ be\ added\ to\ cells$$

45 µL was then pipetted into each well in a 96-well plate with approximately 5×10^3 cells per well.

3.3 Kaplan-Meier survival plots

miR-128 and miR-223 basal expression levels were previously determined (Monchusi and Kaur, 2020), therefore the current study aimed at manipulating the expression of these miRNAs using transfection to observe the effects this had on BC cells. Based on previous analysis in our laboratory, it was predicted that the inhibition of miR-128 expression and the overexpression of miR-223 would attenuate BC cell proliferation by the reduction of intracellular cholesterol accumulation (Monchusi and Kaur, 2020).

Kaplan-Meier survival plots were created using the Kaplan-Meier Plotter [Breast cancer miRNA] analysis tool (https://kmplot.com/analysis/) (Lánczky *et al.*, 2016). The plots represent overall survival in BC patients and were generated in accordance with the presence or absence of ER, PR, and HER2 surface receptors. The miRNAs, hsa-miR-128 and hsa-miR-223 were selected as the miRNAs of interest. In the Luminal A subtype assessing the expression of miR-128, 85 patients were used in the cohort from the GSE40267 dataset. For the plot assessing miR-223 expression in Luminal A patients, 1262 patients were assessed in

the cohort using the METABRIC dataset. For the TNBC plots, 203 patients were assessed using the METABRIC dataset. The findings from the generated plots concluded that miR-128 inhibition and miR-223 overexpression had an overall higher survival rate in BC patients. Therefore, an inhibitor to knockdown miR-128 expression and a mimic to up-regulate miR-223 expression were used for downstream applications.

3.4 Knockdown and overexpression of miRNAs

Transfection is the process of manipulating the expression of a targeted gene by introducing foreign nucleic acids such as plasmid DNA or RNA (small interfering (siRNA) or miRNA) into eukaryotic cells (Rao *et al.*, 2009). In this study, a transient transfection was performed, where cells are typically harvested between 24 and 96 hours (h).

miRNA mimics are small, chemically synthesised dsRNA molecules which mimic mature endogenous miRNA molecules after transfection into cells. Introduction of a miRNA mimic into cells will increase the proportion of RISCs containing that miRNA. miRNA expression changes can be analysed upon transfection with a miRNA mimic, allowing for the detailed study of the gain-of-function effects of target miRNAs on cell function (Thermo Fisher Scientific).

miRNA inhibitors are small, ssRNA molecules that inhibit the expression and function of miRNA molecules (Thermo Fisher Scientific). This enables the down-regulation of miRNA activity to allow for functional analysis. Increased or reduced gene expression after transfection with a miRNA mimic or inhibitor, respectively, provides evidence that the miRNA in question is involved in regulating that specific gene.

A 6-well plate was seeded with 3×10^5 cells per well (as performed according to cell counting above) in a final volume of 2 mL of relevant culturing media with the miScript miRNA mimic (syn-hsa-miR-223-5p) or miScript miRNA inhibitor (anti-hsa-miR-128-3p) (Qiagen, Germany) at a final concentration of 5 nM at 37 °C for 48 h. Previous findings in the laboratory showed similar results were found when cells were treated with 5 nM and 10 nM for 48 and 72 h, therefore this study opted to transfect cells with a concentration of 5 nM of mimic and inhibitor for 48 h. To get a final concentration of 5 nM, 0.5 µL of mimic or inhibitor (20 µM stock) was mixed into 200 µL of serum-free media into a 1.5 mL Eppendorf tube (tube 1). In a separate 1.5 mL Eppendorf tube (tube 2), 1 µL of DharmaFECT™ Transfection Reagent (Dharmacon™, GE Healthcare, UK; Inqaba Biotec™, SA) was gently added and mixed to 200 µL of serum-free media. These tubes were incubated at room temperature (RT) for 5 minutes

(min). This lipid-mediated transfection reagent was used to encapsulate the target miRNA for easy transport of the miRNAs into the cells and nucleus for gain-of-function or loss-of-function effects. This is a highly efficient, rapid, and reliable transfection with low cellular toxicity. A negative control was included to ensure accurate transfection results. The negative control tube contained 1 µL of DharmaFECT™ Transfection Reagent in 200 µL of serum-free media.

Following the 5 min incubation, the contents of tube 1 were gently mixed with the contents in tube 2 for a total volume of 400 µL and incubated at RT for 20 min. Thereafter, 400 µL of the transfection complexes was added dropwise into the appropriate treatment well of interest, with a total volume of 2 mL in each well. Similarly, 200 µL of the negative transfection control complexes was added to the relevant well, with a total volume of 2 mL in the well. To ensure uniform distribution, the 6-well plate was gently swirled and incubated at 37 °C for 48 h.

3.5 RNA extraction

To evaluate miR-128 and miR-223 expression levels post-transfection, total RNA was extracted using the Direct-zol™ RNA MiniPrep kit (Zymo Research, Inqaba Biotec™, SA). Transfected cells were detached using 1 mL of 1 X trypsin/EDTA and deactivated with 1 mL of relevant media as above. Cells were harvested by being transferred into a 2 mL Eppendorf tube and centrifuged at 600 *g* for 8 min in a MiniSpin® centrifuge (Eppendorf, Germany) to pellet cells. The supernatant was discarded, and the pellet was washed twice with 200 µL of 1 X PBS. To each pellet, 100 µL of TRIzol® Reagent (Invitrogen™, Thermo Fisher Scientific, USA) was added to lyse the cells. TRIzol® Reagent is a ready-to-use chemical reagent that lyses cell membranes for the extraction of RNA, DNA and protein from various samples (Simões *et al.*, 2013).

An equal amount of 99.9% RT ethanol was added to the lysed samples and mixed thoroughly to precipitate nucleic acids. Thereafter, samples were transferred into Zymo-Spin™ II CR Columns in collection tubes and centrifuged at 12 100 *g* for 30 seconds (s). The flow-through was discarded and columns were transferred into new collection tubes. The columns were washed with 400 µL of RNA wash buffer and centrifuged as above. A DNase I treatment (5 µL DNase I in 75 µL DNA digestion buffer) was added directly to the column matrix and incubated at RT for 15 min to degrade contaminating DNA in samples. Following treatment, the samples were washed with 400 µL of Direct-zol™ RNA PreWash and centrifuged as above. The flow-through was discarded and this step was repeated. Following, 700 µL of RNA wash buffer was added to the columns and centrifuged for 2 min to ensure complete removal of the

wash buffer. The column was then transferred into an RNase-free tube and RNA was eluted by adding 50 µL of DNase/RNase-free water to the column and centrifuged for 30 s. RNA samples were stored at -80 °C until needed. RNA concentration was quantified using a NanoDrop™ One/One C Microvolume UV-Vis Spectrophotometer (Thermo Fisher Scientific, USA) to quantify (in ng/µL) and observe the quality of RNA. Absorbance readings were taken at wavelengths of 230 nm, 260 nm, and 280 nm to determine the presence of phenol contaminants, nucleic acids, and protein contaminants, respectively. The A_{260}/A_{280} and A_{260}/A_{230} ratios should ideally be greater than 1.8 for pure RNA (Desjardins and Conklin, 2010). Extracted RNA must be of high quality for downstream applications to produce reliable and accurate results. Therefore, samples with A_{260}/A_{280} ratios of 1.9-2 were considered for downstream applications.

3.6 Agarose gel electrophoresis

The integrity of the RNA samples was observed on a 1% agarose gel (0.5 g of agarose powder (BioConcept, Switzerland) in 50 mL of 1 X tris-borate-EDTA (TBE) buffer, with 2.5 µL ethidium bromide (EtBr) (Protea Laboratory Solutions, SA)). A 10 X TBE buffer was prepared according to Table 3.2. The gel was allowed to set for 15 min and RNA samples were normalised by using the following calculation:

$$Volume\ of\ RNA\ sample\ to\ be\ loaded\ (\mu L) = \frac{500\ ng}{Concentration\ of\ RNA\ (\frac{ng}{\mu L})}$$

Table 3.2: Components of 10 X TBE buffer

	Components for 1 L
10 X TBE buffer	1 M Tris base = 108 g 1 M Boric acid = 55 g 0.02 M EDTA = 7.5 g Dissolved in 900 mL of dH_2O Adjusted to pH 8 with hydrochloric acid (HCl) (Honeywell Fluka™, UK) Made up to 1 L with dH_2O (All reagents from Sigma-Aldrich, UK)

Each RNA sample was mixed thoroughly with 2 X RNA loading dye (Thermo Fisher Scientific, USA) prior to being carefully loaded into each well. The loading dye contains the tracking dyes bromophenol blue and xylene cyanol FF (XCFF). Bromophenol blue migrates faster than the human 5S ribosomal RNA (rRNA) band and XCFF migrates slower than the

18S rRNA band. The loading dye also contains the denaturing agent formamide, which stabilises RNA and allows RNA fragments to separate based on size. A RiboRuler High Range RNA Ladder (Thermo Fisher Scientific, USA) was loaded as a positive control on the gel to observe whether unusual results could be attributed to the gel or to the RNA under analysis. The marker was also used to determine the size of any ssRNA bands or smears that appeared. The gel was run for 40 min at 80 volts (V) and imaged on the ChemiDoc XRS+ System (Bio-Rad, USA).

3.7 RT-qPCR

RT-qPCR measures products in real time, during polymerase chain reaction (PCR). It measures fluorescence after each cycle, reflecting the DNA target quantity in each sample (Kralik and Ricchi, 2017). Real time PCR (qPCR) is advantageous as it provides a quick and high-throughput detection and a wide range for quantification of target DNA sequences in different samples.

3.7.1 Polyadenylation

To evaluate miR-128 and miR-223 expression levels post-transfection, a polyadenylation reaction was required. This is because miRNAs are short in length and are difficult to detect with standard qPCR. Polyadenylation is the addition of a poly(A) tail to mRNA and produces mature mRNA for translation. The poly(A) tail consists of several adenosine residues at the 3'-end of the RNA. The 3'-most segment of new pre-mRNA is first cleaved by proteins that then synthesise the poly(A) tail at the 3'-end of the RNA (Proudfoot *et al.,* 2002). To elongate the miRNAs prior to miRNA first strand complementary DNA (cDNA) synthesis, total RNA samples were treated with *Escherichia coli* poly(A) polymerase (PAP) using the miRNA 1st-strand cDNA synthesis kit (Agilent Technologies, USA). This generates a poly(A) tail at the 3'-end of each RNA molecule for miRNAs to be detected. The polyadenylation reactions were prepared according to Table 3.3 below. The following components were added into each 0.2 mL microcentrifuge tube.

All components of each reaction were mixed gently and centrifuged briefly in a microcentrifuge (Starlab, Germany; Celtic Molecular Diagnostics, SA) to collect the contents at the bottom of the tubes. A negative or no template control (NTC) was used where RNase-free water was added instead of RNA to confirm that amplification was due to the RNA samples and not any contaminating species within the reaction tubes. The NTC also monitors primer-dimer formation that could produce false positive results. Reaction tubes were placed in the

T100™ Thermal Cycler (Bio-Rad, USA) to perform PCR at the following cycling conditions: 1 cycle at 37 °C for 30 min and 1 cycle at 95 °C for 5 min to terminate the adenylation reaction. Samples were immediately transferred to ice for immediate use. Alternatively, reactions were stored at -80 °C for long-term storage.

Table 3.3: Components of polyadenylation reaction

Components of reaction	Volume (µL)
5 X poly A polymerase buffer	4
rATP (10 mM)	1
PAP	1
RNA	1 µg
RNase-free water	x
Total volume	**20**

3.7.2 cDNA synthesis

Following polyadenylation, cDNA synthesis was performed using the first strand cDNA synthesis kit (Agilent Technologies, USA). For each polyadenylated reaction, a cDNA synthesis reaction was prepared according to Table 3.4 below. The following components were added into each 0.2 mL microcentrifuge tube.

Table 3.4: Components of cDNA synthesis reaction

Components of reaction	Volume (µL)
10 X AffinityScript RT buffer	2
Polyadenylated sample	8 (~400 ng)
dNTP mix (100 mM)	0.8
RT adaptor primer (10 µM)	1
AffinityScript RT/RNase block enzyme mixture	1
RNase-free water	7.2
Total volume	**20**

All components of each reaction were mixed gently and centrifuged briefly as above. An NTC was used as above, and a no RT control was used to monitor genomic DNA contamination in the target cDNA sample reaction. Reaction tubes were placed in the T100™ Thermal Cycler at the following conditions: 1 cycle at 55 °C for 5 min, 1 cycle at 25 °C for 15 min, 1 cycle at

42 °C for 30 min to allow reverse transcription of first strand cDNA, and 1 cycle at 95 °C for 5 min. Following, 280 µL of RNase-free water was added to each reaction and immediately placed on ice for qPCR. Alternatively, reactions were stored at -20 °C for long-term storage.

3.7.3 SYBR® Green qPCR

Following cDNA synthesis, qPCR was performed on samples using the fluorescent dye, SYBR® Green. A universal reverse primer, an endogenous control primer, and a unique forward primer for miR-128 and miR-223 were used. Once the sequence of the relevant forward primer was determined by Qiagen (Table 3.5), 550 µL of 1 X Tris-EDTA (TE) buffer (prepared according to Table 3.6) was added into the appropriate 10 X miScript Primer Assay (Qiagen, Germany), mixed thoroughly, and stored at -20 °C.

Table 3.5: miRNA primer sequences

Forward primer	Annealing temperature (°C)	Primer sequence (5'-3')
hsa-miR-128-3p	55	UCACAGUGAACCGGUCUCUUU
hsa-miR-223-5p	55	CGUGUAUUUGACAAGCUGAGUU
RNU6	55	CGCAAGGATGACACGCAAAT

Table 3.6: Components of 1 X TE buffer

	Components for 100 mL
1 X TE buffer	10 mM Tris base = 121.14 mg 1 mM EDTA = 37.22 mg 100 mL dH_2O Adjusted to pH 8 with HCl (All reagents from Sigma-Aldrich, UK)

SYBR® Green is an asymmetrical cyanine fluorescent dye that intercalates dsDNA (Zipper *et al.*, 2004). It has an excitation and emission maxima at 497 nm (blue light) and 520 nm (green light), respectively. It is formulated with a hot-start mechanism for increased sensitivity, precision, and accuracy, making this dye ideal for qPCR.

To quantify the desired miRNAs, the following components were set up for each cDNA synthesis reaction according to Table 3.7 below using the miScript SYBR® Green PCR kit

(Qiagen, Germany). The following components were set up in white 0.2 mL 8-tube PCR strips without caps (Starlab, Germany; Celtic Molecular Diagnostics, SA) on ice. RNA, U6 small nuclear 1 (*RNU6*) was used as an endogenous (housekeeping) control to normalise the amount of target miRNA. *RNU6* is a commonly used internal control in miRNA qPCR and is preferred over other genes as it is consistently expressed in several tissues and cell types (Lou *et al*, 2015). *RNU6* expression levels should not be impacted by the various treatments, so it can be utilised to normalise the expression levels of target miRNAs.

Table 3.7: Components of miScript SYBR® Green PCR reaction

Components of reaction	Volume (µL)/reaction (96-well)
2 X QuantiTect SYBR Green PCR Master Mix	12.5
10 X miScript universal primer	2.5
10 X miScript primer assay	2.5
RNase-free water	5.5
Template cDNA	2
Total volume	**25**

Each reaction strip was tightly sealed with optical flat 8-cap strips (Starlab, Germany; Celtic Molecular Diagnostics, SA) and centrifuged briefly as above. Strips were placed in the CFX96 Touch™ Real-Time PCR Detection System (Bio-Rad, USA). Cycling conditions were set up according to Table 3.8 below.

Table 3.8: Cycling conditions

Step	Time	Temperature (°C)
Initial activation step	15 min	95
3 step cycling:		
Denaturation	15 s	94
Annealing	30 s	55
Extension	30 s	70
Cycle number	40 cycles	

A melt curve was added, and the ramp rate was adjusted to 1 °C/s prior to starting the reaction.

Following qPCR, miRNA quantification was calculated using the miScript miRNA PCR Array data analysis tool (Qiagen, Germany). This tool automatically performs quantification using the $2^{-\Delta\Delta Ct}$ method. This method calculates relative quantification and uses *RNU6* to normalise the data.

$$\Delta Ct = Ct\ (target\ miRNA) - Ct\ (endogenous\ control\ RNU6)$$

$$\Delta\Delta Ct = \Delta Ct\ (experimental\ sample) - \Delta Ct\ (normal\ sample)$$

Normalised target miRNA expression in sample (fold change) = $2^{-\Delta\Delta Ct}$

Finally, the $\log_2$ fold change of expression of the sample was calculated as follows:

$$log2(normalised\ target\ miRNA\ expression\ in\ sample)$$

3.8 Cell growth using cell counts (primary screen)

Cell counts were performed 48 h post-transfection to compare the effects of knockdown and overexpression of miRNAs on cell growth. A 6-well plate was seeded with 3×10^5 cells per well in 2 mL of relevant media with mimic or inhibitor and incubated at 37 °C for 48 h (as performed above), with the inclusion of a relevant transfection control containing only transfection reagent. Untreated control wells had equivalent volumes of media to have an accurate representation of comparison. Thereafter, cells were detached using 1 mL of 1 X trypsin/EDTA, deactivated with 1 mL media and counted using a Neubauer haemocytometer as mentioned above. Cell counts were performed three times to ensure accuracy. Relevant graphs and statistical analyses were produced and performed using GraphPad Prism8® indicating BC cell numbers after transfection.

3.9 Cell viability assay (secondary screen)

The viability of BC cells was observed post-transfection and treatment to compare the effects of knockdown and overexpression of miRNAs and drug treatments on cell viability. This was estimated by using a 3-(4,5-Dimethylthiazol-z-yl)-2,5 diphenyltetrazolium bromide (MTT) (Sigma-Aldrich, UK) assay. The MTT assay is a colorimetric assay that measures the reduction of MTT, a yellow tetrazolium salt, by metabolically active (viable) cells resulting in the formation of water-insoluble purple formazan crystals through enzymatic activity of mitochondrial succinate dehydrogenase (van Tonder *et al.*, 2015). The absorbance of the formazan crystals is measured, with the absorbance being directly proportional to cell viability.

A disadvantage of the MTT assay is that it involves interference of various test compounds (van Tonder *et al.*, 2015). It has been reported that the conversion of MTT to formazan crystals could be performed by compounds other than the mitochondrial succinate dehydrogenase enzyme, which would lead to inaccurate readings (van Tonder *et al.*, 2015). However, this assay is a quick and reliable method in determining cell growth inhibition and cell viability.

The *in vitro* cytotoxic effect of knockdown and overexpression of target miRNAs and TAM and AP drug treatments on cell viability was assessed using the MTT assay. Knockdown of miR-128 and overexpression of miR-223 was performed as above for 48 h. Following, 5×10^3 cells/well were seeded into a 96-well plate and maintained at 37 °C for 24 h. Following incubation, 5 µL of sterile 5 mg/mL MTT (Sigma-Aldrich, USA) dissolved in 1 mL 1 X PBS was added to each well. The plate was mixed thoroughly on a MS 3 digital plate shaker (IKA®, Germany) at 500 rpm for 30 s and incubated for 3 h after which the formazan crystals were subsequently dissolved in solubilising solution (10% sodium dodecyl sulfate (SDS) (Sigma-Aldrich, UK) with 10 mM HCl) for at least 16 h. The absorbance of each well was subsequently measured at 570 nm using a Multiskan GO Microplate Reader (Thermo Fisher Scientific, SkanIt™ software). The percentage viability was determined, and relevant graphs and statistical analyses were produced and performed accordingly in GraphPad Prism8®.

Similarly, the effect of 1 µM TAM, 10 µM AP, and 1 µM TAM + 10 µM AP on cell viability was measured. Cells (5×10^3 cells/well) were seeded into a 96-well plate and incubated at 37 °C for 24 h. After incubation, cells were treated with 5 µL of TAM, AP, and a combination of TAM and AP. The plate was mixed on a plate shaker and incubated for 24 h. Following incubation, 5 µL of MTT solution was added to each well and further incubated for 3 h after which the formazan crystals were subsequently dissolved in solubilising solution for at least 16 h. The absorbance of each well was measured, and the percentage viability was determined as above.

Lastly, knockdown of miR-128 and overexpression of miR-223 was performed as above for 48 h. Following this, transfected cells were harvested and seeded into a 96-well plate (5×10^3 cells/well) and incubated at 37 °C for 24 h. After incubation, transfected cells were treated with 5 µL of TAM, AP, and a combination of TAM and AP at concentrations listed above. The plate was mixed thoroughly on a plate shaker and incubated for 24 h. Following incubation, 5 µL of MTT solution was added to each well and incubated for 3 h after which the formazan crystals

were subsequently dissolved in solubilising solution for at least 16 h. The optical density (OD) of each well was subsequently measured, and the percentage viability was determined as above. PL (40 μM) was included as a positive control as it is known to inhibit cell growth, an untreated control (media instead of compound treatment) was included, and a blank control (media only) was also included to consider the background absorption value due to phenol red and serum. These controls were included for all three conditions.

Concentrations of TAM, AP, and PL above were selected as previous findings in our laboratory showed the efficacy of these compounds at inhibiting cell growth and inducing apoptosis at these concentrations (Henriques Palma and Kaur, 2022). Therefore, the combination treatment of TAM and AP was selected for further downstream assays. Cell viability was calculated against the untreated samples, where the untreated control had a cell viability of 100%.

3.10 Cholesterol staining

Cholesterol and lipid raft staining was performed to visualise and confirm the effects of a cholesterol depleting agent (AP) in combination with a cytotoxic therapeutic agent (TAM) on transfected and non-transfected BC cells. This resulted in a qualitative visual representation of fluorescently labelled lipids and lipid rafts in cells. Examining the regulation of lipid rafts is vital in understanding the mechanisms in which cholesterol is depleted from lipid rafts in the cell upon treatment. Lipid raft staining also assists in identifying key membrane proteins that are associated with lipid rafts.

In this study, free cholesterol in the cell was stained blue using a fluorescent probe, filipin III from *Streptomyces filipinensis* (Sigma-Aldrich, UK). Filipin naturally fluoresces and binds to unesterified cholesterol (Maxfield and Wüstner, 2012). Filipin fluorescence is observed with UV excitation at 340-380 nm and emission at 480 nm. Although filipin is widely used to stain lipid molecules for a variety of studies, its disadvantage is that it cannot be used on live cells as its binding to cholesterol disturbs the cell membrane (Maxfield and Wüstner, 2012). Additionally, filipin fluorescent staining photo bleaches rapidly, thus samples must be analysed immediately. Therefore, additional stains were utilised to confirm the reduction of cholesterol post treatments.

CEs or lipid droplets were observed by using the green, fluorescent cholesteryl 4,4-difluoro-5,7-dimethyl-4-bora-3a,4a-diaza-s-indacene-3-dodecanoate (CholEsteryl BODIPY™ FL C_{12}, Thermo Fisher Scientific, USA) dye. This dye is used to track cholesterol transport and

endocytosis of lipoproteins by fluorescence microscopy (Guest *et al.*, 2007). This dye has long-wavelength absorption and fluorescence properties. Fluorescence is observed with excitation typically at 505 nm and emission typically at 515 nm (Maxfield and Wüstner, 2012). BODIPY is suitable for fluorescent lipid probes as it has a low environmental sensitivity (Maxfield and Wüstner, 2012) and higher specificity than other dyes, making this an ideal dye for CE staining.

Finally, lipid rafts were stained red using the Vybrant™ Alexa Fluor™ 594 Lipid Raft Labelling Kit (Invitrogen™, Thermo Fisher Scientific, USA). Lipid rafts are detergent-insoluble plasma membrane microdomains that are rich in cholesterol and glycosphingolipids (GSLs). This study focused on the disruption of lipid rafts via cholesterol depletion by AP therefore, staining lipid rafts was important in observing the effects of treatments on cells. This kit is quick and easy to use, with bright fluorescence of live or fixed cells. Fluorescence is observed with excitation at 590 nm and emission at 617 nm. Cells are labelled with the red-fluorescent Alexa Fluor® 594 conjugate of cholera toxin subunit B (CT-B). An anti-CT-B antibody then crosslinks CT-B labelled lipid rafts on the plasma membrane, which is then visualised by fluorescence microscopy (Janes *et al.*, 1999). The Alexa Fluor® 594 dye is conjugated to an antibody that offers a high fluorescence quantum yield, high photostability and great sensitivity.

In addition to the above lipid stains, nuclei were stained to determine the number and location of cells in each well and the localisation of other stains. Nucleus staining was also performed to observe the shape of the nucleus indicating the state of cells. Nuclei were stained blue with a fluorescent 4',6-diamidino-2-phenylindole (DAPI) (Sigma-Aldrich, UK) nucleic acid stain. This stain binds strongly to adenine–thymine rich regions in the minor groove of dsDNA (Kubista *et al.*, 1987). Fluorescence is observed with UV excitation at 385 nm and emission at 461 nm. Due to filipin's blue fluorescence, DAPI could not be used as a counterstain therefore, NucRed® Dead 647 ReadyProbes® Reagent (Thermo Fisher Scientific, USA) was used. This stain emits bright far-red fluorescence when bound to DNA and is suitable for staining fixed cells only. Fluorescence is observed with excitation at 642 nm and emission at 661 nm. This stain is quick and easy to use as no further dilutions or stocks are required.

Ten thousand transfected and non-transfected cells were seeded onto round coverslips in a 24-well plate in 500 µL of relevant media and incubated at 37 °C for 24 h to allow for the attachment of cells. Following incubation, the cells were treated with the combination treatment of 1 µM TAM and 10 µM AP at 37 °C for 2 h. Control wells had equivalent volumes

of the positive control, 1 mM MβCD. An untreated control and an unstained control were used as references to compare lipid depletion and staining. Following treatment, media was removed from each well and washed gently 3 times with 1 X PBS. Cells were fixed with 200 µL of 4% formaldehyde (Sigma-Aldrich, UK, diluted in 1 X PBS) at RT for 15 min. Cells need to be fixed prior to permeabilization to allow dyes or antibodies to access intracellular structures within the cell. Thereafter, formaldehyde was removed from each well and washed 3 times with 1 X PBS.

3.10.1 Filipin staining

Following the above wash step, free cholesterol was stained blue with 200 µL of 0.05 mg/mL filipin (diluted in 1 X PBS) working solution per well at RT for 2 h in the dark. The filipin solution was removed from each well and washed 3 times with 1 X PBS. Thereafter, 200 µL of 1 X PBS and 1 drop of NucRed® Dead 647 Reagent was added to each well and incubated at RT for 10 min to stain nuclei red. The stain solution was removed from each well and washed 3 times with 1 X PBS. Coverslips were carefully removed from each well and placed face down onto a drop of Fluoromount™ Aqueous Mounting Medium (Sigma-Aldrich, UK) onto microscope slides and allowed to dry. Slides were stored at 4 °C for short-term storage and -20 °C for long-term storage. All images were acquired using the FLoid™ Cell Imaging Station (Thermo Fisher Scientific, USA) using the blue and red filters for filipin (cholesterol) and NucRed® Dead 647 Reagent (nucleic acid) staining, respectively. The fluorescent images were then analysed using the ImageJ1 Software (NIH, USA) (Schneider *et al.,* 2012), by drawing an outline around each cell and measuring area, mean, and integrated density, along with corresponding background readings. The following formula was used to calculate the corrected total cell fluorescence (CTCF): CTCF = integrated density – (area of selected cell × mean fluorescence of background) (Jakic *et al.,* 2017). For each condition, 5 images and 10 cells per image were analysed, from three independent repeats (n=150). Graphs were produced by plotting the mean CTCF and relevant statistical analysis was performed as indicated.

3.10.2 BODIPY staining

Following the wash step after cell fixation, cells were permeabilised with 200 µL of 0.1% Triton X-100 (diluted in 1 X PBS) per well at RT for 15 min. The permeabilization solution was removed from each well and washed 3 times with 1 X PBS. CEs were stained green by adding 200 µL of 1 µg/mL BODIPY (diluted in 1 X PBS) working solution to each well at 37 °C for 30 min in the dark. The BODIPY solution was then removed from each well and washed 3 times with 1 X PBS. Nuclei of cells were stained blue by adding 200 µL of 0.0001 mg/mL

DAPI (diluted in 1 X PBS) working solution to each well for 10 min at RT in the dark. The nucleic acid staining solution was removed from each well and washed 3 times with 1 X PBS. Coverslips were removed and placed onto microscope slides as above. Cells were visualised using the FLoid™ Cell Imaging Station using the green and blue filters for BODIPY (lipid droplets) and DAPI (nucleic acid) staining, respectively. Fluorescent images were analysed as above.

3.10.3 Vybrant™ Alexa Fluor™ 594 lipid raft staining

Following the permeabilization step as above, lipid rafts were stained red by adding 200 µL of 1 µg/mL component A (Alexa Fluor® 594 CT-B conjugate diluted in 1 X PBS) working solution to each well at 37 °C for 30 min in the dark. Subsequently, the fluorescent CT-B conjugate solution was removed from each well and washed 3 times with 1 X PBS. Similarly, 200 µL of component B (0.4 µL of anti-CT-B antibody diluted in 200 µL of 1 X PBS) was then added to each well to crosslink the CT-B-labelled lipid rafts at 37 °C for 30 min in the dark. Cells were washed 3 times with 1 X PBS. Nuclei were stained blue using a DAPI working solution and cells were washed as above. Coverslips were removed and placed onto microscope slides as above. Cells were visualised using the FLoid™ Cell Imaging Station using the red and blue filters for Alexa Fluor® 594 (lipid rafts) and DAPI (nucleic acid) staining, respectively. Fluorescent images were analysed as above.

3.11 Primer optimisation

In the current study, PCR was used to optimise the annealing temperatures of selected primers involved in cancer drug resistance and lipoprotein signalling and cholesterol metabolism (Table S1). Primer sequences were selected using the PrimerBank database (http://pga.mgh.harvard.edu/primerbank/), where genes were inputted using the National Center for Biotechnology Information (NCBI) gene symbol. The length of each primer sequence, PCR amplicon size, melting temperature (T_m) (between 60-63 °C), and GC content (restricted to 35-65%) were validated using the UCSC In-Silico PCR Genome Browser (https://genome.ucsc.edu/index.html), the NCBI Primer-BLAST website (https://www.ncbi.nlm.nih.gov/tools/primer-blast/), and the Integrated DNA Technologies (IDT) OligoAnalyzer™ Tool (https://eu.idtdna.com/pages/tools/oligoanalyzer). Once each primer sequence was validated, sequences were synthesized by IDT (Whitehead Scientific, SA).

3.11.1 cDNA synthesis

Total, intact RNA was extracted as above and was used as a template to synthesise first strand cDNA. The RevertAid First Strand cDNA Synthesis Kit (Thermo Fisher Scientific, USA) was used for downstream PCR and qPCR reactions.

A sample of untreated MCF-7 cells was used to optimise the annealing temperatures of selected primers. The cDNA synthesis reaction was prepared according to Table 3.9 below. The following components were added into each 0.2 mL microcentrifuge tube.

Table 3.9: Components of cDNA synthesis reaction

Components of reaction	Volume (µL)
5X Reaction Buffer 250 mM Tris-HCl (pH 8.3), 250 mM KCl, 20 mM $MgCl_2$, 50 mM DTT	4
RNA	1 µg
10 mM dNTP Mix	2
RevertAid RT (200 U/µL)	1
RiboLock RNase Inhibitor (20 U/µL)	1
Oligo(dT)18 Primer, 100 µM	1
RNase-free water	x
Total volume	**20**

All components of each reaction were mixed gently and centrifuged briefly as above. An NTC was used as above, and a no RT control was used as above. Reaction tubes were placed in the T100™ Thermal Cycler at the following conditions: 1 cycle at 42 °C for 1 h, 1 cycle at 70 °C for 5 min. Following, samples were immediately placed on ice for qPCR. Alternatively, reactions were stored at -20 °C for long-term storage.

3.11.2 PCR

To find the desired annealing temperature for each primer pair, the following PCR reaction components were set up for each cDNA synthesis reaction according to Table 3.10 below using the One*Taq* 2X Master Mix (New England BioLabs Inc; Inqaba Biotec™, SA). The following components were added into each 0.2 mL microcentrifuge tube.

All components of each reaction were mixed gently and centrifuged briefly as above. A NTC and a no RT control was used as above. Glyceraldehyde 3-phosphate dehydrogenase (*GAPDH*) was used as a housekeeping control to ensure cycling conditions were not affected. *GAPDH* is one of the most used housekeeping genes to normalise gene expression data. *GAPDH* is constitutively expressed across samples regardless of treatment. It is necessary to correct for sample differences such as RNA quality, batch to batch variation, and efficiency of reverse transcription (Sikand *et al.,* 2012). Reaction tubes were placed in the T100™ Thermal Cycler and cycling conditions were set up according to Table 3.11 below.

Table 3.10: Components of PCR reaction

Components of reaction	Volume (µL)
OneTaq® 2X Master Mix with Standard Buffer	6.25
Forward primer (10 µM)	0.4
Reverse primer (10 µM)	0.4
RNase-free water	3.45
Template cDNA	2
Total volume	**12.5**

Table 3.11: PCR cycling conditions

Step	Time	Temperature (°C)
Initial activation step (1 cycle)	10 min	95
3 step cycling:		
Denaturation	10 s	95
Annealing	15 s	5 degrees lower than T_m
Extension	20 s	72
Cycle number	40 cycles	
Final extension (1 cycle)	1 min	72

Following PCR, samples were placed on ice immediately to visualise PCR products on an agarose gel. Each sample was mixed thoroughly with 6 X DNA loading dye (Thermo Fisher Scientific, USA) prior to being carefully loaded into each well. A 50 bp DNA ladder (New

England BioLabs Inc; Inqaba Biotec™, SA) was used to determine the amplicon size of PCR products and to detect any non-specific primer-dimers. The gel was run for 40 min at 80 V and imaged on the ChemiDoc XRS+ System. Once the amplicon sizes of PCR products were detected for all selected primers, RT-qPCR was then performed on all samples.

3.11.3 RT-qPCR

To evaluate whether transfection and treatment affected the expression of selected genes involved in cancer drug resistance and lipoprotein signalling and metabolism, the following components were set up for each cDNA synthesis reaction according to Table 3.12 below using the SensiFAST™ Probe No-ROX Kit (Meridian Bioscience®; Celtic Diagnostics, SA). The following components were set up in white 0.2 mL 8-tube PCR strips without caps on ice. GAPDH was used as an endogenous control to normalise the amount of target genes.

Table 3.12: Components of SensiFAST™ Probe No-ROX PCR reaction

Components of reaction	Volume (µL)/reaction (96-well)
2 X SensiFAST Probe No-ROX Mix	5
Forward primer (10 µM)	0.4
Reverse primer (10 µM)	0.4
RNase-free water	2.2
Template cDNA	2
Total volume	**10**

Each reaction strip was tightly sealed with an optical flat 8-cap and centrifuged briefly as above. Strips were placed in the CFX96 Touch™ Real-Time PCR Detection System and cycling conditions were set up as above (Table 3.11). Following RT-qPCR, mRNA quantification of each gene was calculated using the $2^{-\Delta\Delta Ct}$ method of relative quantification as above in an Excel© format and graphs produced accordingly using GraphPad Prism8®.

3.12 SDS-PAGE and western blotting

Western blots were performed to observe the alteration of expression of specific proteins in cell lines once transfected and treated. It was an important step to elucidate whether TAM + AP and miRNA manipulation can play a role in reducing cholesterol accumulation and cancer-related resistance in BC cells.

To harvest cells, transfected and treated cells (1×10^6 cells/well) with relevant controls were detached by using 1 mL 1 X tryspin/EDTA from each well of a 6-well plate as above. Harvested cells were pelleted at 4000 *g* for 5 min using a MiniSpin® centrifuge. The supernatant was removed, and each pellet was re-suspended in 1 X radio-immunoprecipitation assay (RIPA) lysis buffer (prepared according to Table 3.13) (100 µL/10^6 cells) on ice and vortexed thoroughly every 5 min for 30 min. RIPA lysis buffer disrupts or lyses cell membranes thus releasing and solubilizing the internal proteins of the cell that is used for extraction. Following cell lysis, lysates were kept on ice before performing protein quantification. Alternatively, cell lysates were stored at -20 °C for long-term storage. The protein concentrations of each sample were measured using a bicinchoninic acid (BCA) assay.

Table 3.13: RIPA lysis buffer components

	Components for 100 mL
1 X RIPA lysis buffer	50 mM Tris-HCl (pH 7.4) = 1.21 g 300 mM NaCl = 0.876 g 1% Triton X-100 = 1 mL 1% Sodium deoxycholate = 1 g 0.1% SDS (1 mL of 10% SDS) 10 mM EDTA = 1 mL 100 mL dH_2O (All reagents from Sigma-Aldrich, UK)

3.12.1 Protein quantification: BCA assay

In this study, total protein was quantified using the BCA assay. It is a two-step colorimetric technique based on the reduction of copper sulfate Cu^{2+} to cuprous cation Cu^{1+} in the presence of protein in an alkaline environment. In the first step, cuprous cation Cu^{1+} is detected by BCA, forming a light blue complex. In the second step, two BCA molecules react with one reduced Cu^{1+} resulting in the development of a purple colour that is measured at 562 nm using a microplate reader (Smith *et al.*, 1985). Protein quantification is essential to ensure equal loading during sodium dodecyl sulfate polyacrylamide gel electrophoresis (SDS-PAGE). Known protein standards (example shown in Fig. 3.2 below) were used to determine the protein concentration of samples.

Bovine serum albumin (BSA) (Glentham Life Sciences; Inqaba Biotec™, SA) standards were diluted in 1 mL of 1 X RIPA lysis buffer and stored at -20 °C for long-term storage. The BCA working solution was prepared by adding 50 parts of BCA solution (Sigma-Aldrich, UK) to 1 part of Cu^{2+} solution (Sigma-Aldrich, UK) in a 15 mL centrifuge tube in the dark. Following, 25 µL of each standard concentration was added into a 96-well plate in triplicates. For unknown samples, 5 µL of protein lysate was mixed with 20 µL of 1 X RIPA lysis buffer and added into each well in triplicates. Thereafter, 200 µL of the BCA working reagent mix (196 µL of BCA and 4 µL of Cu^{2+}) was added into each well and the plate was mixed thoroughly on a plate shaker for 30 s before being incubated at 37 °C for 30 min in the dark. The absorbance of each well was subsequently measured at 562 nm using a Multiskan GO Microplate Reader (Thermo Fisher Scientific, SkanIt™ software). The protein concentration of each unknown lysate sample was calculated using the standard curve produced in Microsoft Office Excel© with the following calculations.

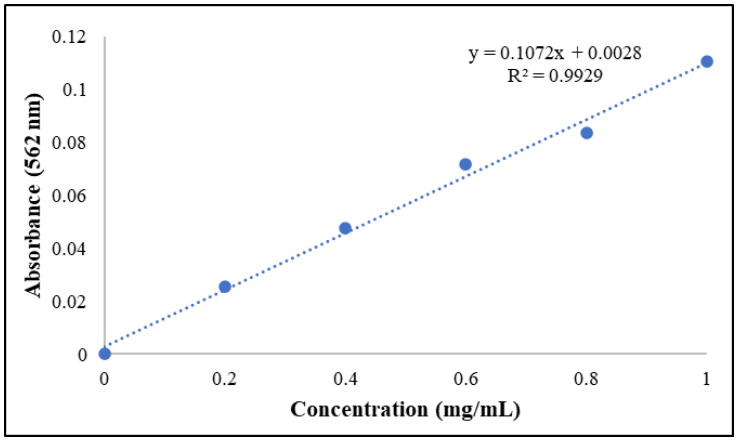

Figure 3.2: A representative BSA protein standard curve

Protein lysate concentrations were calculated as follows:

$$Average\ of\ samples - Average\ of\ blank = (\boldsymbol{a})$$

$$Substituted\ y - value\ with\ (\boldsymbol{a})\ in\ y = mx + c\ formula\ in\ standard\ curve\ above$$

$$\therefore x - value\ \times 5\ (dilution\ factor) = protein\ lysate\ concentration\ (mg/mL)$$

3.12.2 SDS-PAGE

The standard curve above (Fig. 3.2) allowed for the relevant calculations to be made to determine protein concentration in samples, ensuring equal loading before running SDS-PAGE. The polyacrylamide gel was prepared according to Tables 3.14 and 3.15. A 10 %, 1 mm 8-lane comb thickness resolving (separating) gel was used as this gel separates samples containing a broad range of molecular weights (20-250 kDa). Into a 15 mL centrifuge tube, the components of the resolving gel were added and thoroughly mixed before pouring the resolving gel solution into the glass plates of the gel casting mould (Bio-Rad, USA), allowing for sufficient space for the stacking gel. An overlay with 100% isopropanol was added to prevent air bubbles and ensure the gel polymerised with an even surface. The acrylamide was allowed to polymerise for 15 min. Whilst allowing for polymerisation, the components of the stacking gel were added into a separate 15 mL centrifuge tube and mixed thoroughly. The overlay was carefully removed using paper towel and the stacking solution was poured into the gel casting mould on top of the resolving gel. An 8-lane comb was inserted, and the acrylamide was allowed to set for 15 min.

Table 3.14: SDS-PAGE resolving and stacking gel (10 %, 1 mm) components

Components	Resolving gel	Stacking gel
Resolving gel buffer with SDS	3 mL	-
Stacking gel buffer with SDS	-	750 µL
30% Bis-acrylamide (Sigma-Aldrich, UK)	3 mL	500 µL
dH_2O	3 mL	1.75 mL
10% Ammonium persulfate (APS) (Sigma-Aldrich, UK)	100 µL	30 µL
N, N, N′, N′-Tetramethylethylenediamine (TEMED) (Sigma-Aldrich, UK)	10 µL	3 µL

Following polymerisation of the gel, samples were prepared prior to loading. According to the protein concentrations calculated above, relevant amounts of 2 X Laemmli sample buffer (Sigma-Aldrich, UK) were added to each sample lysate (1:1) in a 1.5 mL Eppendorf tube and thoroughly mixed. Laemmli sample buffer contains β-mercaptoethanol, SDS bromophenol blue and glycerol. The sample lysates were heated at 95 °C for 5 min in an AccuBlock™ digital

dry bath (Labnet International, USA) to completely denature the proteins and then placed on ice immediately until further use. The polymerised gel was placed in the Mini-PROTEAN® tetra vertical electrophoresis cell (Bio-Rad, USA) and 1 X running buffer (prepared from 10 X running buffer according to Table 3.16) was poured into the electrophoresis apparatus until the gel was fully submerged. The 8-lane comb was carefully removed, and air bubbles and small pieces of gel were removed with a pipette by flushing the wells.

Table 3.15: SDS-PAGE buffer components

	Components
Resolving gel buffer	36.2 g Tris 0.8 g SDS Dissolved in 150 mL dH_2O Adjusted pH to 8.9 Made up to 200 mL with dH_2O
Stacking gel buffer	5.9 g Tris 0.4 g SDS Dissolved in 70 mL dH_2O Adjusted pH to 6.8 Made up to 100 mL with dH_2O
30% Bis-acrylamide	30 g Acrylamide 0.8 g Bis-acrylamide 0.1 g SDS 100 mL dH_2O
10% APS	100 mg APS in 1 mL dH_2O

Normalised sample (10 mg/mL) and 2 µL of protein molecular weight marker (Precision Plus Protein™ unstained protein standards (Bio-Rad, USA)) was carefully loaded into relevant wells. The apparatus was topped up with 1 X running buffer and plugged into the PowerPac™ basic power supply (Bio-Rad, USA) and ran at 100 V for 90 min. The gel ran until the dye front (bromophenol blue) in the sample buffer reached the bottom of the gel. Following, the gel was carefully removed from the glass plates and prepared for western blotting.

Table 3.16: Running buffer components

	Components for 1 L
10 X running buffer	30.2 g Tris 144 g Glycine 10 g SDS 1 L dH_2O (All reagents from Sigma-Aldrich, UK)
1 X running buffer	100 mL 10 X running buffer 900 mL dH_2O

3.12.3 Western blotting

Western blotting detects the size of a protein of interest and can measure the amount of protein expression in a sample. Following SDS-PAGE, resolved proteins were transferred onto a 0.22 μM polyvinylidene fluoride (PVDF) membrane for 30 min at 25 V using the semi-dry Trans-Blot®Turbo™ Transfer System (Bio-Rad, USA) in 1 X transfer buffer (prepared from 10 X transfer buffer according to Table 3.17). The PVDF membrane was used as opposed to a nitrocellulose membrane as it is a stronger membrane that is generally used for high molecular weight proteins (≥20 kDa) and has a higher adsorption capacity allowing for the detection of lowly expressed proteins and is suitable for re-probing. The PVDF membrane was soaked in 100% methanol for 1 min and then equilibrated in 1 X transfer buffer prior to transfer. This was performed to activate the membrane and allow improved transfer and protein binding. Filter papers and the gel were also soaked and equilibrated in 1 X transfer buffer prior to transfer.

Once transfer was complete, the membrane with transferred proteins was then incubated in a 3 % BSA blocking solution (3 g BSA powder in 100 mL 1 X Tris-buffered saline with Tween-20 (TBST), prepared according to Table 3.18) at RT for 1 h with gentle shaking. Although BSA is a more expensive blocking solution compared to skim milk, it is advantageous to use when the protein of interest is expressed at low levels and when the antibody used has low binding strength. It is also a better alternative to skim milk as there is lower background signal. TBST was used instead of PBST as primary antibodies against phosphorylated forms of proteins were used and this buffer prevented a high background signal and interference with those proteins.

Table 3.17: Transfer buffer components

	Components for 1 L
10 X transfer buffer	38 g Tris 144 g Glycine 1 L dH_2O
1 X transfer buffer	100 mL 10 X transfer buffer 700 mL dH_2O 200 mL methanol (Honeywell Fluka™, UK)

Table 3.18: TBS(T) buffer components

	Components for 1 L
10 X TBS	60.5 g Tris 87.6 g NaCl Dissolved in 700 mL dH_2O Adjusted pH to 7.5 Made up to 1 L with dH_2O
1 X TBST	100 mL 10 X TBS buffer 900 mL dH_2O 1 mL TWEEN® 20 (Sigma-Aldrich, UK)

Following blocking, the membrane was probed with the relevant primary antibody at a 1:2000 dilution (in 10 mL of 3 % BSA blocking solution) against the protein of interest with gentle shaking overnight at 4 °C (Table 3.19). A monoclonal anti-β-Tubulin antibody was used as a loading control. Since this protein is constitutively expressed in cells, the protein expression levels of this protein were used to normalise the results obtained from protein expression levels of all other proteins used in the study. Moreover, this loading control ensured that the primary antibodies used were indeed specific for the targeted proteins (ERα, CETP, ABCG1, PCSK9, SREBP1, SREBP2, HMGCR, and LXRα).

Thereafter, the membrane was washed 5 times with 1 X TBST for 5 min each at RT with gentle agitation. This was performed to wash off any unbound antibodies. Following, the membrane was probed with the relevant HRP-labelled secondary antibody at a 1:5000 dilution (in 10 mL

of 3 % BSA blocking solution with 1 µL of Precision Protein™ StrepTactin-HRP conjugate (Bio-Rad, USA)) incubated at RT for 1 h with gentle agitation in the dark. The addition of the StrepTactin-HRP conjugate was for the chemiluminescent detection of the Precision Plus Protein™ unstained protein standards molecular weight marker. Subsequent 5 min 1 X TBST washes were performed as above. The secondary antibodies were specific to isotypes of the primary antibody (Table 3.20).

Table 3.19: Primary antibodies

Antibody name	Source	Size (kDa)	Vendor
Anti-β-Tubulin	Mouse monoclonal	50	Sigma-Aldrich, UK
Anti-CETP	Mouse monoclonal	60	Abcam, Biocom Africa, SA
Anti-ERα	Mouse monoclonal	66	Novus Biologicals, Whitehead Scientific, SA
Recombinant anti-ABCG1	Rabbit monoclonal	100	Abcam, Biocom Africa, SA
Anti-SREBP1	Rabbit polyclonal	125 and 68	Novus Biologicals, Whitehead Scientific, SA
Anti-SREBP2	Rabbit polyclonal	125, 68, and 58	Novus Biologicals, Whitehead Scientific, SA
Anti-PCSK9	Goat polyclonal	60	Novus Biologicals, Whitehead Scientific, SA
Anti-HMGCR	Rabbit monoclonal	100	Novus Biologicals, Whitehead Scientific, SA
Anti-LXRα	Rabbit polyclonal	55	Novus Biologicals, Whitehead Scientific, SA

Chemiluminescence was performed by adding Clarity™ Western ECL Substrates (Bio-Rad, USA) to the membrane. This substrate is compatible with HRP conjugates and is highly sensitive for detecting proteins bound to membranes. It yields high signals with a low background and long signal duration. The membrane was incubated in equal volumes of Peroxidase solution and Luminol/enhancer solution for 2 min in the dark before viewing on the ChemiDoc XRS+ System (Bio-Rad, USA).

Table 3.20: Secondary antibodies

Antibody name	Source	Vendor
Anti-mouse IgG (H+L)-HRP conjugate	Goat	Bio-Rad, USA
Anti-rabbit IgG (H+L)-HRP conjugate	Goat	Bio-Rad, USA
Anti-goat IgG-HRP conjugate	Mouse	Sigma-Aldrich, UK

3.13 Statistical analyses

Mean and standard deviation (S.D) calculations were performed using Microsoft Office Excel© and/or GraphPad Prism version 8 Software (California, USA) from at least three independent experiments, each performed in triplicates for reproducibility. The statistical significance of differences between control and treated sample cells (between two groups) were calculated using a two-tailed student's *t*-test. This test was used as it tests for a change (increase or decrease) in the variable and determines if there is any difference between groups (untreated vs. treated). A two-way analysis of variance (ANOVA) followed by the Bonferroni *post-hoc* test was also used to analyse the statistical differences between the means of two or more groups. It examines the influence of two different categorical independent variables (treatment and transfection) on one continuous dependent variable (fluorescence). ANOVA determines if the means of these groups are significantly different from one another and is useful in analysing the data of several treatment groups. A p-value of less than 0.05 (*) was the standard estimation of measuring significance of the observations. A Z-factor was calculated for each assay performed in 96-well plates, indicating good to excellent robustness (Zhang *et al.*, 1999). A Z-factor above > 0.6 was considered the acceptable range in which the technicality of the experiments was trustworthy.

Percentage increase/decrease was calculated according to the formulae below:

$$\%\ Increase = \frac{(B - A)}{A} \times 100$$

$$\%\ Decrease = \frac{(A - B)}{A} \times 100$$

$$Where\ A = Initial\ value\ and\ B = Final\ value$$

4. RESULTS

4.1 Patient survival outcomes based on miRNA expression

Kaplan-Meier survival plots were generated to confirm patient survival outcomes depending on the relevant miRNA expression. The survival plots shown below (Fig. 4.1), indicate higher overall survival in BC patients over time when miR-128 expression was down-regulated and when miR-223 expression was up-regulated. In BC patients with the Luminal A subtype exhibiting high miR-128 expression, the probability of overall survival at 150 months dropped to 10% as compared to 30% for BC patients exhibiting low miR-128 expression (logrank p-value = 0.13). These patients with low miR-128 expression were anticipated to survive up to 61 months as compared to 46 months (Fig. 4.1a). Patients with the same subtype exhibiting low miR-223 expression had an overall survival probability of 55% as compared to 65% for patients exhibiting high miR-223 expression (logrank p-value = 0.00057). Patients with high miR-223 expression were anticipated to survive up to 203 months as compared to 179 months (Fig. 4.1b). In basal-like patients (TNBC subtype) exhibiting low miR-128 expression, there was a 13% increase in overall survival at 150 months compared to patients with high miR-128 expression (logrank p-value = 0.12). Additionally, these patients were expected to survive for more than 20 months longer than patients with higher miR-128 expression (Fig. 4.1c). Similarly, patients with the TNBC subtype exhibiting higher miR-223 expression had a 20% increase in overall survival compared to those with lower miR-223 expression at 150 months (logrank p-value = 0.0054). Patients were expected to survive for more than 60 months when there was a high miR-223 expression (Fig. 4.1d).

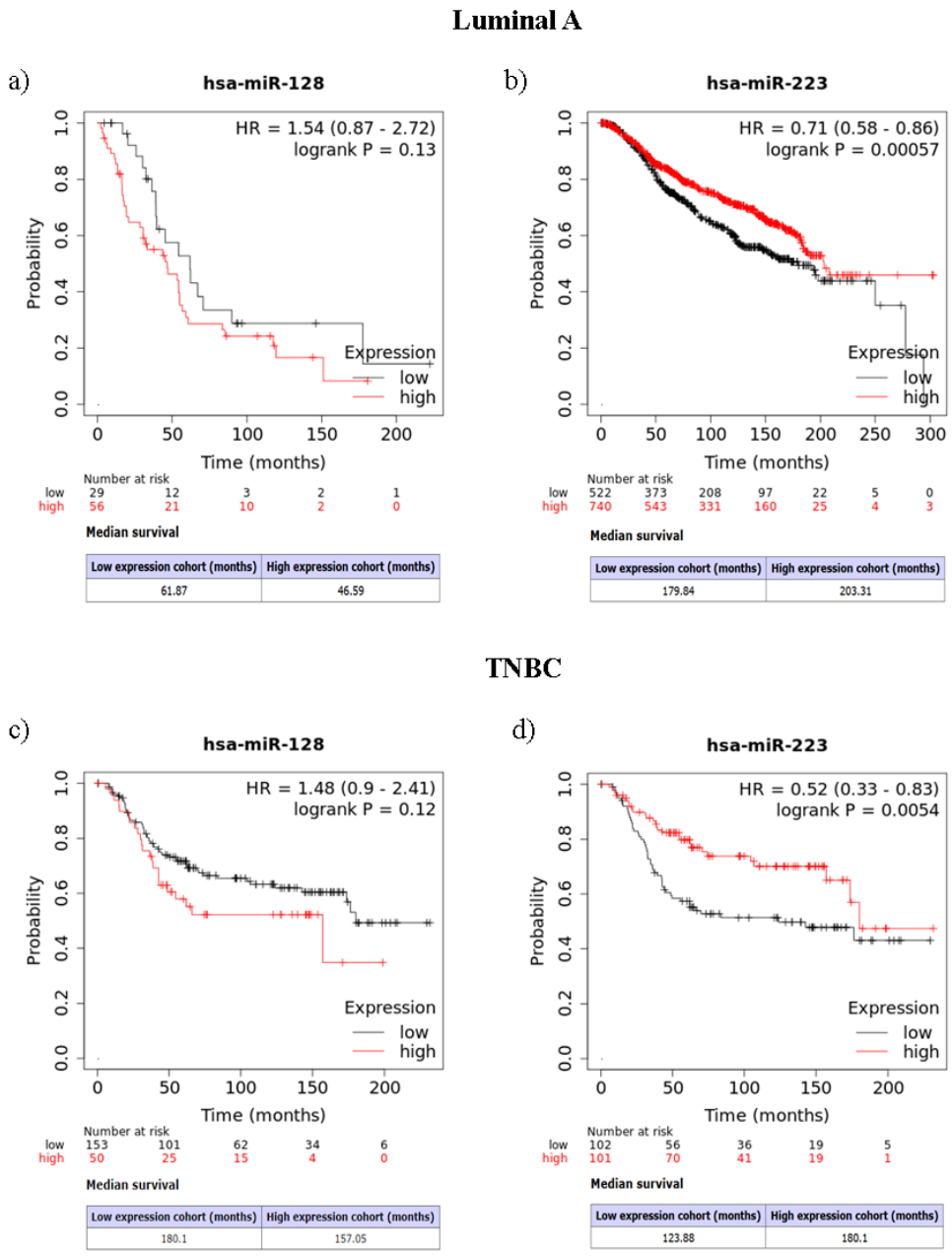

Figure 4.1: The effects of miR-128 and miR-223 expression on BC patient survival

Kaplan-Meier survival plots were generated using the Kaplan-Meier Plotter [Breast cancer miRNA] analysis tool (https://kmplot.com/analysis/) (Lánczky et al., 2016). Luminal A and TNBC subtypes were selected, and the plots represent the probability of overall survival over time with red lines representing high miRNA expression and black lines representing low miRNA expression. An overall increase in patient survival was observed when miR-128 ***(a)*** *had a low expression and when miR-223* ***(b)*** *had a high expression in the Luminal A subtype. Similarly, an overall increase in patient survival was observed when miR-128 was lowly expressed* ***(c)*** *and when miR-223 was highly expressed* ***(d)*** *in the TNBC subtype. The overall*

*logrank p-value for miR-128 was 0.13 and 0.00057 for miR-223 for the Luminal A subtype and 0.12 and 0.0054 for TNBC, respectively. The logrank p-value indicates if survival distribution between two groups occurring at any given time is significant, where * P < 0.05, ** P < 0.01, *** P < 0.001. The hazard ratio (HR) indicates the relative odds of patients' probability of survival up to a certain time interval. The number of patients at risk for each group at each time point is shown below the plots.*

4.2 Alteration of miRNA expression using an inhibitor or mimic

Following the confirmation that a reduction in miR-128 expression and an increase in miR-223 expression had higher overall survival in BC patients, the alteration of the expression of these miRNAs was performed. An inhibitor was used to knockdown the expression of miR-128 and a mimic was used to overexpress miR-223 via transient transfection in BC cell lines.

Cells were transfected with the relevant inhibitor or mimic with a transfection control as indicated above, and miRNA expression levels were observed using RT-qPCR. The integrity of each RNA sample was examined (Fig. S1) prior to RT-qPCR to confirm that RNA was intact. Analysis by RT-qPCR indicated that upon transfection with an inhibitor, there was a significant down-regulation of miR-128 expression in MCF-7 and LTED cells compared to the non-transfection control (Fig. 4.2). Similarly, upon transfection with a mimic, miR-223 expression was significantly up-regulated in all cell lines when compared to the non-transfection control. MCF-7 cells had a log2 fold change of -1.7 in miR-128 expression and a log2 fold change of 3 in miR-223 expression (Fig. 4.2a). Similarly, in MDA-MB-231 cells there was a log2 fold change of -2.13 and 8.52 in miR-128 and miR-223 expression, respectively (Fig. 4.2b). In resistant LTED cells, there was a log2 fold change of -0.81 and 18.5 in miR-128 and miR-223 expression, respectively (Fig. 4.2c). In the HEK293 cell line, there was a log2 fold change of -3.12 in miR-128 expression and a log2 fold change of 15.39 in miR-223 expression (Fig. 4.2d).

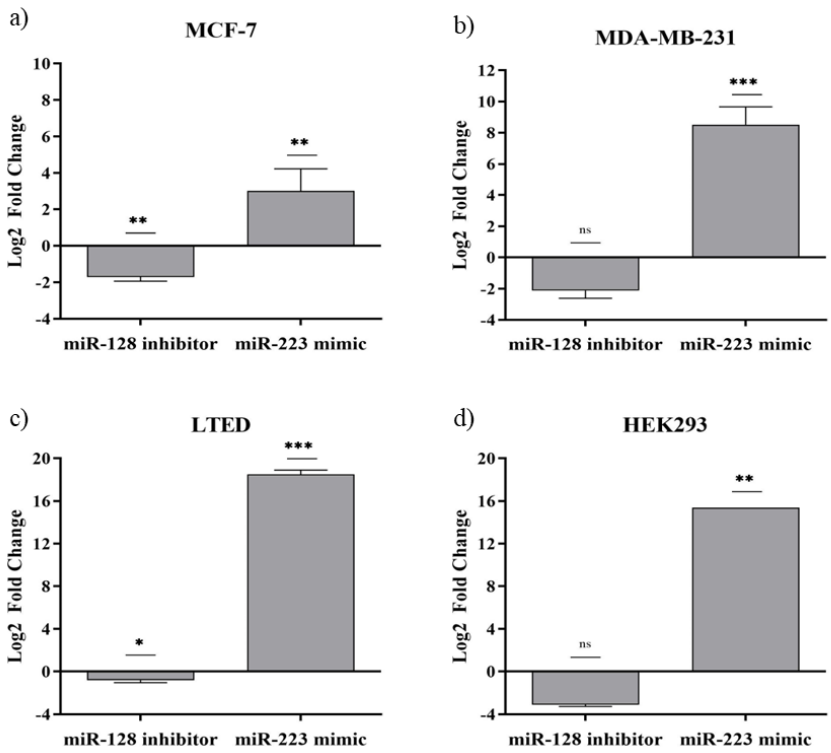

Figure 4.2: Changes in miRNA expression upon transfection with a miR-128 inhibitor and a miR-223 mimic

RT-qPCR analysis of miR-128 and miR-223 expression in MCF-7 ***(a)****, MDA-MB-231* ***(b)****, LTED* ***(c)****, and HEK293* ***(d)*** *cells relative to the non-transfection control. Cells were transiently transfected with 5 nM of a hsa-miR-128-3p inhibitor or a hsa-miR-223-5p mimic. Relative expression is presented as log2 fold change. The expression of RNU6 was used to normalise the data. Statistical analysis was calculated using a two-tailed student's t-test, where * P < 0.05, ** P < 0.01, *** P < 0.001, and ns = non-significant compared to non-transfection control. Data represents the mean ± S.D; (n=3).*

4.3 Cell viability in BC cells with altered miRNA expression

4.3.1 Cell counting

Following the confirmation that the use of an inhibitor down-regulated miR-128 expression and a mimic up-regulated miR-223 expression, cell numbers of transfected cells were observed. Cells were transfected as previously described and were counted after 48 h. Cell counting determined whether altering the expression of these miRNAs affected the ability of BC cells to proliferate. It was pertinent to determine whether the alteration of miRNA expression only affected BC cells whilst having little to no effect in HEK293 cells, indicating the specific roles that miR-128 and miR-223 play in BC alone.

Cell counts demonstrated a significant reduction in BC cell numbers with a slight reduction in HEK293 cells (Fig. 4.3), relative to the non-transfection control. In MCF-7 cells, the down-regulation of miR-128 expression led to a 17.45% reduction in cell numbers compared to the non-transfection control. Similarly, the up-regulation of miR-223 expression led to a 18.99% reduction in cell numbers (Fig. 4.3a). In aggressive MDA-MB-231 cells, the down-regulation of miR-128 and the up-regulation of miR-223 led to an 18.25% and 20.49% reduction in cell numbers, respectively (Fig. 4.3b). The reduction of cell numbers was most prominent in TNBC cells, indicating that these miRNAs play more complex and vital roles in the aggressive TNBC subtype than in the Luminal A, hormone-dependent subtype. There was no significant reduction in cell numbers in resistant LTED and HEK293 cells when miR-128 was down-regulated and when miR-223 was up-regulated (Figs. 4.3c and d); however, the same trend in cell number reduction was observed as in MCF-7 and MDA-MB-231 cells. A significant reduction in cell numbers was observed in the transfection control in MCF-7 and MDA-MB-231 cells. However, upon miRNA transfection, there was a more prominent reduction in cell numbers compared to the transfection control, indicating the little effect the transfection control had on cell growth.

4.3.2 MTT assay

Following the primary screen of cell counting to determine cell numbers post-transfection, a secondary screen was performed to observe the viability of these cells using an MTT assay. In this secondary screen, non-transfected (control) cells and transfected cells were treated with a single treatment of 1 μM TAM, a single treatment of 10 μM AP, and a combination of the two (1 μM TAM + 10 μM AP).

In non-transfected MCF-7 cells (Fig. 4.4a), cell viability post TAM treatment was 72.35%, 53.28% post AP treatment, and 44.84% post combination treatment (TAM + AP). In MCF-7 cells, when miR-128 expression was down-regulated, cell viability was significantly reduced when cells were treated with TAM alone (cell viability of 46.86%), relative to the untreated control. When cells were treated with the combination, cell viability was 34.79%, indicating another significant reduction in cell viability. Similarly, when miR-223 was overexpressed in these cells, viability was reduced when cells were treated with TAM alone (cell viability of 55.33%), with AP alone (viability of 49.6%), and with the combination (viability of 41.26%).

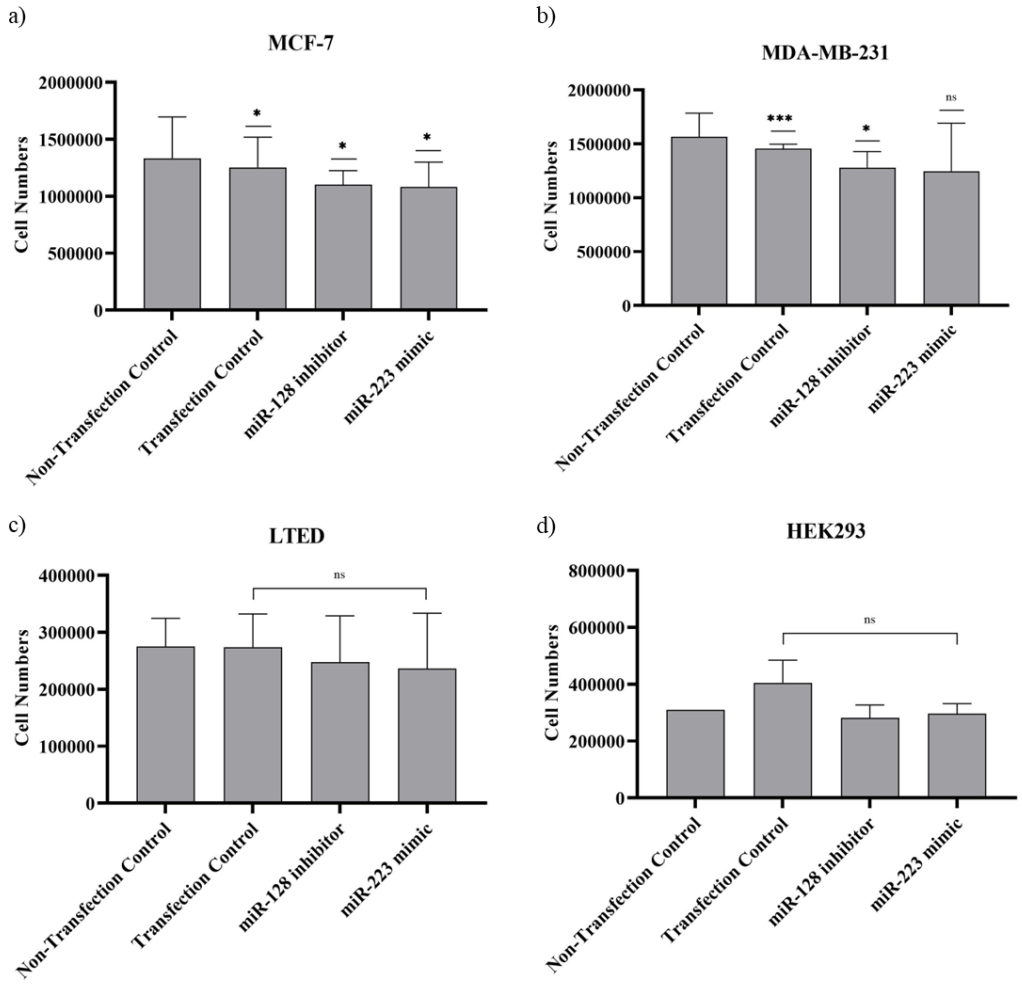

Figure 4.3: Cell numbers upon transfection with a miR-128 inhibitor and a miR-223 mimic

Graphs indicating cell numbers per well in MCF-7 ***(a)****, MDA-MB-231* ***(b)****, LTED* ***(c)****, and HEK293* ***(d)*** *cells after a 48 h transfection with a miR-128 inhibitor or a miR-223 mimic. Cell numbers were analysed using the trypan blue cell counting method in a Neubauer haemocytometer in triplicates after a 48 h transfection where 300 000 cells were originally plated per well in a 6-well plate. A transfection control (empty liposome) was also included. Data represents the mean ± S.D; (n=3). A two-tailed student's t-test was used for statistical analysis, where * P < 0.05, ** P < 0.01, *** P < 0.001, and ns = non-significant indicates a significant or non-significant difference compared to the non-transfection control.*

Non-transfected MDA-MB-231 cells had similar results to that of MCF-7 cells. When treated with TAM alone, cell viability was 74.11%, AP alone yielded 52.65% cell viability, and the combination had a cell viability of 48.34% (Fig. 4.4b). A significant reduction in cell viability was observed in cells with down-regulated miR-128 expression. When these cells were treated with TAM alone, viability was 41.83% in comparison to the untreated control. When these cells were treated with AP alone, cell viability was 37.38%, and when treated with the combination, cell viability was further reduced to 25.25%. When miR-223 expression was up-regulated, cells treated with TAM alone showed an increase in cell viability (viability of 88%). This demonstrates that the up-regulation of miR-223 expression does not increase TAM's efficacy in reducing cellular viability as effectively as miR-128 down-regulation. The viability of these cells was 44.1% when treated with AP alone, and 38.59% when treated with the combination.

In resistant LTED cells, non-transfection control cells did not respond well to single or combination treatments, due to their highly resistant nature. In non-transfected LTED cells, viability did not go below 70% irrespective of treatments (Fig. 4.4c). Although not as prominent as in the previous cell lines, there was a slight reduction in cell viability when non-transfected LTED cells were treated with the combination treatment. When miR-128 expression was down-regulated and when these cells were treated with TAM alone, cell viability was 99.48%, indicating an increase in viability compared to the non-transfection control. When cells were treated with AP alone, viability was 82.73%, and when cells were treated with the combination, viability was 69.59%. When miR-223 was overexpressed and when cells were treated with TAM alone, cell viability was 95.33%, AP alone reduced viability to 81.82%, and the combination further reduced viability to 72.72%.

The HEK293 cell line was used as a control to demonstrate the differences in cell viability when miRNA expression was altered and when cells were treated with endocrine therapies relative to BC cells. This was performed to indicate the selectivity of these compounds and miRNAs to BC cells whilst have little effect in HEK293 cells. Cell viability in HEK293 cells was above 100% in all conditions regardless of treatment and miRNA expression (Fig. 4.4d), indicating that this treatment did not affect HEK293 cell viability, as calculations were performed against the untreated control that had a set viability of 100%.

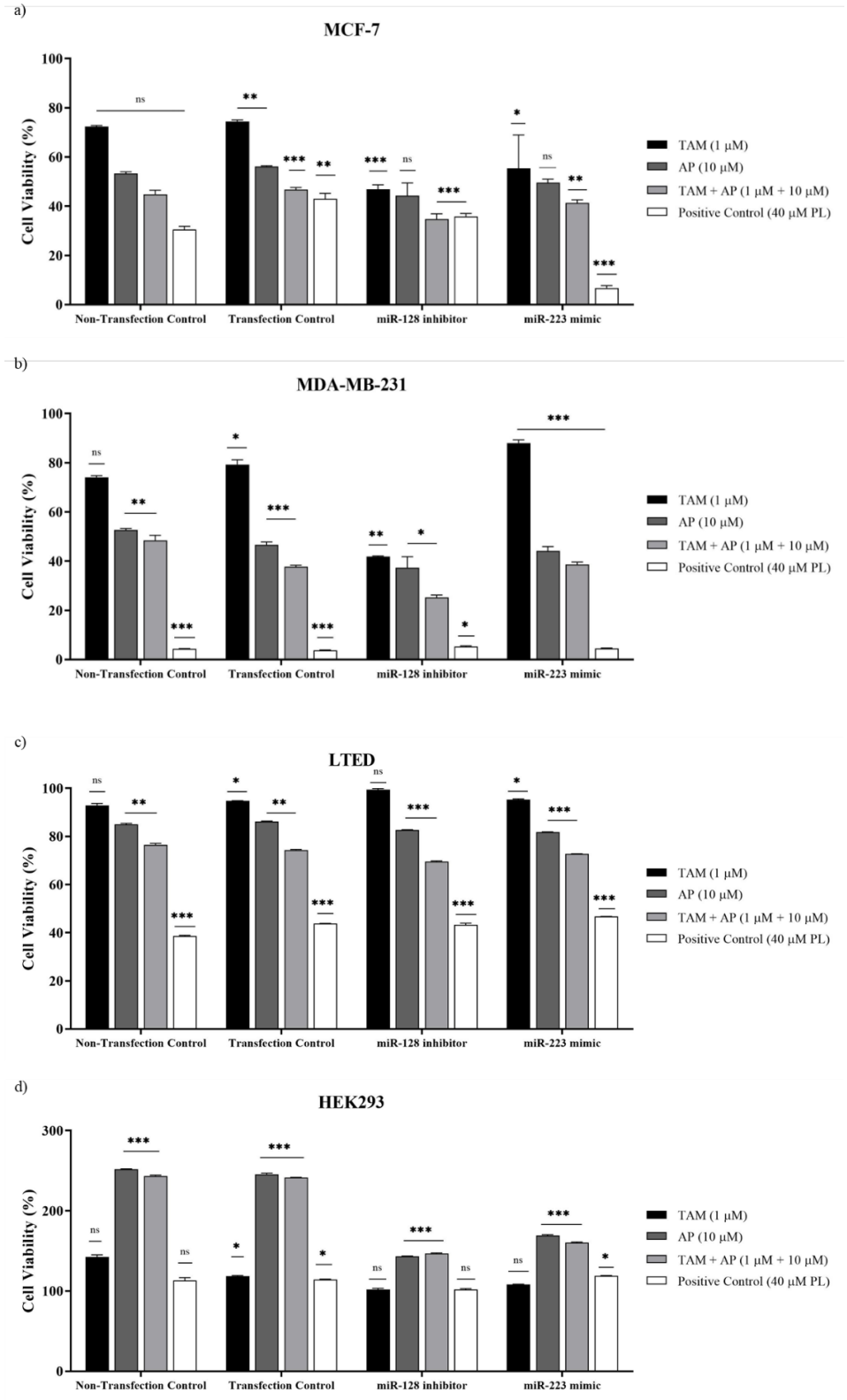

Figure 4.4: Cell viability post miRNA transfection and combination treatment

Graphs indicating percentage cell viability in MCF-7 ***(a)****, MDA-MB-231* ***(b)****, LTED* ***(c)****, and HEK293* ***(d)*** *cell lines at concentrations of 1 μM TAM (black bar), 10 μM AP (dark grey bar), and 1 μM TAM + 10 μM AP (light grey bar) after 24 h treatment at selected conditions. Cells*

*were transfected for 48 h with an inhibitor to down-regulate miR-128 expression or a mimic to up-regulate miR-223 expression prior to treatments. A positive control (PL at 40 µM, white bar) was used for all conditions. Cell viability was assessed using an MTT assay relative to the untreated control (100% viability). Data are mean ± S.D; (n=3) from raw data. Statistical analysis was calculated using a two-tailed student's t-test, where * P < 0.05, ** P < 0.01, *** P < 0.001, and ns = non-significant indicates a significant or non-significant difference to the untreated control. Z-factor was > 0.6 for each 96-well plate.*

4.4 Cholesterol levels in BC cells with altered miRNA expression

To measure the changes in cholesterol levels in BC cells, several cholesterol stains were used. These stains targeted free intracellular cholesterol, CEs (lipid droplets), and lipid rafts located in the cellular membrane.

4.4.1 Free cholesterol

Free intracellular cholesterol (unesterified cholesterol) was stained blue with the fluorescent probe, filipin. Free cholesterol is an important component of lipid rafts and is converted into CEs. Therefore, an overall reduction of free cholesterol could lower lipid raft and CE accumulation, thereby possibly lowering cell survival, proliferation, viability, and aggression. When miR-128 expression was down-regulated and when miR-223 expression was up-regulated in MCF-7 cells, there was a 77% reduction in free cholesterol compared to the non-transfection control (Fig. 4.5a). There was no significant change in free cholesterol when transfected cells were treated with TAM + AP, compared to the corresponding untreated controls.

A reduction in free cholesterol was observed in MDA-MB-231 cells upon down-regulation of miR-128 expression (Fig. 4.5b). When cells had lowered miR-128 expression, free cholesterol was reduced by 40% in comparison to the non-transfection control, whereas when miR-223 expression was up-regulated, free cholesterol increased. There was no significant difference in free cholesterol when transfected cells were treated with TAM + AP, compared to the corresponding untreated controls.

A reduction in free cholesterol was not observed in LTED cells (Fig. 4.5c). When miR-128 expression was down-regulated, and when miR-223 expression was up-regulated, free cholesterol was increased in comparison to the non-transfection control. Indicating that the alteration of these target miRNAs is not effective at reducing free cholesterol in resistant BC cells.

Interestingly, the HEK293 cell line showed a reduction in free cholesterol post-transfection and treatment (Fig. 4.5d). When cells had lowered miR-128 expression, free cholesterol was reduced by 40% in comparison to the non-transfection control, and when miR-223 expression was up-regulated, free cholesterol increased. However, when miR-223 expression was up-regulated and when cells were treated with TAM + AP, a significant reduction of free cholesterol was observed compared to the corresponding untreated control. Similarly, cells with lowered miR-128 expression and treated with TAM + AP led to a significant reduction in free cholesterol in these cells. Although there was a reduction in free cholesterol found in HEK293 cells, cell viability was not affected (Fig. 4.4d), indicating that this transfection and treatment does not affect HEK293 cell viability.

4.4.2 Cholesteryl esters

An increase in lipid droplets in the form of CE accumulation has been implicated in cancer drug resistance. A reduction in this accumulation lowers cell proliferation and aggression through the reduction of cholesterol-mediated drug resistance. CEs in the form of lipid droplets were stained green with a fluorescent BODIPY probe. When MCF-7 cells had a down-regulation of miR-128 expression and an up-regulation of miR-223, there was more than a 70% reduction in CEs in comparison to the non-transfection control (Fig. 4.6a). When non-transfected MCF-7 cells were treated with TAM + AP, there was a 78% reduction in CEs compared to the untreated control. When transfected MCF-7 cells were treated with TAM and AP, there was no significant change in CEs; however, a trend towards a reduction in CEs was observed.

When MDA-MB-231 cells had a down-regulation of miR-128 expression, there was a 69% reduction in CEs, and when miR-223 expression was up-regulated, there was a 75% reduction in CEs, compared to the non-transfection control (Fig. 4.6b). When non-transfected MDA-MB-231 cells were treated with the combination treatment of TAM and AP, there was a 58% reduction in CEs compared to the untreated control. When transfected cells were treated with TAM and AP, there was no significant change in CEs; however, a trend towards a reduction in CEs was observed, as with MCF-7 cells.

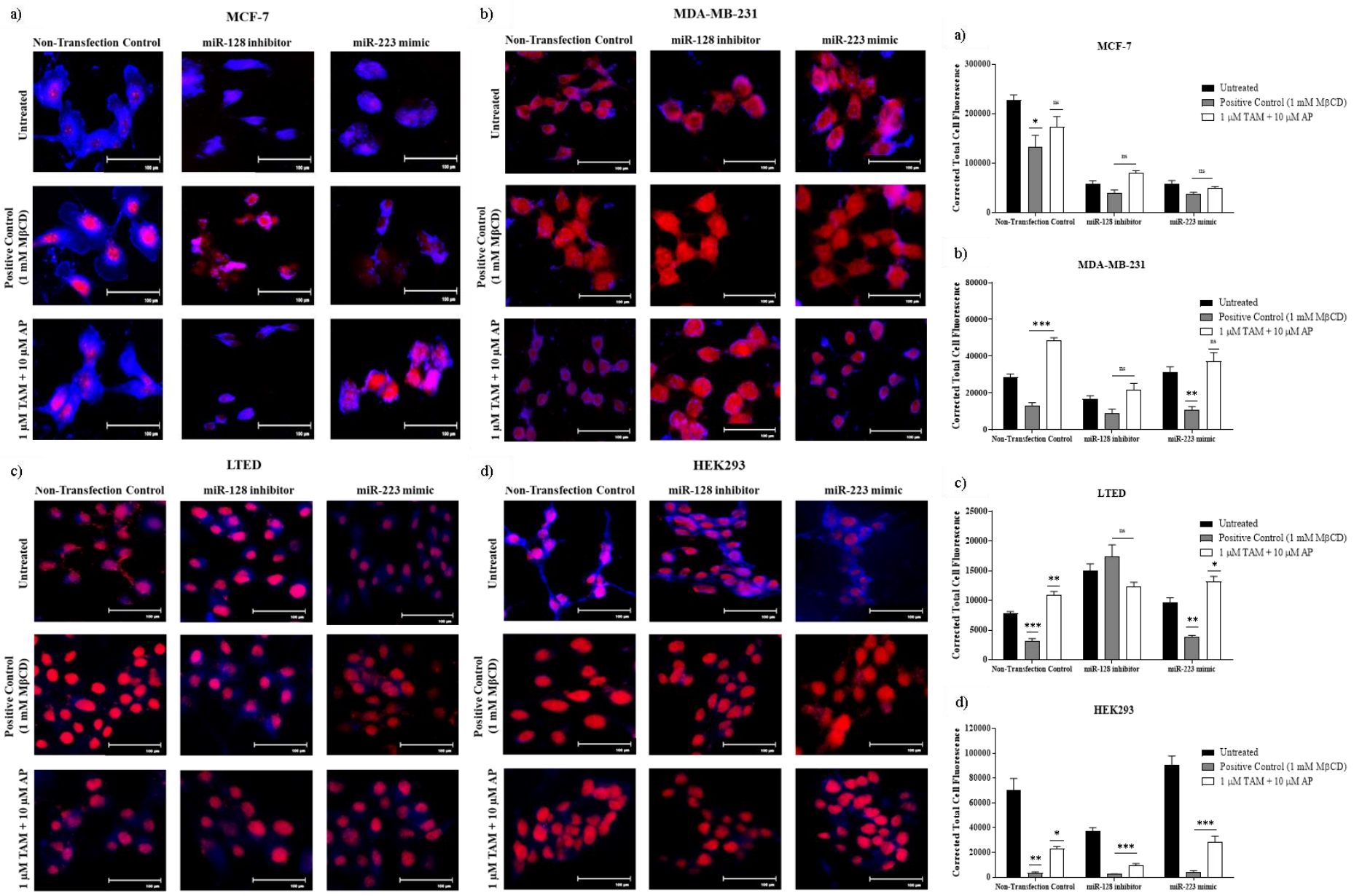
a)
MCF-7
Non-Transfection Control
miR-128 inhibitor
miR-223 mimic
Untreated
Positive Control (1 mM MβCD)
1 μM TAM + 10 μM AP
b)
MDA-MB-231
c)
LTED
d)
HEK293
Corrected Total Cell Fluorescence
Untreated
Positive Control (1 mM MβCD)
1 μM TAM + 10 μM AP
ns

Figure 4.5: Changes in free cholesterol florescence upon miRNA transfection and combination treatment

Representative images from non-transfected MCF-7 ***(a),*** *MDA-MB-231* ***(b),*** *LTED* ***(c),*** *and HEK293* ***(d)*** *cells, cells transfected with a miR-128-3p inhibitor, and a miR-223-5p mimic upon TAM + AP treatment, with a positive control. Cells were transfected with relevant mimic or inhibitor for 48 h prior to treatment with TAM + AP or MβCD for 2 h before filipin staining. Free cholesterol is shown in blue, and nuclei are shown in red. Images were taken using the EVOS FLoid™ Cell Imaging Station for quantification. The scale bars indicate 100 µm. Images are representative of three separate experiments. Corresponding bar graphs depicting mean values of the CTCF in transfected cells relative to the non-transfection control, from three independent repeats. The ImageJ1 software was used for fluorescence quantification. Data are mean ± S.D; (n=150) from raw data, where n is the total number of cells quantified per condition. The data was analysed by a two-way ANOVA followed by a Bonferroni post-hoc test to compare individual differences, where * P < 0.05, ** P < 0.01, *** P < 0.001, and ns = non-significant indicates a significant or non-significant difference to the untreated control.*

Non-transfected LTED cells had similar CE levels to that of non-transfected MCF-7 cells. When LTED cells had a down-regulation of miR-128 expression, there was a 23% reduction in CEs compared to the non-transfection control (Fig. 4.6c). When miR-223 expression was up-regulated, there was a 55% reduction in CEs in these cells. When non-transfected LTED cells were treated with TAM + AP, there was a 43% reduction in CEs compared to the untreated control. When transfected LTED cells were treated with TAM + AP, there was no significant change in CEs, relative to corresponding untreated controls.

Non-transfected HEK293 cells had higher CE levels than BC cells. There was no reduction in CEs when these cells had a down-regulation of miR-128 expression, and a slight reduction when miR-223 was up-regulated (Fig. 4.6d). When transfected cells were treated with TAM + AP, there was a significant reduction in CEs (68% reduction) compared to respective untreated controls. However, the most prominent reduction in CEs was observed when non-transfected cells were treated with TAM + AP (75% reduction). Overall, the most prominent reduction in CE fluorescence was observed in both MCF-7 and MDA-MD-231 cells, upon manipulation of miRNA expression together with TAM + AP treatment.

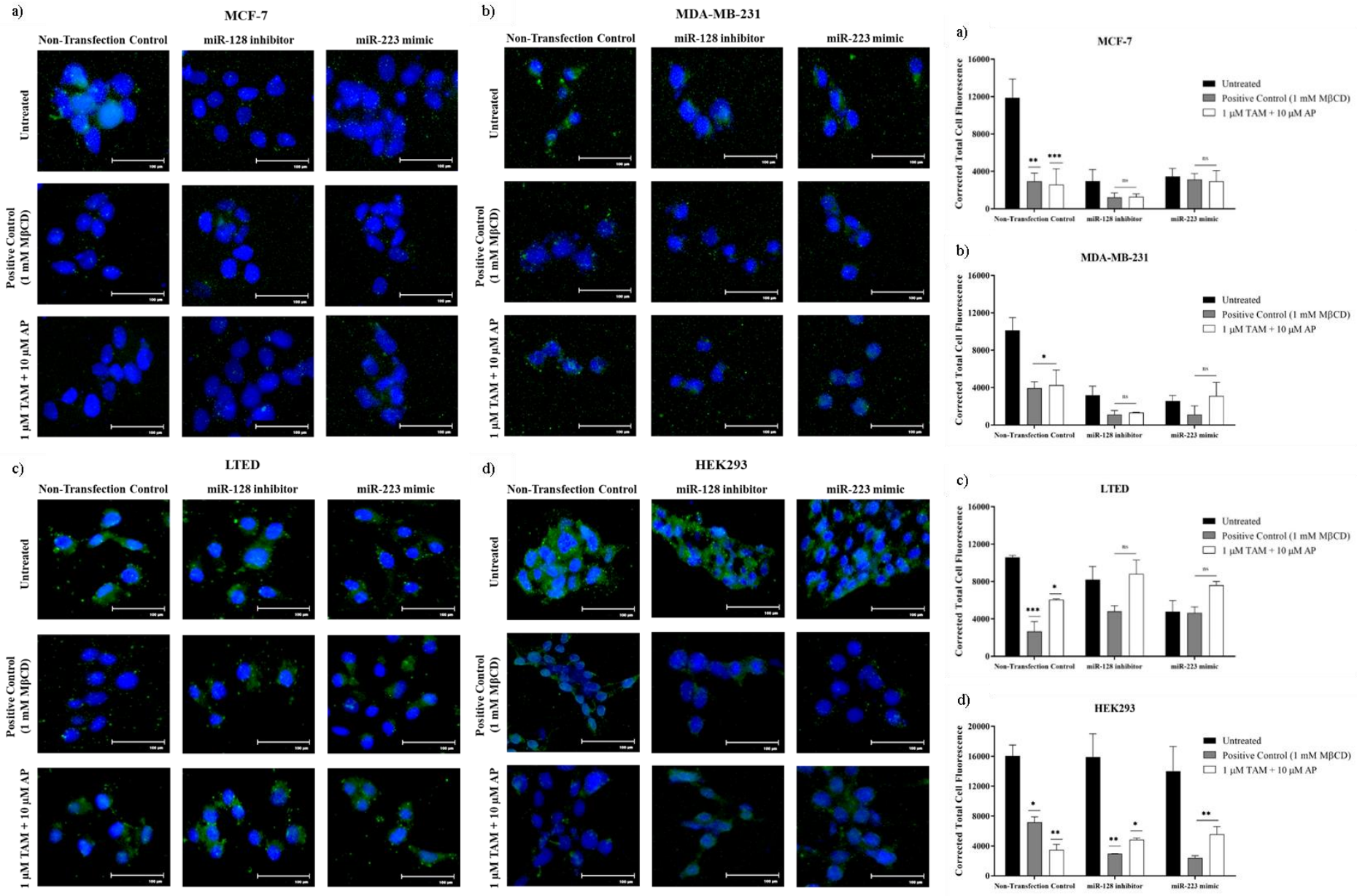
a)
MCF-7
b)
MDA-MB-231
c)
LTED
d)
HEK293
Non-Transfection Control
miR-128 inhibitor
miR-223 mimic
Untreated
Positive Control (1 mM MβCD)
1 μM TAM + 10 μM AP
Corrected Total Cell Fluorescence
Untreated
Positive Control (1 mM MβCD)
1 μM TAM + 10 μM AP
Non-Transfection Control
miR-128 inhibitor
miR-223 mimic

Figure 4.6: Changes in CE fluorescence upon miRNA transfection and combination treatment

Representative images from non-transfected MCF-7 ***(a),*** *MDA-MB-231* ***(b),*** *LTED* ***(c),*** *and HEK293* ***(d)*** *cells, cells transfected with a miR-128-3p inhibitor, and a miR-223-5p mimic upon TAM + AP treatment, with a positive control. Cells were transfected with relevant mimic or inhibitor for 48 h prior to treatment with TAM + AP or MβCD for 2 h before BODIPY staining. CEs are shown as green dots, and nuclei are shown in blue. Images were taken using the EVOS FLoid™ Cell Imaging Station for quantification. The scale bars indicate 100 µm. Images are representative of three separate experiments. Corresponding bar graphs depicting mean values of the CTCF in transfected cells relative to the non-transfection control, from three independent repeats. The ImageJ1 software was used for fluorescence quantification. Data are mean ± S.D; (n=150) from raw data, where n is the total number of cells quantified per condition. The data was analysed by a two-way ANOVA followed by a Bonferroni post-hoc test to compare individual differences, where * P < 0.05, ** P < 0.01, *** P < 0.001, and ns = non-significant indicates a significant or non-significant difference to the untreated control.*

4.4.3 Lipid rafts

When MCF-7 cells had a down-regulation of miR-128 expression, there was a 71% reduction in lipid raft fluorescence compared to the non-transfection control (Fig. 4.7a). When miR-223 expression was up-regulated, there was a 66% reduction in lipid raft florescence in comparison to the non-transfection control. When MCF-7 cells had lowered miR-128 expression and were treated with TAM + AP, there was no significant reduction in lipid raft florescence compared to the corresponding untreated control. However, a trend towards a reduction in fluorescence was observed. When these cells had increased miR-223 expression and were treated with the combination treatment, there was a significant reduction in lipid raft florescence compared to the untreated control. This indicates that increasing miR-223 expression, with TAM + AP treatment significantly reduces lipid rafts in MCF-7 cells.

When MDA-MB-231 cells had a down-regulation of miR-128 expression, there was a 62% reduction in lipid raft florescence compared to the non-transfection control (Fig. 4.7b). When miR-223 expression was up-regulated, there was a 60% reduction in lipid raft florescence in comparison to the non-transfection control. There was no significant change in lipid raft fluorescence when cells had lowered miR-128 expression and were treated with TAM + AP, compared to the corresponding untreated control. However, when MDA-MB-231 cells had

higher miR-223 expression and were treated with the combination treatment, there was a significant reduction in lipid raft florescence compared to the untreated control.

When LTED cells had a down-regulation of miR-128 expression, there was a 62% reduction in lipid raft florescence compared to the non-transfection control (Fig. 4.7c). When miR-223 expression was up-regulated, there was a 17% reduction in lipid raft florescence in comparison to the non-transfection control. There was no significant change in lipid raft fluorescence when cells had lowered miR-128 expression and were treated with TAM + AP, compared to the corresponding untreated control. However, when LTED cells had increased miR-223 expression and were treated with the combination treatment, there was a significant reduction in lipid raft fluorescence compared to the untreated control.

The up-regulation of miR-223 led to similar lipid raft levels to that of the non-transfection control in the HEK293 cell line (Fig. 4.7d). The knockdown of miR-128 expression led to a 41% reduction in lipid raft fluorescence in comparison to the non-transfection control. When these transfected cells were treated with the combination treatment, lipid raft fluorescence was significantly reduced compared to corresponding untreated controls. Overall, the most prominent reduction in lipid raft fluorescence was observed in both MCF-7 and MDA-MD-231 cells, upon manipulation of miRNA expression together with TAM + AP treatment.

Overall, these findings indicate that altering the expression of these target miRNAs with TAM + AP treatment changes the fluorescence intensity of free cholesterol, CEs, and lipid rafts in BC cells, which could possibly lead to decreased cellular viability as seen in Fig. 4.4 above. To investigate this further, several cholesterol-related and cancer drug resistance genes and proteins were selected for further pathway analysis to find the mechanisms in which these miRNAs and treatment function. This was achieved by RT-qPCR and western blotting validation.

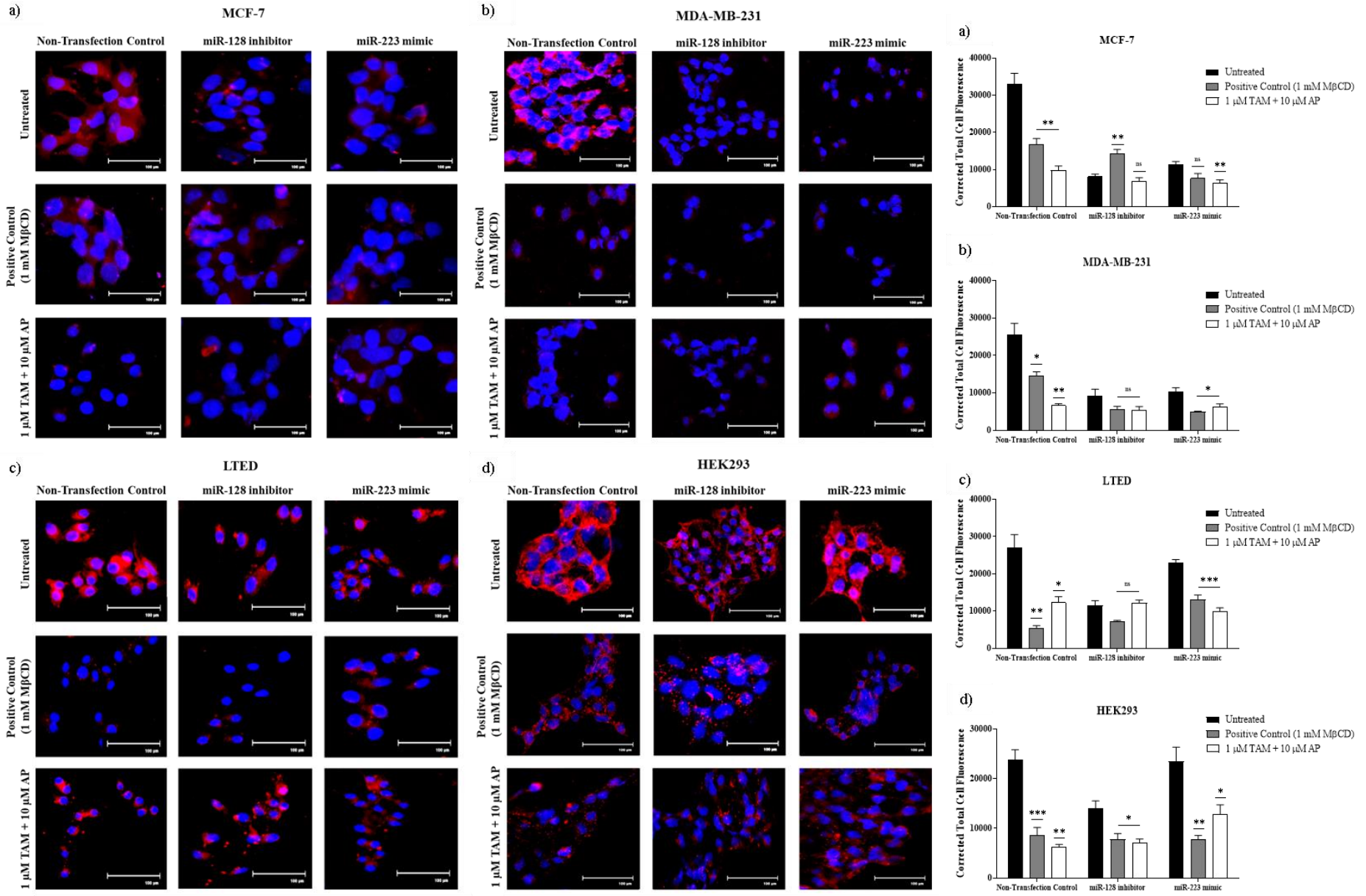
a)
MCF-7
Non-Transfection Control
miR-128 inhibitor
miR-223 mimic
Untreated
Positive Control (1 mM MβCD)
1 μM TAM + 10 μM AP
b)
MDA-MB-231
c)
LTED
d)
HEK293
Corrected Total Cell Fluorescence
Untreated
Positive Control (1 mM MβCD)
1 μM TAM + 10 μM AP
Non-Transfection Control
miR-128 inhibitor
miR-223 mimic

Figure 4.7: Changes in lipid raft fluorescence upon miRNA transfection and combination treatment

Representative images from non-transfected MCF-7 ***(a),*** *MDA-MB-231* ***(b),*** *LTED* ***(c),*** *and HEK293* ***(d)*** *cells, cells transfected with a miR-128-3p inhibitor, and a miR-223-5p mimic upon TAM + AP treatment, with a positive control. Cells were transfected with relevant mimic or inhibitor for 48 h prior to treatment with TAM + AP or MβCD for 2 h before Vybrant™ Alexa Fluor™ 594 Lipid Raft staining. Lipid rafts are shown in red, and nuclei are shown in blue. Images were taken using the EVOS FLoid™ Cell Imaging Station for quantification. The scale bars indicate 100 µm. Images are representative of three independent experiments. Corresponding bar graphs depicting mean values of the CTCF in transfected cells relative to the non-transfection control, from three separate repeats. The ImageJ1 software was used for fluorescence quantification. Data are mean ± S.D; (n=150) from raw data, where n is the total number of cells quantified per condition. The data was analysed by a two-way ANOVA followed by a Bonferroni post-hoc test to compare individual differences, where * P < 0.05, ** P < 0.01, *** P < 0.001, and ns = non-significant indicates a significant or non-significant difference to the untreated control.*

4.5 Gene and protein expression changes following miRNA alteration and treatment

Several genes were selected based on the findings by Monchusi and Kaur (2020), as they had the most significant changes upon miR-128 and miR-223 expression alteration. These genes are known to be involved in many signalling pathways that promote BC drug resistance.

4.5.1 Molecular mechanisms of cancer drug resistance upon miRNA alteration and TAM + AP treatment in BC

The expression levels of relevant genes were observed using RT-qPCR. Each RNA sample had good integrity prior to RT-qPCR. Cancer drug resistance and BC genes analysed using RT-qPCR included: *ABCC5, BRCA2, EGFR,* estrogen receptor 1 (*ESR1*), *IGF1R, PTEN*, tumour protein P53 *(TP53),* and UDP-Glucose Ceramide Glucosyltransferase (*UGCG*).

A heatmap indicating log2 fold change of each gene compared to the untreated or non-transfection control is shown below (Fig. 4.8). Individual graphs of the log2 fold change of each gene and each treatment are shown in Fig. S2. From Fig. 4.8, in general, either the alteration of expression of target miRNAs or the combination of miRNA alteration with TAM + AP treatment led to a down-regulation in expression of most cancer drug resistance genes in MCF-7 and MDA-MB-231 cells, whereas there was a higher expression of these genes seen in

resistant LTED cells. However, when LTED cells were treated with TAM + AP and when miRNA alteration occurred, there was a down-regulation of select genes, compared to just TAM + AP treatment alone or just miRNA alteration alone.

When LTED cells had a decreased expression of miR-128 with TAM + AP treatment, or when these cells had increased miR-223 expression with TAM + AP treatment, genes such as *BRCA2* and *PTEN* (tumour suppressors) were up-regulated, and growth factor receptors like *EGFR* and *IGF1R*, and *ESR1*, were down-regulated. In MCF-7 cells, the combination of a miR-128 inhibitor and TAM + AP treatment led to a reduction in all genes, including tumour suppressors. However, the combination of a miR-223 mimic and TAM + AP treatment led to an increase in the tumour suppressor genes, *BRCA2* and *TP53*, whilst reducing *EGFR*, *IGF1R*, and *ESR1* expression. Similarly, in MDA-MB-231 cells, upon transfection with a miR-223 mimic, an up-regulation of tumour suppressors, *BRCA2*, *PTEN*, and *TP53*, and a down-regulation of *ABCC5* (MDR gene), *EGFR*, and *ESR1* was observed. These findings demonstrate the differences within BC subtypes and confirm the efficacy of increasing miR-223 expression with TAM + AP treatment in combating cholesterol-mediated drug resistance in BC cells.

Further analysis to validate the above findings was performed by use of western blotting. Non-transfection control (lane 1), transfection control (lane 2), miR-223 mimic (lane 3) and miR-128 inhibitor (lane 4) samples were compared in all three BC cell lines and the HEK293 cell line. Comparison of lanes 4 show that a down-regulation of ERα expression was observed when BC cells had reduced miR-128 expression together with TAM + AP treatment in comparison to the non-transfection control (Fig. 4.9). However, this trend was no observed in HEK293 cells. This result confirms the findings reported in Fig. 4.8. Interestingly, LTED cells showed increased ERα expression upon TAM + AP treatment compared to untreated samples, indicating the inherent resistance of these cells to TAM treatment.

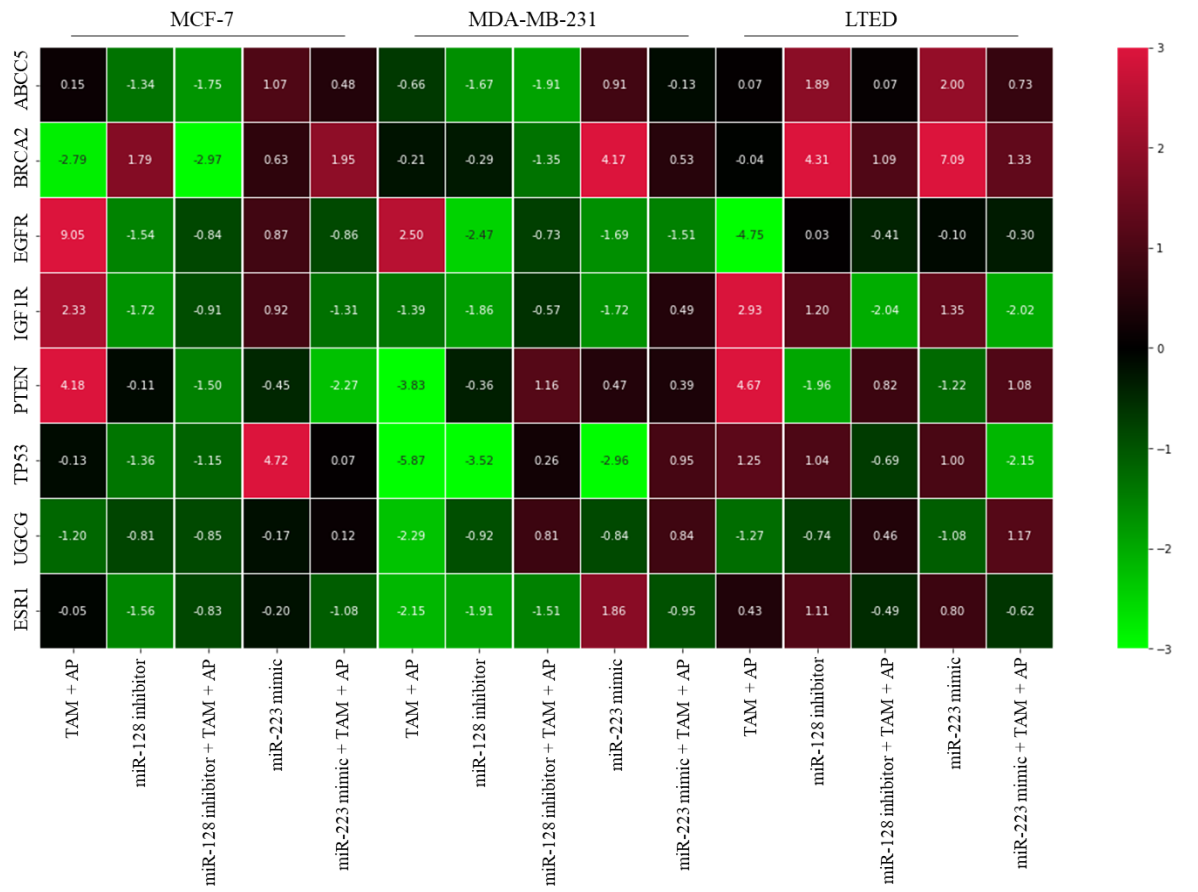

Figure 4.8: Changes in BC drug resistance-related gene expression upon miRNA transfection and TAM + AP treatment

*RT-qPCR expression analysis of genes involved in cancer drug resistance pathways (ABCC5, EGFR, IGF1R, PTEN, TP53, and UGCG) and in BC pathways (BRCA2 and ESR1) in BC cells post-transfection and treatment. Each gene is represented on the y-axis, and each cell line (MCF-7, MDA-MB-231, and LTED) is represented on the x-axis. Cells were either solely treated with TAM + AP (column 1), solely transfected with miR-128 inhibitor (column 2), transfected with miR-128 inhibitor and treated with TAM + AP (column 3), solely transfected with miR-223 mimic (column 4), or transfected with miR-223 mimic and treated with TAM + AP (column 5). Red (positive log2 fold-regulation) represents increase, black represents no change and green (negative log2 fold-regulation) represents decrease in expression of genes in indicated conditions compared to respective untreated or non-transfection controls. The heatmap was generated using the Python software. Data are mean ± S.D; (n=3) from raw data. Statistical significance was calculated using a student's t-test, where * P < 0.05, ** P < 0.01, *** P < 0.001, and ns = non-significant indicates a significant or non-significant difference to the untreated or non-transfection control.*

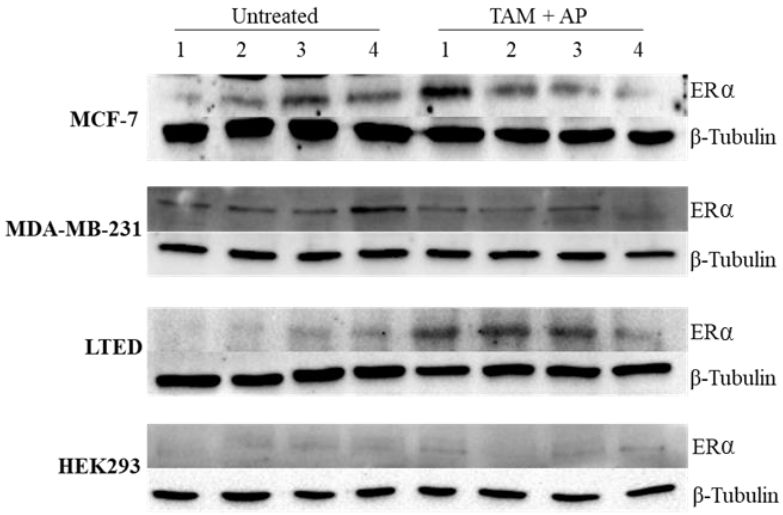

Figure 4.9: Protein expression levels of ERα upon miRNA transfection and combination treatment

Representative western blots comparing the expression levels of ERα in different cell lines post-transfection that were either untreated or treated with TAM + AP. The blots depict ERα (66 kDa) and β-Tubulin (50 kDa) in each cell line. β-Tubulin was used as a loading control. Similar results were obtained in three independent experiments (n=3). ***Lane 1:*** *non-transfection control,* ***Lane 2:*** *transfection control,* ***Lane 3:*** *miR-223 mimic, and* ***Lane 4:*** *miR-128 inhibitor.*

4.5.2 Molecular mechanisms of cholesterol metabolism upon miRNA alteration and TAM + AP treatment in BC

The expression levels of relevant genes were observed using RT-qPCR as above. Genes involved in cholesterol signalling and metabolism included: *ABCA1*, *ABCG1*, *CETP*, *LCAT*, *HMGCR*, *HMGCS1*, *INSIG2*, *SREBF1*, *SREBF2*, and *LDLR*. These genes were selected as they had the most significant changes upon miRNA expression alteration as above.

A heatmap indicating log2 fold change of each gene compared to the untreated control is shown below (Fig. 4.10). Individual graphs of the log2 fold change of each gene and each treatment are shown in Fig. S3. Like in Fig. 4.8, the heatmap below demonstrates a down-regulation in expression of most cholesterol-related genes in MCF-7 and MDA-MB-231 cells, regardless of condition. On the contrary, there was a higher expression of these genes seen in LTED cells; however, when these cells were treated with TAM + AP and when miRNA alteration occurred, there was a down-regulation of select genes.

The knockdown of miR-128 expression alone was the most effective treatment in MCF-7 cells, as the cholesterol efflux transporter, *ABCG1*, and negative cholesterol biosynthesis regulator,

INSIG2 were up-regulated. With the knockdown of miR-128 expression in these cells, genes involved in lipogenesis (*HMGCR, HMGCS1, SREBF1/2*), transport, and uptake (*CETP, LCAT,* and *LDLR*) were down-regulated, indicating that miR-128 is a direct target of various cholesterol synthesis and homeostasis genes in BC cells. In MDA-MB-231 cells, the most effective treatment was the up-regulation of miR-223 with TAM + AP treatment, like what was found in Fig. 4.8 above. This was the most effective condition, as *ABCG1* and *INSIG2* were up-regulated, and *CETP, LCAT, HMGCR, HMGCS1, SREBF1*, and *LDLR* were down-regulated. This further confirms the efficacy of up-regulating the expression of miR-223 with a TAM + AP treatment in the aggressive MDA-MB-231 cell line.

When the expression of miR-128 was down-regulated and when resistant LTED cells were treated with TAM + AP, a slight increase in *HMGCR* and *HMGCS1* occurred, indicating increased cholesterol synthesis; however, the expression of both *ABCA1* and *ABCG1* was heavily up-regulated indicating the sufficient efflux of cholesterol out of these cells. The expression of *CETP*, *SREBF1/2*, and *LDLR* were down-regulated upon miR-128 knockdown and TAM + AP treatment, while *INISG2* expression was up-regulated. These findings were similar to what was found in Fig. 4.8, where miRNA alteration with TAM + AP treatment was effective at reducing the expression of drug resistance-related genes.

Taken together, both Figs. 4.8 and 4.10, showed that in MCF-7 cells, the most effective treatment in reducing cholesterol-mediated drug resistance, was the knockdown of miR-128 expression with or without TAM + AP treatment. In MDA-MB-231 cells, the increased expression of miR-223 with TAM + AP treatment, was most effective, and in LTED cells, the down-regulation of miR-128 with TAM + AP treatment was most effective. It is evident that varying conditions affect BC subtypes in different ways, which could be used as a personalised novel approach in overcoming cholesterol-mediated drug resistance in BC.

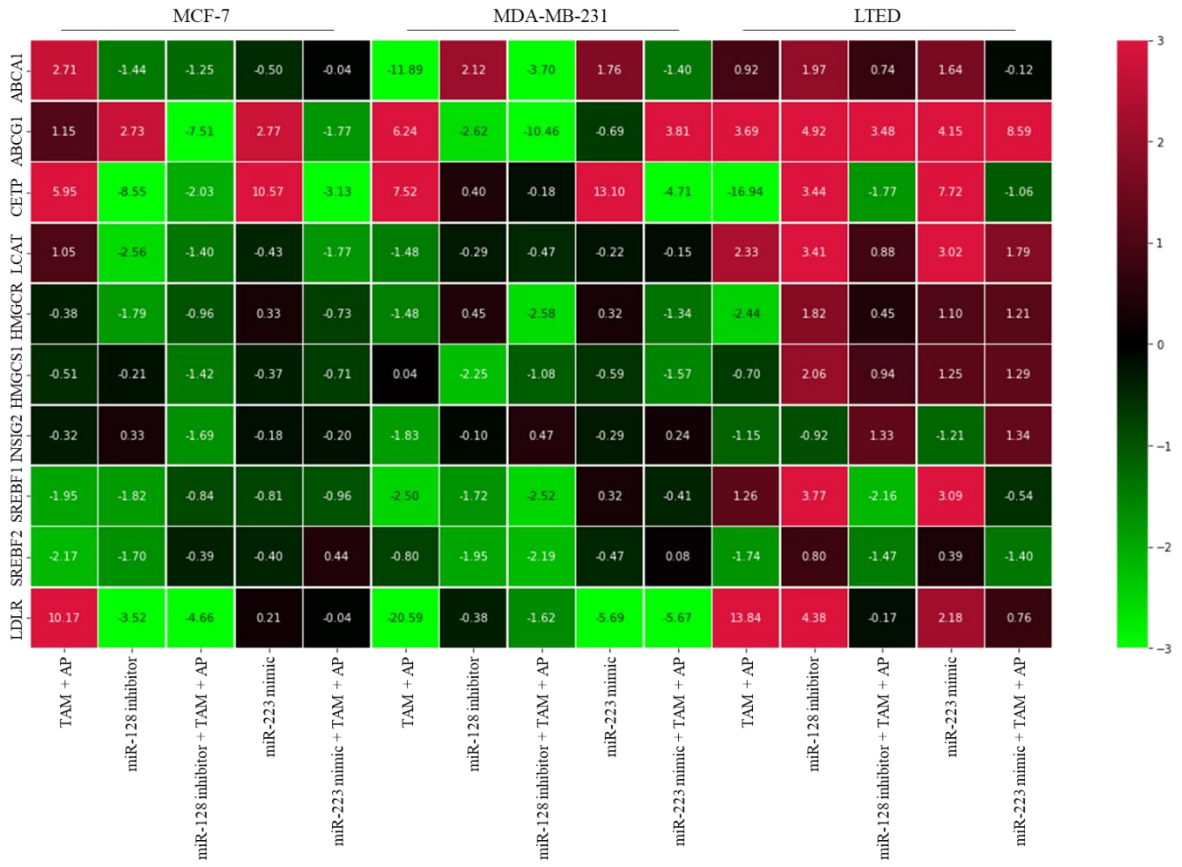

Figure 4.10: Changes in cholesterol-related gene expression upon miRNA transfection and TAM + AP treatment

*RT-qPCR expression analysis of genes involved in cholesterol signalling and metabolism pathways. Genes were separated based on their cellular functions. Cholesterol efflux: ABCA1 and ABCG1; cholesterol transport: CETP and LCAT; cholesterol biosynthesis: HMGCR, HMGCS1, INSIG2, SREBF1 and SREBF2; and cholesterol uptake: LDLR, in BC cells post-transfection and treatment. Each gene is represented on the y-axis, and each cell line (MCF-7, MDA-MB-231, and LTED) is represented on the x-axis. Cells were either solely treated with TAM + AP (column 1), solely transfected with miR-128 inhibitor (column 2), transfected with miR-128 inhibitor and treated with TAM + AP (column 3), solely transfected with miR-223 mimic (column 4), or transfected with miR-223 mimic and treated with TAM + AP (column 5). Red (positive log2 fold-regulation) represents increase, black represents no change and green (negative log2 fold-regulation) represents decrease in expression of genes in indicated conditions compared to respective untreated or non-transfection controls. The heatmap was generated using the Python software. Data are mean ± S.D; (n=3) from raw data. Statistical significance was calculated using a student's t-test, where * P < 0.05, ** P < 0.01, *** P <*

0.001, and ns = non-significant indicates a significant or non-significant difference to the untreated or non-transfection control.

Further analyses to validate the above findings were performed by western blots. The protein expression levels of CETP, ABCG1, LXRα, PCSK9, SREBP1, and SREBP2 are shown in Figs. 4.11-4.16 below.

Reduced CETP expression was observed in general in MDA-MB-231 cells as compared to MCF-7 cells, specifically a visible reduction in CETP (lanes 4 comparison) after miR-128 expression inhibition together with TAM + AP treatment in MDA-MB-231 cells (Fig. 4.11). CETP expression in LTED cells has not been reported in the literature before, therefore, a detailed investigation of gene and protein expression under varied experimental conditions is necessary going forward.

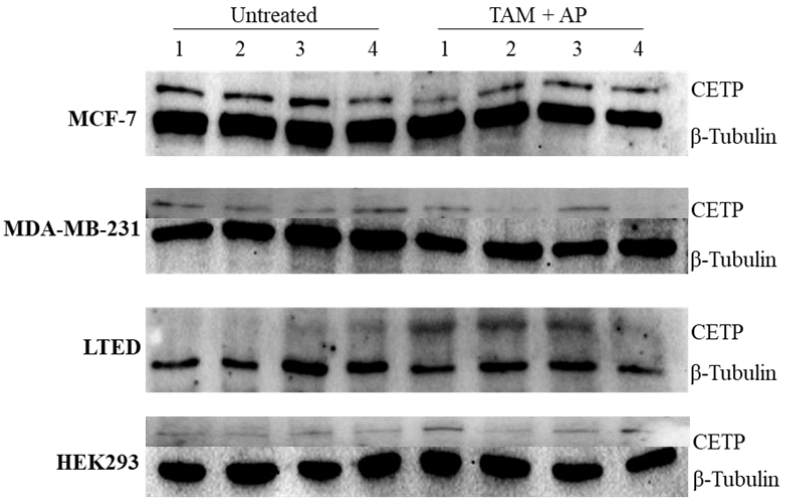

Figure 4.11: Protein expression levels of CETP upon miRNA transfection and combination treatment

Representative western blots comparing the expression levels of CETP in different cell lines post-transfection that were either untreated or treated with TAM + AP. The blots depict CETP (60 kDa) and β-Tubulin (50 kDa) in each cell line. β-Tubulin was used as a loading control. Similar results were obtained in three independent experiments (n=3). ***Lane 1:*** *non-transfection control,* ***Lane 2:*** *transfection control,* ***Lane 3:*** *miR-223 mimic, and* ***Lane 4:*** *miR-128 inhibitor.*

The expression levels of the cholesterol efflux protein, ABCG1 were similar regardless of the condition in MCF-7 cells (Fig. 4.12). In MDA-MB-231 and LTED cells, barely any ABCG1

expression was observed, therefore further investigations are required to make additional conclusions.

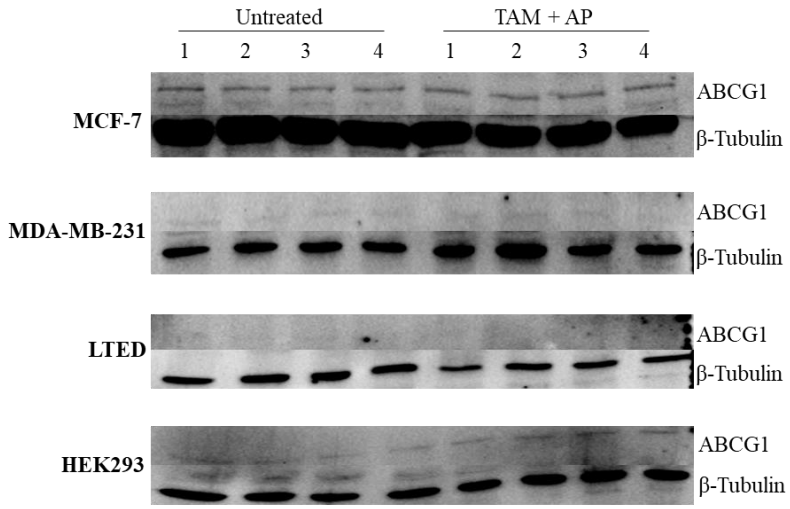

Figure 4.12: Protein expression levels of ABCG1 upon miRNA transfection and combination treatment

Representative western blots comparing the expression levels of ABCG1 in different cell lines post-transfection that were either untreated or treated with TAM + AP. The blots depict ABCG1 (100 kDa) and β-Tubulin (50 kDa) in each cell line. β-Tubulin was used as a loading control. Similar results were obtained in three independent experiments (n=3). ***Lane 1:*** *non-transfection control,* ***Lane 2:*** *transfection control,* ***Lane 3:*** *miR-223 mimic, and* ***Lane 4:*** *miR-128 inhibitor.*

The cholesterol biosynthesis protein, LXRα, is a nuclear receptor that controls lipid homeostasis and drives SREBF1 processing and lipogenesis. It is shown that LXRα expression was reduced generally in MCF-7, MDA-MB-231, and LTED cells, especially in lanes 4 of treated samples upon transfection with a miR-128 inhibitor and TAM + AP treatment (Fig. 4.13). Further confirming that miR-128 knockdown and TAM + AP treatment is sufficient in reducing cholesterol biosynthesis in these cell lines. HEK293 cells also showed a slight reduction in LXRα expression post TAM + AP treatment.

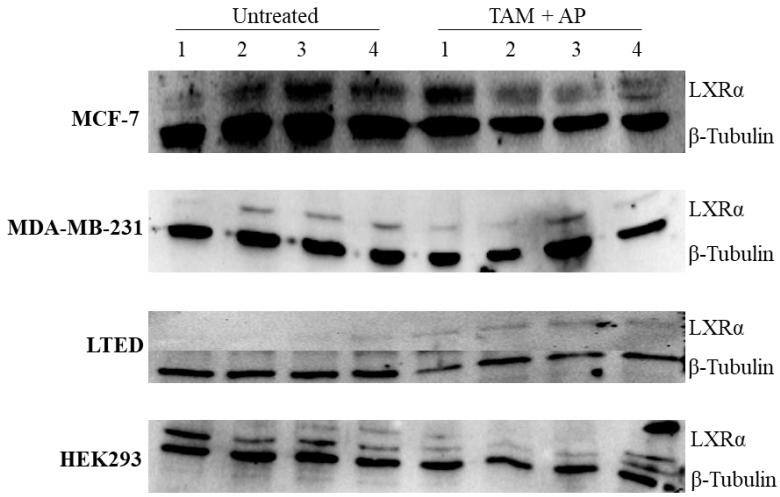

Figure 4.13: Protein expression levels of LXRα upon miRNA transfection and combination treatment

Representative western blots comparing the expression levels of LXRα in different cell lines post-transfection that were either untreated or treated with TAM + AP. The blots depict LXRα (55 kDa) and β-Tubulin (50 kDa) in each cell line. β-Tubulin was used as a loading control. Similar results were obtained in three independent experiments (n=3). ***Lane 1:*** *non-transfection control,* ***Lane 2:*** *transfection control,* ***Lane 3:*** *miR-223 mimic, and* ***Lane 4:*** *miR-128 inhibitor.*

Another crucial protein involved in cholesterol metabolism and plasma cholesterol homeostasis is PCSK9. Like LXRα expression above, PCSK9 expression was down-regulated upon transfection with a miR-128 inhibitor and TAM + AP treatment in MCF-7, MDA-MB-231, and LTED cells compared to the non-transfection control (Fig. 4.14). As with ERα and CETP, PCSK9 expression was up-regulated in LTED cells upon TAM + AP treatment compared to untreated samples. However, a reduction post miR-128 inhibition was observed in this cell line relative to the non-transfection control. Interestingly, HEK293 cells showed an up-regulation of PCSK9 expression post miR-128 inhibition and TAM + AP treatment.

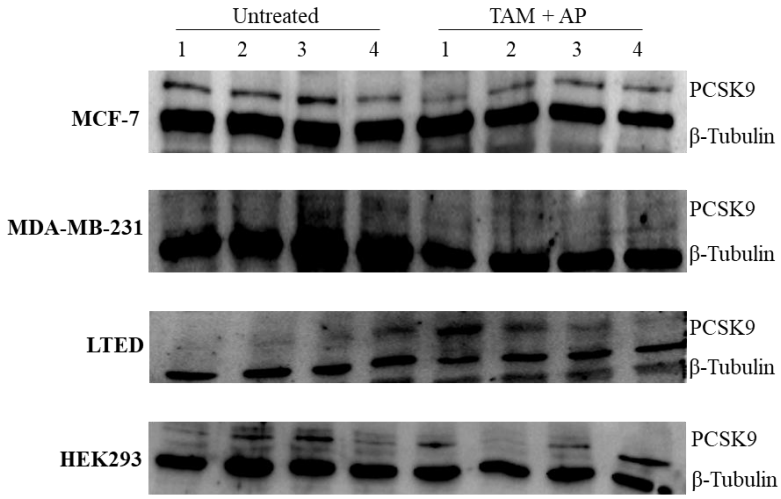

Figure 4.14: Protein expression levels of PCSK9 upon miRNA transfection and combination treatment

Representative western blots comparing the expression levels of PCSK9 in different cell lines post-transfection that were either untreated or treated with TAM + AP. The blots depict PCSK9 (60 kDa) and β-Tubulin (50 kDa) in each cell line. β-Tubulin was used as a loading control. Similar results were obtained in three independent experiments (n=3). ***Lane 1:*** *non-transfection control,* ***Lane 2:*** *transfection control,* ***Lane 3:*** *miR-223 mimic, and* ***Lane 4:*** *miR-128 inhibitor.*

Western blot analysis of SREBP1 below indicates two isoforms (Fig. 4.15). The first form is the precursor or unprocessed form of SREBP1 (P-SREBP1) at 125 kDa, and the second is the activated, processed nuclear form (N-SREBP1) at 68 kDa. In MCF-7cells, not much difference was observed in the expression of P-SREBP1 in comparison to N-SREBP1, whereas P-SREBP1 expression was clearly higher in comparison to N-SREBP1 in MDA-MB-231 cells. This indicates that MDA-MB-231 cells had high intracellular cholesterol levels at the time of processing the samples, thus not requiring activation of SREBP1 for cholesterol biosynthesis. This was in accordance with Fig. 4.10 above, where most conditions led to a down-regulation in *SREBF1*, which is the processed transcription factor form (N-SREBP1). When these cells were transfected with a miR-128 inhibitor and treated with TAM + AP, N-SREBP1 expression was reduced compared to the non-transfection control (lanes 4). No clear expression of P-SREBP1 and N-SREBP1 was detected in LTED cells and not much changes in expression of these two proteins was observed in HEK293 cells.

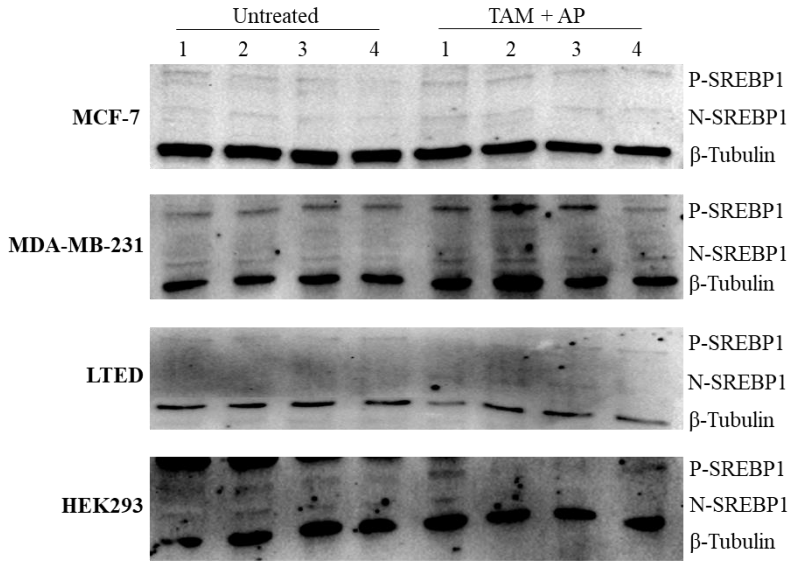

Figure 4.15: Protein expression levels of SREBP1 upon miRNA transfection and combination treatment

Representative western blots comparing the expression levels of SREBP1 in different cell lines post-transfection that were either untreated or treated with TAM + AP. The blots depict the unprocessed (precursor, P-SREBP1 at 125 kDa) and the processed (nuclear, N-SREBP1 at 68 kDa) forms of SREBP1 and β-Tubulin (50 kDa) in each cell line. β-Tubulin was used as a loading control. Similar results were obtained in three independent experiments (n=3). ***Lane 1:*** *non-transfection control,* ***Lane 2:*** *transfection control,* ***Lane 3:*** *miR-223 mimic, and* ***Lane 4:*** *miR-128 inhibitor.*

Similarly, SREBP2 expression was observed, which is indicated in three forms: P-SREBP2 at 125 kDa, N-SREBP2 at 68 kDa, and N-SREBP2 at 58 kDa (Fig. 4.16). Like SREBP1 above, P-SREBP2 is the inactive precursor initially embedded in the endoplasmic reticulum, whereas N-SREBP2 (68 kDa) is the activated, nuclear form of this protein. Once translocated to the nucleus, SREBP2 activates cholesterol biosynthesis genes. A second N-SREBP2 (58 kDa) isoform is often formed due to a premature truncation in the amino acid sequence of this protein. In all cell lines, there was an up-regulation of N-SREBP2 (58 kDa) expression in comparison to P-SREBP2 expression, indicating low intracellular cholesterol levels across these cells. In MCF-7 cells, there was more N-SREBP2 (58 kDa) expression in untreated samples, showing the increased production of cholesterol in these cells as compared to TAM + AP treated cells. In MDA-MB-231 and LTED cells, there was no demarcated difference observed in the expression patterns of both N-SREBP2 bands, indicating not much impact of

TAM + AP treatment on cholesterol homeostasis in therapeutically resistant cell lines at a molecular level. HEK293 cells also did not show cholesterol dyshomeostasis.

Altogether, the use of a miR-128 inhibitor or a miR-223 mimic, with TAM + AP treatment impacted the expression of some of the tested cholesterol-related and cell signalling proteins in BC cell lines. These results demonstrate that altering the expression of miR-128 and miR-223 prior to a combination treatment of an endocrine compound (TAM) and a cholesterol depleting agent (AP) may impact cholesterol-mediated drug resistance in BC.

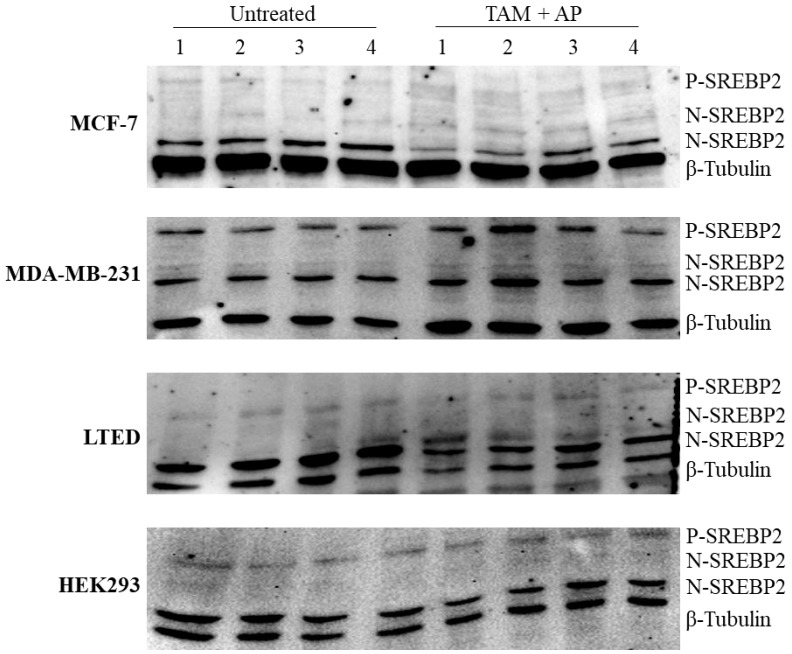

Figure 4.16: Protein expression levels of SREBP2 upon miRNA transfection and combination treatment

Representative western blots comparing the expression levels of SREBP2 in different cell lines post-transfection that were either untreated or treated with TAM + AP. The blots depict P-SREBP2 at 125 kDa and the two nuclear (N-SREBP2 at 68 and 58 kDa, respectively) forms of SREBP2, and β-Tubulin (50 kDa) in each cell line. β-Tubulin was used as a loading control. Similar results were obtained in three independent experiments (n=3). ***Lane 1:*** *non-transfection control,* ***Lane 2:*** *transfection control,* ***Lane 3:*** *miR-223 mimic, and* ***Lane 4:*** *miR-128 inhibitor.*

5. DISCUSSION

Combating the resistance associated with TAM treatment by targeting cholesterol accumulation in BC cell lines is a novel concept. Previous studies have shown that when the cholesterol depleting agent, AP, is used in combination with an endocrine therapy such as TAM, cytotoxicity of normal cells decreases while increasing the cytotoxicity of BC cells through cholesterol depletion (Esau *et al.*, 2016; Henriques Palma and Kaur, 2022). Despite the progress in treatments of lowering intracellular cholesterol levels, mortality rates are still high, emphasising the need for novel therapeutic strategies. miRNAs have recently been shown to regulate cholesterol, triglyceride, glucose homeostasis, and cancer drug resistance (Monchusi and Kaur, 2020; Wagschal *et al.*, 2015). Therefore, targeting these miRNAs in BC cells could be used for the development of new treatments in combating cholesterol-mediated drug resistance. Several miRNAs regulate lipid metabolism and have been found to control cellular cholesterol homeostasis; however, evidence is lacking on the exact molecular mechanisms in which these miRNAs function. Therefore, the current study aimed at altering the expression of miR-128 and miR-223 with a combination treatment of TAM + AP, to investigate whether this treatment could be successful as a novel anticancer therapy for the reduction of cholesterol-mediated drug resistance in BC. This was achieved by subjecting BC cells to three conditions. The first condition was that BC cells were either exclusively transfected with a miR-128 inhibitor to reduce miR-128 expression, or a miR-223 mimic to increase miR-223 expression. The second condition was a combination treatment of 1 µM TAM and 10 µM AP, and the third condition was a combination of miRNA alteration with TAM + AP treatment.

miRNAs are known to possess tumour suppressor and oncogenic properties. miR-128 is known to be a tumour suppressor in glioblastoma, bladder, and lung cancers (Li *et al.*, 2013a). A study showed that miR-223 is dysregulated in pancreatic, gastric, lung, prostate, and BC (Dou *et al.*, 2019). A study found that miR-128 expression was up-regulated in letrozole-resistant BC cells, whereas the inhibition of miR-128 resulted in the re-sensitisation of letrozole-resistant cells to transforming growth factor (TGF)-β growth inhibitory effects, indicating that miR-128 could play a crucial role in regulating TGFβ signalling and could possibly overcome resistance associated with AIs (Li *et al.*, 2013a; Masri *et al.*, 2010). On the contrary, another study showed high miR-128 expression in patients with grades I and II BC, and a decrease in miR-128 expression in grade III BC (Xiao *et al.*, 2017). This study also observed that TNBC cells had lower miR-128 expression than luminal A cells. However, another study demonstrated that

high miR-128 expression was linked to poor prognosis in BC patients (Buffa *et al.*, 2011), and this was corroborated by the Kaplan-Meier survival plots shown in the current study (Fig. 4.1a and 4.1c), where higher miR-128 expression led to a reduced overall survival in BC patients. To further support these claims, the current study demonstrated that the use of an inhibitor for the down-regulation of miR-128 expression had the highest effect in reducing cell numbers in TNBC (MDA-MB-231) cells (Fig. 4.3b), suggesting a potential therapeutic and prognostic use in reducing cell proliferation in this aggressive BC subtype. When miR-128 is overexpressed, hormone-dependent BC cells become resistant to endocrine treatments (Masri *et al.*, 2010), indicating the significance in reducing miR-128 expression in all BC subtypes. Although there are several contradictory findings regarding the effects of miR-128 expression in BC, our findings demonstrate that inhibition of this miRNA reduces BC cell numbers, viability, and cholesterol content. However, further investigations into the pathways affected by miR-128 expression are warranted.

Similarly, studies have revealed the pleiotropic effects of miR-223 expression in different cancer types (Gao *et al.*, 2017). This miRNA acts as an oncogene in prostate and gastric cancers, whereas in acute myeloid leukaemia, cervical, and non-small cell lung cancer (NSCLC), it acts as a tumour suppressor (Gao *et al.*, 2017). This pleiotropic effect depends on its target genes in different tissue types. A study demonstrated that miR-223 levels were significantly lower in MCF-7, MDA-MB-231, and T-47D cells compared to non-tumourigenic MCF-10A cells (Gong *et al.*, 2013). The most aggressive BC cell line, MDA-MB-231, had the lowest miR-223 expression, and overexpression of this miRNA led to reduced proliferation and invasion of these cells (Gong *et al.*, 2013). In addition, high miR-223 expression was associated with increased overall survival of TNBC patients, acting as a positive prognostic marker (Chen *et al.*, 2021b). The findings of this study are in accordance with the literature, where increased miR-223 expression correlated with increased overall survival in TNBC patients (Fig. 4.1d). Another study revealed that miR-223 overexpression in BC cells led to decreased migration and invasion, increased anoikis-related cell death, and enhanced sensitivity to chemotherapy (Pinatel *et al.*, 2014). On the contrary, a study found that stage III BC patients had higher miR-223-3p expression compared to stage I BC patients, and when MCF-7 cells were transfected with a mimic, there was increased proliferation and invasion in these cells (Yoshikawa *et al.*, 2018). However, this was not observed in the current study as increased expression of miR-223-5p led to reduced cell numbers and viability in all BC cells (Figs. 4.3-4.4). Taken together, several studies have suggested that miR-223 acts in suppressing

BC tumour progression, suggesting a potential novel strategy for BC treatment (Gong *et al.,* 2013; Lim *et al.,* 2011; Pinatel *et al.,* 2014; Yang *et al.,* 2018). It is therefore predicted that miR-128 and miR-223 may be potential prognostic and diagnostic biomarkers for BC; however, further elucidation into the molecular mechanisms of miRNA expression in tumour suppression is required. Nonetheless, miRNA regulation is a promising tool for reducing BC cell growth, proliferation, and invasion (Aziz *et al.,* 2022).

Cancers such as prostate cancer and BC, are known to have cholesterol-enriched cell membrane domains (lipid rafts) for increased survival and proliferation. Studies have found that cancer cells are six to eight times richer in cholesterol than normal cells for increased cell growth and survival (Cruz *et al.,* 2020; Gu *et al.,* 2019). Therefore, an effective treatment in targeting this excess cholesterol, is by use of cholesterol lowering agents. Cholesterol plays an important role in maintaining membrane fluidity and permeability, cell signalling, drug trafficking, and the formation of lipid rafts (Mahammad and Parmryd, 2015). Cholesterol is also an important precursor for the synthesis of steroid hormones (estrogen and testosterone), bile acids, and vitamin D production. Therefore, reducing the excess cholesterol levels found in cancer cells is essential in reducing the proliferative capabilities of these cells, and could be a novel and effective anticancer treatment.

There are currently two strategies that target cholesterol for anticancer therapy. These strategies are the use of statins, and the use of cholesterol depleting agents. The first approach lowers cholesterol by inhibiting HMGCR, the rate-limiting enzyme of the mevalonate pathway that produces cholesterol. This blocks *de novo* synthesis of cholesterol within the cell. Studies have found statins to be effective in lowering cholesterol in patients and therefore, recent preclinical studies have investigated the efficacy of statins in combination with current chemotherapeutics as a possible anticancer therapy. However, epidemiologic studies remain controversial. Several studies have found that statin use increases the efficacy of current anticancer therapies and have shown a reduction in BC cell proliferation and a reduction in the risk of BC recurrence (Borgquist *et al.,* 2017; Chae *et al.,* 2015; Dulak and Józkowicz, 2005; Harborg *et al.,* 2020; Jakobisiak and Golab, 2003; Kumar *et al.,* 2008; Sim *et al.,* 2022). Although, there have been positive preclinical results with the use of statins for anticancer therapy, numerous adverse side effects have been reported (Jakobisiak and Golab, 2003). These side effects include hepatoxicity, peripheral neuropathy, myopathy, rhabdomyolysis, autoimmune diseases, and impaired myocardial contractility (Bełtowski *et al.,* 2009). Furthermore, increased mortality of type 2 diabetes mellitus patients hospitalised for coronavirus disease 2019 on statin treatment

has been reported (Cariou *et al.,* 2021). In addition, recent evidence has shown that 26% of patients are intolerant to statin treatment (Snejdrlova *et al.,* 2020) and another study showed that females (especially Asian and African) have a higher risk of being intolerant to statin treatment (Bytyçi *et al.,* 2022). For these reasons, a safer and more effective anticancer treatment targeting excess cholesterol accumulation is by use of cholesterol depleting agents.

The compound known as AP was used in the current study, and has been shown to be involved in the atherosclerosis pathway by altering apolipoprotein genes (Esau *et al.,* 2016). This suggests that this compound can be used as a cholesterol depleting agent in combination with an endocrine treatment (TAM), to reduce lipid raft levels in cholesterol-rich plasma membranes, thereby increasing permeability to allow for drug passage for the induction of apoptosis within these cells. However, the molecular mechanisms of AP require further investigation. It has been shown however, that AP induces cytotoxicity in a range of cancer cells, including ER+ MCF-7 cells, and regressed tumour growth, with normal cells demonstrating no associated toxicity. It also showed a reduction in intracellular cholesterol levels (Esau *et al.,* 2016; Sagar *et al.,* 2014). Indicating the safe and effective use of AP as a cholesterol depleting agent in conjunction with current endocrine therapies for the reduction of cholesterol in BC cells. The findings of the current study support these claims as AP was found to reduce cell viability in BC cells, whilst having little effect in HEK293 cells (Fig. 4.4). These findings also showed that combining AP with TAM led to a greater reduction in BC cell viability.

A study performed by Mohammad and colleagues (2014), demonstrated that the combinatorial effect of TAM and MβCD significantly suppressed tumour growth in mice, with no toxicity to vital organs. Tumour regression occurred due to enhanced anti-proliferative and anti-angiogenic effects of the combination treatment (Mohammad *et al.,* 2014). The reduction of tumour size was due to increased TAM levels in tumours, which therefore reduced the accumulation of TAM in vital organs such as the kidney and liver. This led to the conclusion that TAM has lower toxicity in vital organs in the presence of a cholesterol depleting agent, which is one of the major concerns in chemotherapeutic treatment (Mohammad *et al.,* 2014). The results obtained from the current study in Fig. 4.4, further confirm these claims, as it was shown that the combination treatment (TAM + AP) effectively reduced BC cell viability, particularly in MCF-7 and MDA-MB-231 cells. In addition, the down-regulation of miR-128 expression together with the combination treatment was the most effective condition in reducing cell viability across all three BC cell lines. BC cells accumulate excess cholesterol to

aid in cellular proliferation, survival, and invasion. It can be seen from Figs. 4.3 and 4.4 above that the alteration of target miRNA expression reduced cellular numbers and viability by enhancing the efficacy of TAM treatment. This could possibly be due to the reduction in cholesterol content within BC cells as miR-128 and miR-223 are known to play several roles in cholesterol homeostasis and metabolism. Therefore, several cholesterol stains were used to observe the changes in cholesterol levels post transfection with a miR-128 inhibitor or a miR-223 mimic and post treatment with an endocrine treatment (TAM) and a cholesterol depleting agent (AP).

Lipid rafts of plasma membranes are responsible for many biological processes in the cell and the disruption of signalling molecules on these lipid rafts leads to impaired signalling events (Mohammad *et al.,* 2014). Therefore, many components of plasma membranes have been targeted for alternative therapeutic strategies in the treatment of cancer. The accumulation and dysregulation of cholesterol has recently been reported in various cancers, including BC, and has been linked to BC aggressiveness and progression (Di Vizio *et al.,* 2008; Duncan *et al.,* 2004; Esau *et al.,* 2016). Drug trafficking of cell membranes is influenced by the amount of cholesterol present in lipid rafts (Mohammad *et al.,* 2014). Therefore, cholesterol depleting compounds such as AP may enhance the efficacy of TAM treatment. As AP depletes cholesterol from the plasma membrane, cell membrane permeability is increased thereby altering the transport and signalling of molecules within cells (Esau *et al.,* 2016; Mohammad *et al.,* 2014). It also induces apoptosis which could be due to cholesterol depletion (Sagar *et al.,* 2014). A previous study revealed that lipid rafts were disrupted in MCF-7 cells treated with AP while normal cells (BJ cell line) remained unaffected (Esau *et al.,* 2016). Quantitative measurements revealed that cholesterol was reduced by 35% in MCF-7 cells treated with AP (Esau *et al.,* 2016). This was in accordance with what was found in the current study, where a reduction in lipid raft fluorescence was observed in all BC cell lines upon TAM + AP treatment (Fig. 4.7). In addition, the alteration of miR-128 and miR-223 expression in combination with TAM + AP led to a reduction in lipid raft fluorescence in these cells. Lipid raft accumulation inhibits cholesterol efflux in the plasma membrane through reduced ABCA1 expression. Interestingly, both miRNAs directly and indirectly regulate ABCA1 expression. Therefore, altering the expression of these target miRNAs could prevent lipid raft accumulation through increased ABCA1 expression, which increases cholesterol efflux thereby sensitising these cells to chemotherapeutic treatments.

The RCT pathway is crucial in maintaining cholesterol homeostasis. This system comprises several key proteins such as ABC efflux transporters, LDLs, HDLs, apolipoproteins, CETP, and LCAT. These proteins function together in transporting excess cholesterol from the cell to the liver for excretion (Tosheska Trajkovska and Topuzovska, 2017). Increased accumulation of intracellular cholesterol activates ABCA1 and ABCG1 activity via the cholesterol efflux process, whereby APOA1 initiates esterification of cholesterol via LCAT in HDLs to be transported to the liver to be converted to bile acids (Cooke et al., 2018). CETP mediates this transfer of CEs from HDLs to LDLs for excretion by the liver (Gu et al., 2019). In cancer cells, these pathways are dysregulated leading to an imbalance in cholesterol homeostasis. Studies have found that cells lacking CETP expression, have lower intracellular cholesterol levels due to the possible accumulation of CEs at the synthesis site (endoplasmic reticulum) (Esau *et al.*, 2016; Gu *et al.,* 2019). Since CE transport is impeded, there is inefficient removal of CEs from the endoplasmic reticulum, signalling sterol abundance, which was found in LTED cells upon miR-128 inhibition and TAM + AP treatment (Fig. 4.6c). This leads to the down-regulation of pathways that synthesize cholesterol and the up-regulation of pathways involved in cholesterol efflux (Esau *et al.,* 2016).

Overall, the above findings indicate that altering the expression of target miRNAs with TAM + AP treatment changes the fluorescence intensity of lipid rafts, free cholesterol, and CEs in BC cells (Figs. 4.5-4.6), which could possibly lead to decreased cellular viability as seen in Fig. 4.4 above. The current study provides evidence that cholesterol depletion sensitises cells towards TAM-mediated cytotoxicity. To investigate this further, several cholesterol-related and cancer drug resistance genes and proteins were selected for further pathway analysis to find the mechanisms in which these miRNAs and treatment function. This was achieved by RT-qPCR and western blotting validation. Several genes involved in BC and MDR pathways were analysed to further understand the molecular mechanisms involved in TAM-related resistance in BC. These genes included *ABCC5, BRCA2, EGFR, IGF1R, PTEN, TP53, UGCG*, and *ESR1* (Fig. 4.8). The protein expression of ERα was also analysed post-transfection and treatment (Fig. 4.9). The current study found that upon miRNA transfection and TAM + AP treatment, the expression of *EGFR, IGF1R, ESR1,* and *ABCC5* were generally down-regulated in all BC cells, while the expression of tumour suppressors, *PTEN* and *TP53,* were up-regulated.

Steroid hormones such as estrogen are crucial in maintaining cellular proliferation in ER+ BC cells, through the activation of the PI3K/Akt and MAPK signalling pathways (Liang and

Shang, 2013). These signalling pathways are activated by the increased expression of EGFR, IGF1R, and HER2. These receptor tyrosine kinases have been implicated in BC resistance (Li *et al.*, 2013b), and regulate cell proliferation and cell death. Increased activation of these signalling pathways enhances tumour growth, invasion, and metastasis. Studies have found a crosstalk between the EGFR and IGF1R signalling pathways (van der Veeken *et al.*, 2009), and the co-inhibition of EGFR and IGF1R was found to induce apoptosis in BC cells (Camirand *et al.*, 2005). A study demonstrated that miR-223 directly targets IGF1R and its downstream PI3K/Akt/mTORC1 pathway to suppress cancer cell growth (Gao *et al.*, 2017). It has also been found to function as a tumour suppressor via the IGF1R/MAPK pathway, and reverses EMT in cervical cancer (Gao *et al.*, 2017). In addition, miR-223 overexpression has been shown to suppress EGFR, PI3K, and phosphorylated Akt protein expression in NSCLC cells to regulate apoptosis (Ma *et al.*, 2019). In line with the literature, the current study demonstrated the ability of miR-223 overexpression in reducing *EGFR* and *IGF1R* expression in all three BC cell lines (Fig. 4.8). The down-regulation of these genes could therefore reduce cellular proliferation and chemoresistance in BC cells via inhibiting the proto-oncogenic PI3K/Akt and MAPK signalling pathways.

The exact mechanisms of TAM resistance are not fully elucidated; however, TAM-R BC cells remain responsive to anti-estrogen therapy while maintaining ER content. Thus, the loss of ER signalling alone is unlikely to contribute to TAM resistance (Knowlden *et al.*, 2003). Therefore, it was proposed that BC cells could make use of alternative growth factor pathways, and the inhibition of growth factor receptors and signalling pathways in combination with TAM could be an effective treatment in resistant BC cells by reverting these cells back to initial estrogen dependent ER-mediated pathways to promote cell growth (Wong and Chen, 2012). A study found that the combination therapy of TAM and an EGFR inhibitor aided in overcoming *de novo* resistance and delayed acquired resistance in BC cells (Wong and Chen, 2012). *In vitro* studies revealed that LTED cells showed re-sensitisation to TAM and estrogen deprivation when treated with lapatinib (inhibitor of HER2 and EGFR) (Wong and Chen, 2012). In addition, clinical trials showed that combination therapies were superior to just single therapies alone in terms of progression-free survival (Wong and Chen, 2012). Several other studies have shown significant results when MAPK and PI3K inhibitors were used in the treatment of TAM-R BC cell lines (Viedma-Rodríguez *et al.*, 2014). The findings of the current study demonstrate the re-sensitisation of resistant cells (LTED cells) to TAM treatment, possibly through the

inhibition of *EGFR, IGF1R,* and *ESR1* in BC cells (Fig. 4.8-4.9), following miRNA alteration and TAM + AP treatment, lowering cell viability.

Despite the development of several anticancer therapeutics in overcoming cancer mortalities, MDR remains a major obstacle in cancer recurrence. One of the major contributors to MDR, is the ABC superfamily, which is primarily involved in drug efflux. The ABC proteins are involved in extra- and intracellular transport. An increase in the activity of ABC drug efflux transporters reduces intracellular drug accumulation, whereby downstream apoptotic pathways cannot be initiated, leading to increased cell survival and MDR (Jaramillo *et al.,* 2018). One of the major contributors to BC MDR, is the increased expression of the drug efflux transporter, ABCC5 (Jansen *et al.,* 2015). This protein is part of the MRP subfamily of ABC transporters, which is highly involved in MDR. A study has shown that MCF-7 cells had high *ABCC5* expression, which led to reduced sensitivity and accumulation of an anticancer therapeutic, eventually leading to increased resistance and repression of programmed cell death (Chen *et al.,* 2021a). *ABCC5* was shown to be significantly overexpressed in BC patients receiving neoadjuvant chemotherapy (Park *et al.,* 2006), indicating that a reduction in this drug efflux transporter is crucial in reducing the resistance found in BC. The current study indicated the effective reduction of *ABCC5* expression in MCF-7 and MDA-MB-231 cells when miR-128 expression was inhibited and when cells were treated with TAM + AP (Fig. 4.8). Therefore, possibly indicating that miR-128 may be involved in MDR in BC cells.

Various studies have revealed a link between cancer drug resistance (through growth factor receptor signalling pathways) and intracellular cholesterol levels. Cholesterol metabolism may play a role in TAM-R BC cells (Hultsch *et al.,* 2018) and ER+ BC patients that are receiving cholesterol depleting agents and endocrine therapy show improved clinical outcome (Borgquist *et al.,* 2017). The cholesterol depleting agent, MβCD was found to act with TAM to suppress pro-survival signalling and induced apoptosis in TAM-R BC cells (Tiwary *et al.,* 2011). Overexpression of oncogenes that activate PI3K/Akt signalling (such as EGFR, HER2, IGF1R, and activated mutant Akt1) confer resistance to TAM in ER+ BC cells. *In vivo* studies have found that TAM-R MCF-7 xenografts showed an increase in EGFR, IGF1R, and HER2 expression. Moreover, LTED ER+ BC cell lines showed up-regulated PI3K/Akt/mTOR signalling and hyper-activation of IGF1R (Miller *et al.,* 2011). Altogether, these studies demonstrate the link between cholesterol dyshomeostasis and chemoresistance in BC. Therefore, altering the expression of target miRNAs with a TAM + AP combination treatment could reveal new strategies in which to overcome cholesterol-mediated drug resistance in BC.

Studies have found that increased CE accumulation significantly contributes to BC resistance and aggressiveness (de Gonzalo-Calvo *et al.,* 2015). Increased CE accumulation observed in cancer cells has been associated with increased signalling of the PI3K/Akt pathway as with lipid raft accumulation (Cruz *et al.,* 2020). Several genes and proteins involved in CE and lipid raft accumulation were observed in this study to identify the molecular mechanisms involved in cancer-related resistance. Although many genes are involved in the cholesterol pathway, a select few were chosen and separated based on cellular function (Fig. 4.10). These genes were separated based on cholesterol transport (*CETP* and *LCAT*), cholesterol uptake (*LDLR* and *PCSK9*), cholesterol efflux (*ABCA1* and *ABCG1*), and cholesterol biosynthesis (*HMGCR, HMGCS1, LXRα, INSIG2, SREBF1*, and *SREBF2*). Following gene expression analysis, the expression of selected cholesterol-related proteins was also observed (Figs. 4.11-4.16). The results found in Figs. 4.10-4.16 above, show that BC cells with altered miRNA expression and TAM + AP treatment, reduced the expression of genes and proteins (ABCG1, CETP, LCAT, LDLR, and PCSK9) found in the RCT pathway. The reduction in expression of these genes and proteins is crucial in reducing lipid raft and CE accumulation within the cell, thereby possibly reducing cholesterol-mediated drug resistance. This was further confirmed as lipid rafts and CE levels were reduced in BC cells (Figs. 4.6-4.7), demonstrating the potential of these miRNAs in reducing BC drug resistance through cholesterol depletion.

A reduction in SREBF1/2 expression was observed at an mRNA (Fig. 4.10) and at a protein level (Figs. 4.15-4.16) in all BC cell lines, post miRNA alteration and TAM + AP treatment. SREBF1 activates LDLR expression in low cholesterol conditions in the cell. *In vivo* experiments revealed that when SREBP1 was overexpressed, lipogenesis increased leading to fatty livers in mice (Chouinard *et al.,* 1998). Another study showed that moving glioblastoma cells into low cholesterol conditions led to a significant up-regulation of *de novo* lipogenesis which is SREBP-dependent (Guo *et al.,* 2011). The current study confirms these findings where low hormone growing conditions (LTED cell line) resulted in the up-regulation of *HMGCR* and *HMGCS1* expression in these cells, while reducing *SREBF1/2* expression (Fig. 4.10). Another study also revealed increased levels of SREBP1 expression in BC tissues with the promotion of cell migration and invasion *in vitro* (Bao *et al.,* 2016). SREBP1 inhibition has shown to increase the sensitivity of chemo-resistant cancer cells to chemotherapeutic drugs, inducing cytotoxicity in these cells (Zhao *et al.,* 2022). Increased SREBP1 signalling is therefore a critical feature for cancer cell growth; however, the mechanism by which SREBP supports tumour growth is still unclear.

Although findings have demonstrated the high levels of cholesterol found in cancer cells, little is known about how these cells sustain cholesterol levels. There is a link between CE accumulation and hyper-activation of the EGFR-linked PI3K/Akt/mTOR pathway via SREBP and LDLR activation. This leads to cell proliferation and invasion of aggressive cancer cells as these cells have a need for increased lipogenesis (Guo *et al.*, 2011; Yue *et al.*, 2014). It was elucidated that the PI3K/Akt/mTOR signalling pathway plays a critical role in up-regulating SREBP expression. Up-regulation of the PI3K/Akt/mTOR pathway leads to SREBP and LDLR activation, which initiates esterification of cholesterol into lipid droplets, allowing for fatty acid uptake thus leading to increased cell proliferation (Peck and Schulze, 2014). SREBP and the PI3K/Akt/mTOR pathway are associated in two parts. Firstly, activated Akt can stabilise the nuclear form of SREBP1 and sequentially promote its target gene expression by down-regulating an E3 ubiquitin enzyme that regulates SREBP1 N-terminus degradation (Guo *et al.*, 2014). Secondly, PI3K/Akt signalling via mammalian target of rapamycin complex 1 (mTORC1) regulates SREBP1 transcriptional activity and nuclear localisation (Guo *et al.*, 2014; Wen *et al.*, 2018). However, SREBP1 regulation by the PI3K/Akt/mTOR pathway appears to be much more complex in cancer cells. Recent studies show that high SREBP1 expression is directly implicated with tumour metastasis and predicts poor prognosis in BC patients (Wen *et al.*, 2018). Furthermore, mTORC1-related SREBP1 activation is shown to induce BC cell proliferation and growth (Wen *et al.*, 2018). In addition, lipid droplets are central organelles where several signalling-associated proteins localise. These proteins include PI3K and ERK1/2, which are involved in the MAPK signalling pathway, leading to an increase in cell survival and progression (Cruz *et al.*, 2020). The results found in Figs. 4.6-4.16 demonstrate the ability of targeted miRNA alteration and TAM + AP treatment in reducing lipid droplets and the expression of *SREBF1/2, LDLR, EGFR*, and *IGF1R*, thereby deactivating the EGFR-linked PI3K/Akt/mTOR pathway, in turn reducing cell survival and progression.

A study showed that miR-128-2 increased SREBP2, HMGCS1, LXR, and LDLR expression and decreased SREBP1, ABCA1, and ABCG1 expression in MCF-7 cells (Adlakha *et al.*, 2013). This study also demonstrated that reduced miR-128-2 expression increased ABCA1 and ABCG1 expression in HepG2, MCF-7, and HEK293 cells, demonstrating that cholesterol efflux was stimulated by miR-128 inhibition, thereby reducing cholesterol accumulation (Adlakha *et al.*, 2013). However, silencing of miR-128 could also increase cholesterol accumulation by increasing SREBP2 expression (Adlakha *et al.*, 2013). Therefore, SREBP2 not only controls cholesterol synthesis genes (*HMGCR, HMGCS1*, and *LDLR*), but could also

control pro-apoptotic miR-128-2 and regulates cholesterol metabolism. miRNAs often have dual roles in the body; therefore, manipulation of miRNA expression warrants further investigation. However, the results from the current study (Figs. 4.10-4.16) and the study conducted by Adlakha and colleagues (2013), confirm that inhibition of miR-128 may be a useful therapeutic strategy for maintaining cholesterol homeostasis and could be used for the treatment of BC.

Increased intracellular cholesterol accumulation, either via increased cholesterol synthesis, or increased cholesterol uptake, leads to the up-regulation of *ABCA1* and *ABCG1*, to maintain cholesterol homeostasis. *ABCA1* pumps cholesterol out of the cell that is then transported by HDL back to the liver (Wagschal *et al.,* 2015). Interestingly, *LDLR* and *ABCA1* are directly targeted by miR-128, and overexpression of this miRNA strongly reduced *ABCA1* and *LDLR* expression (Wagschal *et al.*, 2015). *In vivo* studies showed that the overexpression of miR-128 reduced plasma HDL levels due to the reduction of *ABCA1* expression (Wagschal *et al.*, 2015). It was concluded that miR-128 regulates circulating lipoprotein-cholesterol levels *in vivo* through the regulation of cholesterol transporters and cholesterol production and clearance. Further studies found that miR-223 expression inhibited lipogenesis and increased cholesterol efflux (Vickers *et al.,* 2014). miR-223 directly targets and represses SR-BI, thereby repressing cholesterol uptake, and inhibits cholesterol biosynthesis through direct *HMGCS1* inhibition (Vickers *et al.,* 2014). In addition, this miRNA indirectly promotes *ABCA1* expression for enhanced cellular cholesterol efflux. Therefore, both miR-128 and miR-223 are key players in cholesterol metabolism through the regulation of cholesterol biosynthesis, uptake, and efflux. Moreover, these miRNAs could potentially serve as biomarkers for altered cholesterol homeostasis in BC cells.

In the current study, it was found that in MCF-7 cells, the reduction of miR-128 expression alone was the most effective condition in increasing the cholesterol efflux transporter, *ABCG1*, while down-regulating the genes involved in cholesterol transport, synthesis, and uptake (Fig. 4.10). In the MDA-MB-231 cell line, the most effective condition for increasing cholesterol efflux while simultaneously reducing cholesterol synthesis, transport, and uptake, was when these cells were transfected with the miR-223 mimic and treated with TAM + AP. Finally, in the resistant LTED cell line, the reduction of miR-128 expression with TAM + AP treatment was the most effective condition in overcoming cholesterol dyshomeostasis. It is evident from the results obtained above, that each BC subtype responds differently to the same treatments, indicating the potential effective use of miRNAs as diagnostic and prognostic biomarkers in

BC patients. Targeting these miRNAs could also be used as a valid form of therapy via encapsulating these miRNAs in lipid nanoparticles (NPs) and introducing these NPs into the solid tumour.

Taken together, the findings from the current study reveal that both target miRNAs have direct effects in down-regulating MDR and cholesterol-related genes in BC cells. It is evident that manipulating the expression of miRNAs is effective in reducing the signalling of the EGFR-linked PI3K/Akt and MAPK pathways. These signalling pathways are critical for increased cell survival and chemoresistance in BC cells and have been linked to cholesterol synthesis and metabolism pathways. The hypothetical figure shown below (Fig. 5.1) summarises the interaction between miR-128 knockdown and miR-223 overexpression and genes related to cancer drug resistance and cholesterol homeostasis. This study provides evidence that reduced miR-128 expression and increased miR-223 expression can reduce BC cell viability and cholesterol-mediated drug resistance through a complex network of signalling pathways that are yet to be fully elucidated.

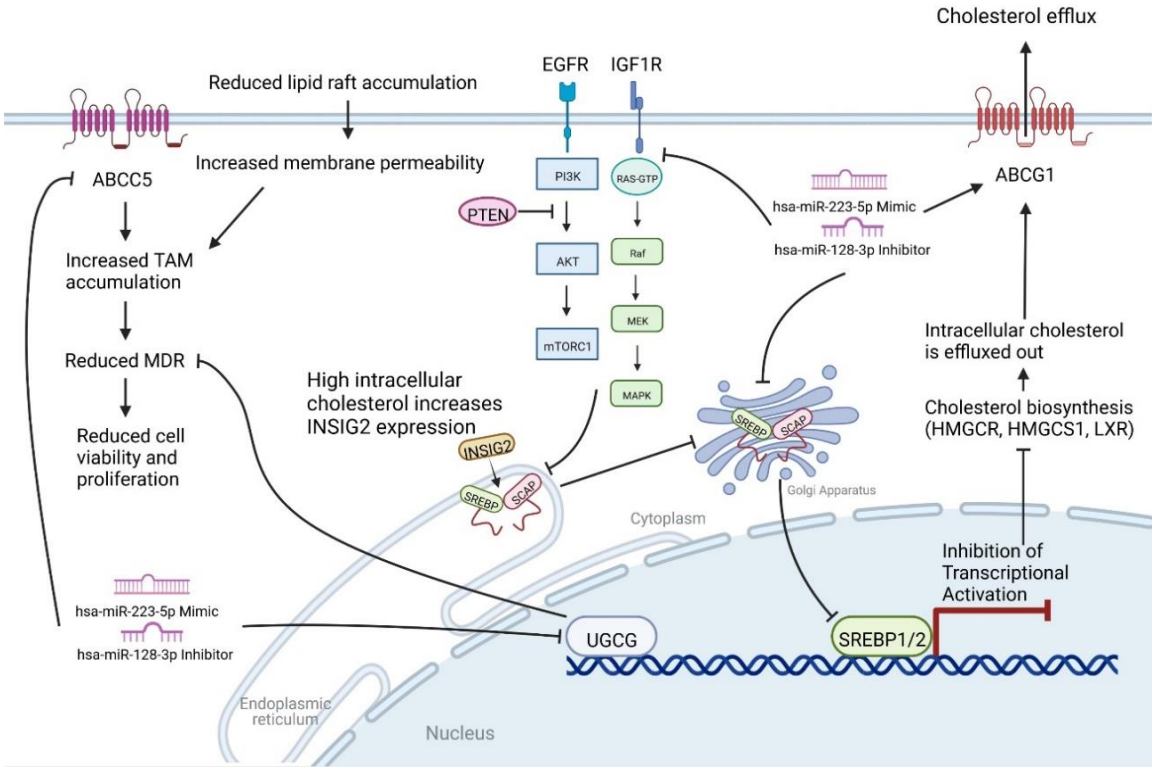

Figure 5.1: The signalling pathways affected by miR-128 and miR-223 in BC

A summary of the involvement of miR-128 and miR-223 and selected genes in BC signalling, cancer drug resistance, and cholesterol homeostasis pathways. Inhibition of miR-128 and overexpression of miR-223 directly inhibit ABCC5 and UGCG expression, thereby reducing MDR through increased intracellular drug accumulation leading to BC cytotoxicity. The aberrant expression of these miRNAs also reduces lipid raft accumulation which increases membrane permeability allowing for the intracellular accumulation of TAM, thus reducing TAM resistance. Altered miR-128 and miR-223 expression inhibits the expression of several cholesterol biosynthesis genes such as SREBP1/2, HMGCR, HMGCS1, and LXRα, thereby reducing cell survival and proliferation. When there is high intracellular cholesterol, INSIG2 is activated which binds to the SREBP-SCAP complex, inhibiting the translocation of SREBP into the nucleus, thereby inhibiting transcriptional activation for lipogenesis. There is an increase in intracellular cholesterol efflux via increased ABCG1 expression which is a target of miR-128 and miR-223. Finally, altered miR-223 and miR-128 expression directly inhibits cell signalling genes, EGFR and IGF1R, while increasing PTEN expression. Down-regulation of the PI3K/Akt/mTORC1 and MAPK signalling pathways reduces BC cell proliferation and survival and inhibits SREBP expression, thereby reducing cholesterol-mediated drug resistance in BC. Source: [Image created with BioRender.com]

6. CONCLUSIONS

In summary, there is a complex network of genes that are heavily implicated in BC cell progression and resistance. These genes are associated with both the cholesterol biosynthesis and homeostasis pathways, as well as cancer drug resistance pathways. This study demonstrates the differences in each BC cell line and highlights the different pathways in which each BC subtype function at reducing cholesterol and resistance. In MCF-7 cells, miR-128 down-regulation was favoured as several genes involved in cholesterol synthesis and transport (*HMGCR, HMGCS1, SREBF1, SREBF2, CETP, LCAT,* and *LDLR*), MDR (*ABCC5* and *UGCG*), and cell signalling (*EGFR, IGF1R,* and *ESR1*) were down-regulated, with increased cholesterol efflux (*ABCG1*). In the aggressive MDA-MB-231 cell line, the up-regulation of miR-223 with TAM + AP treatment was favoured as the cell signalling genes (*EGFR* and *ESR1*), the MDR gene (*ABCC5*), and cholesterol transport and synthesis genes (CETP, *LCAT, LDLR, HMGCR, HMGCS1, SREBF1,* and *SREBF2*) were all down-regulated, with increased expression in cholesterol efflux (*ABCG1*) and tumour suppressors (*PTEN* and *TP53*). In the resistant LTED cell line however, both miRNAs with TAM + AP treatment had similar effects, implying that either miRNA could be used as a target for the reduction of MDR found in these cells. In this cell line, the down- or up-regulation of miR-128 and miR-223, respectively with a TAM + AP treatment led to a reduction in cholesterol transport and synthesis (*CETP, SREBF1,* and *SREBF2*), and cell signalling expression (*EGFR, IGF1R,* and *ESR1*), while increasing cholesterol efflux (*ABCA1* and *ABCG1*) and *PTEN* expression. The differences highlighted in each cell line following miRNA alteration and TAM + AP treatment is a good indication of how different BC subtypes reprogramme their cell signalling and metabolic pathways to adapt to various treatments. Therefore, understanding the molecular mechanisms involved in each BC subtype is crucial for developing new anticancer therapeutics. The current study attempted to improve our understanding of the molecular mechanisms through which miRNA expression can alleviate cholesterol-mediated TAM resistance in BC and provide new avenues to identify useful biomarkers to overcome this resistance. However, miRNAs have a plethora of off-target effects and further investigation is warranted for targeting miRNA expression as a possible anticancer strategy. Nevertheless, this study demonstrated the positive effects in the use of miRNAs as possible diagnostic and prognostic biomarkers in resistance and cholesterol metabolism in BC. This study also revealed the effective strategy of using a cholesterol depleting agent (AP) to significantly re-sensitise BC cells towards enhanced TAM treatment; therefore, reducing cancer-related drug resistance via cholesterol depletion.

7. FUTURE WORK

The biological mechanisms for the observations made in the current study are still unknown as literature is limited. Therefore, future work will be focused on observing and understanding the effects of combination treatments and miRNA alteration on cholesterol-related proteins. Apoptotic assays should be performed to confirm early- and late-stage apoptosis in BC cells. This can be achieved by use of several assays such as an APOPercentage™ assay, a MOMP assay, and a caspase 3/7 assay. This will give a clear view of whether the current treatment induces apoptosis in BC cells. Cell cycle analysis should also be performed to uncover where cell proliferation changes are occurring and give better insights into what is happening in the cells upon miRNA transfection and which genes the miRNAs are targeting at a broader level.

The effects of a miR-128 mimic and a miR-223 inhibitor should also be investigated to confirm whether the chosen mimic and inhibitor for this current study were most appropriate in reducing cholesterol-mediated drug resistance in BC cells. In addition, a dual transfection of the miR-128 inhibitor and miR-223 mimic should be performed to observe and understand the synergistic effects of these target miRNAs on BC cell viability.

Several more genes and proteins involved in highlighted pathways should be investigated to confirm the expression changes in BC cells upon treatment and transfection. In addition, methods such as next-generation or RNA sequencing and bioinformatic analyses on the transcriptome should be incorporated to discover pathways that are induced or silenced upon overexpression or knockdown of target miRNAs with and without TAM + AP. This will provide a deeper understanding of the molecular mechanisms involved in cholesterol-mediated drug resistance in BC. Furthermore, knocking down or overexpressing selected genes from these analyses should be assessed to indicate the roles of candidate genes in cancer drug resistance downstream of TAM + AP treatment.

Preliminary studies have found that encapsulating 5 nM of the miR-128 inhibitor into lipid NPs for 96 h was effective at reducing miR-128 expression in MDA-MB-231 cells (Fig. S4). Therefore, it is pertinent to further confirm whether NPs can enter BC cells to inhibit the expression of target miRNAs before performing *in vivo* studies. Once this has been confirmed, the use of NPs as a delivery system in a preclinical mouse model should be performed to highlight the use of miRNAs as viable targets for the treatment of BC.

8. LIMITATIONS OF THE STUDY

The use of *in vitro* models to study the molecular mechanisms involved in cholesterol-mediated drug resistance in the treatment of BC is important. Although these models are useful, the limitation in this is that they are not true representations of the disease state and does not account for other modifications present *in vivo*, which does not allow for the complete understanding of BC and resistance. Investigating the combination of an endocrine treatment and a cholesterol depleting agent in a cell line model is not an accurate representation observed in the whole-body system. A compound may show great efficacy *in vitro* but will not have the same effect on the tumour. Additionally, compounds may show great efficacy *in vivo* due to high toxicities, which could render the combination treatment from advancing to clinical trials. Animal models allow us to take the tumour microenvironment and whole system of the organism into consideration, whereas cell line models do not allow for this. Using cell line models alone is not enough in a study dealing with so many factors of resistance in a tumour microenvironment; therefore, an *in vivo* mouse model needs to be conducted to compare the results of cell line models. However, the current study is a novel concept where baseline findings were needed in a cell line model before advancing into animal studies. The current findings provided us with insightful information to design future *in vivo* experiments and clinical trials going forward. These *in vivo* experiments could not be performed due to time and financial constraints.

In addition, the current study made use of the HEK293 cell line as a control cell line, as opposed to the normal-like MCF10A epithelial cell line. The MCF10A cell line would be the preferential control cell line given the nature of the study, however; due to limited funds and availability, this was not possible. The authors deemed the HEK293 cell line as an acceptable control cell line due to these cells being non-breast cancer like and would give insights into how miRNA manipulation with a combination treatment would affect various cells differently. The results obtained herein confirm the specificity of the proposed combination treatments to BC cells, whilst having little to no effect on HEK293 cells.

Another limitation of this study is the use of miRNAs which are quickly degraded and subjected to RNAses. For this reason, the miRNA needs to be encapsulated into stable lipid NPs for an easier delivery mechanism directly into the tumour. The use of a liposomal transfection reagent used in this preliminary study was sufficient in encapsulating the target miRNA and allowing for the transport and release of these miRNAs directly into the cell. However, in an *in vivo*

setting, this will not suffice. Therefore, the encapsulation of target miRNAs into stable NPs needs further investigation before advancing to animal studies.

This study only investigated the effects of miR-128-3p and miR-223-5p expression. Further analysis is required for miR-128-5p and miR-223-3p expression and the effects of this altered expression. This will aid in a deeper understanding of the direct and indirect target genes in which these miRNAs regulate. This will also provide us with an overall understanding of miRNA expression in BC patients for a more personalised approach in using these miRNAs as prognostic and diagnostic factors.

Finally, the biggest limitation of the current study was the financial constraint imposed throughout. For this reason, several assays could not have been performed to supplement the conclusions that were made. For example, the expression of several more BC and drug resistance-related proteins needs to be observed to achieve a deeper understanding of the pathways affected by miRNA manipulation and TAM + AP treatment. In addition, assays such as confocal microscopy, RNA sequencing, cell cycle analysis, cholesterol quantitation, and apoptotic assays need to be further investigated. Nonetheless, this study provides a significant amount of baseline data and opens new avenues for future research in this exciting field. The results of this study warrant further investigations into the roles of these two miRNAs in cholesterol-mediated drug resistance not only in BC, but also in other cholesterol-rich cancers such as prostate, pancreatic and colon.

9. TROUBLESHOOTING

All experiments were standardised in MCF7, MDA-MB-231, LTED, and HEK293 cells and assays were performed in several ways for optimal results.

Transfection of miRNAs

Differing concentrations (5 nM and 10 nM) of the miR-128 inhibitor and miR-223 mimic were tested in cell lines upon transfection for different periods of time (48 h, 72 h, 96 h). Upon RT-qPCR analysis, it was found that concentrations of 5 nM and 10 nM of inhibitor or mimic had similar effects at altering the expression of the target miRNA; therefore, a concentration of 5 nM was used for transfection. Similarly, 48 h and 72 h incubation periods led to similar results in altering expression and for this reason, a 48 h incubation period was selected for a shorter transfection period before performing subsequent experiments.

All other assays performed in the current study (cell counts, cell viability, cholesterol staining, RT-qPCR, SDS-PAGE, and western blotting) were previously optimised and did not require further troubleshooting.

10. REFERENCES

Ackermann, T., and Tardito, S. (2019). Cell Culture Medium Formulation and Its Implications in Cancer Metabolism. Trends Cancer *5*, 329-332.

Acunzo, M., Romano, G., Wernicke, D., and Croce, C.M. (2015). MicroRNA and cancer – A brief overview. Advances in Biological Regulation *57*, 1-9.

Adlakha, Y.K., Khanna, S., Singh, R., Singh, V.P., Agrawal, A., and Saini, N. (2013). Pro-apoptotic miRNA-128-2 modulates ABCA1, ABCG1 and RXRalpha expression and cholesterol homeostasis. Cell death & disease *4*, e780.

Afonso, M.S., Machado, R.M., Lavrador, M.S., Quintao, E.C.R., Moore, K.J., and Lottenberg, A.M. (2018). Molecular Pathways Underlying Cholesterol Homeostasis. Nutrients *10*, 760.

Ali, S., Rasool, M., Chaoudhry, H., N Pushparaj, P., Jha, P., Hafiz, A., Mahfooz, M., Abdus Sami, G., Azhar Kamal, M., Bashir, S., *et al.* (2016). Molecular mechanisms and mode of tamoxifen resistance in breast cancer. Bioinformation *12*, 135-139.

Anderson, E., and Clarke, R.B. (2004). Steroid Receptors and Cell Cycle in Normal Mammary Epithelium. Journal of Mammary Gland Biology and Neoplasia *9*, 3-13.

Angius, A., Cossu-Rocca, P., Arru, C., Muroni, M.R., Rallo, V., Carru, C., Uva, P., Pira, G., Orrù, S., and De Miglio, M.R. (2020). Modulatory Role of microRNAs in Triple Negative Breast Cancer with Basal-Like Phenotype. Cancers (Basel) *12*.

Antalis, C., and Buhman, K. (2012). Lipoproteins and cancer. INTECH Open Access Publisher, 623-646.

Aziz, F., Chakraborty, A., Khan, I., and Monts, J. (2022). Relevance of miR-223 as Potential Diagnostic and Prognostic Markers in Cancer. Biology *11*.

Badana, A.K., Chintala, M., Gavara, M.M., Naik, S., Kumari, S., Kappala, V.R., Iska, B.R., and Malla, R.R. (2018). Lipid rafts disruption induces apoptosis by attenuating expression of LRP6 and survivin in triple negative breast cancer. Biomedicine & Pharmacotherapy *97*, 359-368.

Bao, J., Zhu, L., Zhu, Q., Su, J., Liu, M., and Huang, W. (2016). SREBP-1 is an independent prognostic marker and promotes invasion and migration in breast cancer. Oncology letters *12*, 2409-2416.

Bełtowski, J., Wójcicka, G., and Jamroz-Wiśniewska, A. (2009). Adverse effects of statins - mechanisms and consequences. Current drug safety *4*, 209-228.

Ben Hassen, C., Gutierrez-Pajares, J.L., Guimaraes, C., Guibon, R., Pinault, M., Fromont, G., and Frank, P.G. (2020). Apolipoprotein-mediated regulation of lipid metabolism induces distinctive effects in different types of breast cancer cells. Breast Cancer Research *22*, 38.

Borgquist, S., Giobbie-Hurder, A., Ahern, T.P., Garber, J.E., Colleoni, M., Láng, I., Debled, M., Ejlertsen, B., Moos, R.v., Smith, I., *et al.* (2017). Cholesterol, Cholesterol-Lowering Medication Use, and Breast Cancer Outcome in the BIG 1-98 Study. *35*, 1179-1188.

Boudreau, D.M., Yu, O., and Johnson, J. (2010). Statin Use and Cancer Risk: A Comprehensive Review. Expert opinion on drug safety *9*, 603-621.

Buffa, F.M., Camps, C., Winchester, L., Snell, C.E., Gee, H.E., Sheldon, H., Taylor, M., Harris, A.L., and Ragoussis, J. (2011). microRNA-Associated Progression Pathways and Potential Therapeutic Targets Identified by Integrated mRNA and microRNA Expression Profiling in Breast Cancer. Cancer research *71*, 5635-5645.

Buhaescu, I., and Izzedine, H. (2007). Mevalonate pathway: A review of clinical and therapeutical implications. Clinical Biochemistry *40*, 575-584.

Bytyçi, I., Penson, P.E., Mikhailidis, D.P., Wong, N.D., Hernandez, A.V., Sahebkar, A., Thompson, P.D., Mazidi, M., Rysz, J., Pella, D., *et al.* (2022). Prevalence of statin intolerance: a meta-analysis European Heart Journal *43*, 3213-3223.

Calin, G.A., Dumitru, C.D., Shimizu, M., Bichi, R., Zupo, S., Noch, E., Aldler, H., Rattan, S., Keating, M., Rai, K., *et al.* (2002). Frequent deletions and down-regulation of micro- RNA genes miR15 and miR16 at 13q14 in chronic lymphocytic leukemia. Proceedings of the National Academy of Sciences of the United States of America *99*, 15524-15529.

Camirand, A., Zakikhani, M., Young, F., and Pollak, M. (2005). Inhibition of insulin-like growth factor-1 receptor signaling enhances growth-inhibitory and proapoptotic effects of gefitinib (Iressa) in human breast cancer cells. Breast cancer research : BCR *7*, R570-579.

Campbell, M.J., Esserman, L.J., Zhou, Y., Shoemaker, M., Lobo, M., Borman, E., Baehner, F., Kumar, A.S., Adduci, K., Marx, C., *et al.* (2006). Breast Cancer Growth Prevention by Statins. Cancer research *66*, 8707-8714.

Cariou, B., Goronflot, T., Rimbert, A., Boullu, S., Le May, C., Moulin, P., Pichelin, M., Potier, L., Smati, S., Sultan, A., *et al.* (2021). Routine use of statins and increased COVID-19 related mortality in inpatients with type 2 diabetes: Results from the CORONADO study. Diabetes & metabolism *47*, 101202.

Chae, Y.K., Yousaf, M., Malecek, M.K., Carneiro, B., Chandra, S., Kaplan, J., Kalyan, A., Sassano, A., Platanias, L.C., and Giles, F. (2015). Statins as anti-cancer therapy; Can we translate preclinical and epidemiologic data into clinical benefit? Discovery medicine *20*, 413-427.

Chan, K.K.W., Oza, A.M., and Siu, L.L. (2003). The Statins as Anticancer Agents. Clinical Cancer Research *9*, 10-19.

Chang, M. (2012). Tamoxifen resistance in breast cancer. Biomol Ther (Seoul) *20*, 256-267.

Chang, T.Y., Chang, C.C., and Cheng, D. (1997). Acyl-coenzyme A:cholesterol acyltransferase. Annual review of biochemistry *66*, 613-638.

Chen, J., Wang, Z., Gao, S., Wu, K., Bai, F., Zhang, Q., Wang, H., Ye, Q., Xu, F., Sun, H., *et al.* (2021a). Human drug efflux transporter ABCC5 confers acquired resistance to pemetrexed in breast cancer. Cancer cell international *21*, 136.

Chen, L., Zhu, X., Han, B., Ji, L., Yao, L., and Wang, Z. (2021b). High Expression of microRNA-223 Indicates a Good Prognosis in Triple-Negative Breast Cancer. Frontiers in oncology *11*, 630432.

Chimento, A., Casaburi, I., Avena, P., Trotta, F., De Luca, A., Rago, V., Pezzi, V., and Sirianni, R. (2019). Cholesterol and Its Metabolites in Tumor Growth: Therapeutic Potential of Statins in Cancer Treatment *9*.

Chouinard, R.A., Luo, Y., Osborne, T.F., Walsh, A., and Tall, A.R. (1998). Sterol Regulatory Element Binding Protein-1 Activates the Cholesteryl Ester Transfer Protein Gene in Vivobut Is Not Required for Sterol Up-regulation of Gene Expression. J Biol Chem *273*, 22409-22414.

Cianfrocca, M., and Goldstein, L.J. (2004). Prognostic and predictive factors in early-stage breast cancer. The oncologist *9*, 606-616.

Clemons, M., and Goss, P. (2001). Estrogen and the risk of breast cancer. N Engl J Med *344*, 1804.

Clendening, J.W., and Penn, L.Z. (2012). Targeting tumor cell metabolism with statins. Oncogene *31*, 4967-4978.

Cooke, A.L., Morris, J., Melchior, J.T., Street, S.E., Jerome, W.G., Huang, R., Herr, A.B., Smith, L.E., Segrest, J.P., Remaley, A.T., *et al.* (2018). A thumbwheel mechanism for APOA1 activation of LCAT activity in HDL. Journal of lipid research *59*, 1244-1255.

Cruz, A.L.S., Barreto, E.d.A., Fazolini, N.P.B., Viola, J.P.B., and Bozza, P.T. (2020). Lipid droplets: platforms with multiple functions in cancer hallmarks. Cell death & disease *11*, 105.

Cruz, P.M., Mo, H., McConathy, W., Sabnis, N.A., and Lacko, A.G. (2013). The role of cholesterol metabolism and cholesterol transport in carcinogenesis: a review of scientific findings, relevant to future cancer therapeutics. Frontiers in pharmacology *4*, 119.

Davison, Z., de Blacquière, G.E., Westley, B.R., and May, F.E.B. (2011). Insulin-like growth factor-dependent proliferation and survival of triple-negative breast cancer cells: implications for therapy. Neoplasia *13*, 504-515.

Dawson, S.J., Provenzano, E., and Caldas, C. (2009). Triple negative breast cancers: Clinical and prognostic implications. European Journal of Cancer *45*, 27-40.

de Gonzalo-Calvo, D., López-Vilaró, L., Nasarre, L., Perez-Olabarria, M., Vázquez, T., Escuin, D., Badimon, L., Barnadas, A., Lerma, E., and Llorente-Cortés, V. (2015). Intratumor cholesteryl ester accumulation is associated with human breast cancer proliferation and aggressive potential: a molecular and clinicopathological study. BMC Cancer *15*, 460.

de Groot, S., Charehbili, A., van Laarhoven, H.W.M., Mooyaart, A.L., Dekker-Ensink, N.G., van de Ven, S., Janssen, L.G.M., Swen, J.J., Smit, V.T.H.B.M., Heijns, J.B., *et al.* (2016). Insulin-like growth factor 1 receptor expression and IGF1R 3129G > T polymorphism are associated with response to neoadjuvant chemotherapy in breast cancer patients: results from the NEOZOTAC trial (BOOG 2010-01). Breast cancer research : BCR *18*, 3-3.

DeBose-Boyd, R.A., and Ye, J. (2018). SREBPs in Lipid Metabolism, Insulin Signaling, and Beyond. Trends Biochem Sci *43*, 358-368.

Desjardins, P., and Conklin, D. (2010). NanoDrop microvolume quantitation of nucleic acids. J Vis Exp, 2565.

Di Vizio, D., Solomon, K.R., and Freeman, M.R. (2008). Cholesterol and Cholesterol-Rich Membranes in Prostate Cancer: An Update. Tumori Journal *94*, 633-639.

Didichenko, S.A., Navdaev, A., Cukier, A.M., Gille, A., Schuetz, P., Spycher, M.O., Therond, P., Chapman, M.J., Kontush, A., and Wright, S.D. (2016). Enhanced HDL functionality in small HDL species produced upon remodeling of HDL by reconstituted HDL, CSL112: effects on cholesterol efflux, anti-inflammatory and antioxidative activity. Circulation research *119*, 751-763.

DiMarco, D.M., and Fernandez, M.L. (2015). The Regulation of Reverse Cholesterol Transport and Cellular Cholesterol Homeostasis by MicroRNAs. Biology *4*, 494-511.

Dou, L., Han, K., Xiao, M., and Lv, F. (2019). miR-223-5p Suppresses Tumor Growth and Metastasis in Non-Small Cell Lung Cancer by Targeting E2F8. Oncology research *27*, 261-268.

Dulak, J., and Józkowicz, A. (2005). Anti-angiogenic and anti-inflammatory effects of statins: relevance to anti-cancer therapy. Current cancer drug targets *5*, 579-594.

Duncan, R.E., El-Sohemy, A., and Archer, M.C. (2004). Mevalonate Promotes the Growth of Tumors Derived from Human Cancer Cells in Vivo and Stimulates Proliferation in Vitro with Enhanced Cyclin-dependent Kinase-2 Activity. J Biol Chem *279*, 33079-33084.

Duncan, R.E., El-Sohemy, A., and Archer, M.C. (2005). Statins and Cancer Development. Cancer Epidemiology Biomarkers & Prevention *14*, 1897-1898.

Encarnación-Medina, J., Ortiz, C., Vergne, R., Padilla, L., and Matta, J. (2019). MicroRNA Expression Changes in Women with Breast Cancer Stratified by DNA Repair Capacity Levels. J Oncol *2019*, 7820275-7820275.

Esau, L., Sagar, S., Bangarusamy, D., and Kaur, M. (2016). Identification of CETP as a molecular target for estrogen positive breast cancer cell death by cholesterol depleting agents. Genes & cancer *7*, 309-322.

Fagan, D.H., Uselman, R.R., Sachdev, D., and Yee, D. (2012). Acquired Resistance to Tamoxifen Is Associated with Loss of the Type I Insulin-like Growth Factor Receptor: Implications for Breast Cancer Treatment. *72*, 3372-3380.

Gajate, C., Gonzalez-Camacho, F., and Mollinedo, F. (2009). Lipid raft connection between extrinsic and intrinsic apoptotic pathways. Biochemical and Biophysical Research Communications *380*, 780-784.

Gallagher, E.J., Zelenko, Z., Neel, B.A., Antoniou, I.M., Rajan, L., Kase, N., and LeRoith, D. (2017). Elevated tumor LDLR expression accelerates LDL cholesterol-mediated breast cancer growth in mouse models of hyperlipidemia. Oncogene *36*, 6462-6471.

Gao, Y., Lin, L., Li, T., Yang, J., and Wei, Y. (2017). The role of miRNA-223 in cancer: Function, diagnosis and therapy. Gene *616*, 1-7.

Garcia-Bermudez, J., Baudrier, L., Bayraktar, E.C., Shen, Y., La, K., Guarecuco, R., Yucel, B., Fiore, D., Tavora, B., Freinkman, E., *et al.* (2019). Squalene accumulation in cholesterol auxotrophic lymphomas prevents oxidative cell death. Nature *567*, 118-122.

Gong, B., Hu, H., Chen, J., Cao, S., Yu, J., Xue, J., Chen, F., Cai, Y., He, H., and Zhang, L. (2013). Caprin-1 is a novel microRNA-223 target for regulating the proliferation and invasion of human breast cancer cells. Biomedicine & Pharmacotherapy *67*, 629-636.

Gstraunthaler, G., Lindl, T., and van der Valk, J. (2013). A plea to reduce or replace fetal bovine serum in cell culture media. Cytotechnology *65*, 791-793.

Gu, L., Saha, S.T., Thomas, J., and Kaur, M. (2019). Targeting cellular cholesterol for anticancer therapy. Federation of European Biochemical Societies *286*, 4192-4208.

Guan, X., Liu, Z., Zhao, Z., Zhang, X., Tao, S., Yuan, B., Zhang, J., Wang, D., Liu, Q., and Ding, Y. (2019). Emerging roles of low-density lipoprotein in the development and treatment of breast cancer. Lipids in health and disease *18*, 137-137.

Guest, C.B., Hartman, M.E., O'Connor, J.C., Chakour, K.S., Sovari, A.A., and Freund, G.G. (2007). Phagocytosis of cholesteryl ester is amplified in diabetic mouse macrophages and is largely mediated by CD36 and SR-A. PloS one *2*, e511-e511.

Guo, D., Bell, EH., Mischel, P., Chakravarti, A. (2014). Targeting SREBP-1-driven lipid metabolism to treat cancer. Current Pharmaceutical Design *20*, 2619-2626.

Guo, D., Reinitz, F., Youssef, M., Hong, C., Nathanson, D., Akhavan, D., Kuga, D., Amzajerdi, A.N., Soto, H., Zhu, S., *et al.* (2011). An LXR agonist promotes glioblastoma cell death through inhibition of an EGFR/AKT/SREBP-1/LDLR-dependent pathway. Cancer discovery *1*, 442-456.

Györffy, B., Lanczky, A., Eklund, A.C., Denkert, C., Budczies, J., Li, Q., and Szallasi, Z. (2010). An online survival analysis tool to rapidly assess the effect of 22,277 genes on breast cancer prognosis using microarray data of 1,809 patients. Breast cancer research and treatment *123*, 725-731.

Hanahan, D. (2022). Hallmarks of Cancer: New Dimensions. Cancer Discovery *12*, 31-46.

Hanahan, D., and Weinberg, R.A. (2000). The hallmarks of cancer. Cell *100*, 57-70.

Haneklaus, M., Gerlic, M., O'Neill, L.A.J., and Masters, S.L. (2013). miR-223: infection, inflammation and cancer. Journal of Internal Medicine *274*, 215-226.

Harborg, S., Heide-Jørgensen, U., Ahern, T.P., Ewertz, M., Cronin-Fenton, D., and Borgquist, S. (2020). Statin use and breast cancer recurrence in postmenopausal women treated with adjuvant aromatase inhibitors: a Danish population-based cohort study. Breast Cancer Res Treat *183*, 153-160.

Hata, A., and Kashima, R. (2016). Dysregulation of microRNA biogenesis machinery in cancer. Crit Rev Biochem Mol Biol *51*, 121-134.

He, H., Tian, W., Chen, H., and Jiang, K. (2016). MiR-944 functions as a novel oncogene and regulates the chemoresistance in breast cancer. Tumor Biology *37*, 1599-1607.

Heffner, L.J., and Schust, D.J. (2010). The Reproductive System at a Glance, J.W.a. Sons, ed., pp. pp. 16.

Henriques Palma, G.B., and Kaur, M. (2022). Cholesterol Depletion Modulates Drug Resistance Pathways to Sensitize Resistant Breast Cancer Cells to Tamoxifen. Anticancer research *42*, 565-579.

Hodges, L.C., Cook, J.D., Lobenhofer, E.K., Li, L., Bennett, L., Bushel, P.R., Aldaz, C.M., Afshari, C.A., and Walker, C.L. (2003). Tamoxifen Functions As a Molecular Agonist Inducing Cell Cycle-Associated Genes in Breast Cancer Cells. Molecular Cancer Research *1*, 300-311.

Horton, J.D., Bashmakov, Y., Shimomura, I., and Shimano, H. (1998). Regulation of sterol regulatory element binding proteins in livers of fasted and refed mice. PNAS *95*, 5987-5992.

Horton, J.D., Cohen, J.C., and Hobbs, H.H. (2007). Molecular biology of PCSK9: its role in LDL metabolism. Trends Biochem Sci *32*, 71-77.

Hultsch, S., Kankainen, M., Paavolainen, L., Kovanen, R.-M., Ikonen, E., Kangaspeska, S., Pietiäinen, V., and Kallioniemi, O. (2018). Association of tamoxifen resistance and lipid reprogramming in breast cancer. BMC cancer *18*, 850-850.

Hutchinson, S., Battaglia, S., Røberg-Larsen, H., Hughes, T., and Thorne, J. (2018). Cholesterol metabolism and chemo-resistance in breast cancer. Endocrine Abstracts *59*, 111.

Jakic B, Buszko M, Cappellano G, Wick G. (2017). Elevated sodium leads to the increased expression of HSP60 and induces apoptosis in HUVECs. PLoS One *12*(6):e0179383.

Jakobisiak, M., and Golab, J. (2003). Potential antitumor effects of statins (Review). International journal of oncology *23*, 1055-1069.

Janes, P.W., Ley, S.C., and Magee, A.I. (1999). Aggregation of lipid rafts accompanies signaling via the T cell antigen receptor. The Journal of cell biology *147*, 447-461.

Jansen, R.S., Mahakena, S., de Haas, M., Borst, P., and van de Wetering, K. (2015). ATP-binding Cassette Subfamily C Member 5 (ABCC5) Functions as an Efflux Transporter of Glutamate Conjugates and Analogs. J Biol Chem *290*, 30429-30440.

Jaramillo, A.C., Saig, F.A., Cloos, J., Jansen, G., and Peters, G.J. (2018). How to overcome ATP-binding cassette drug efflux transporter-mediated drug resistance? Cancer Drug Resistance *1*, 6-29.

Jeng, M.-H., Shupnik, M.A., Bender, T.P., Westin, E.H., Bandyopadhyay, D., Kumar, R., Masamura, S., and Santen, R.J. (1998). Estrogen Receptor Expression and Function in Long-Term Estrogen-Deprived Human Breast Cancer Cells. Endocrinology *139*, 4164-4174.

Jeng, M.-H., Yue, W., Eischeid, A., Wang, J.-P., and Santen, R.J. (2000). Role of MAP kinase in the enhanced cell proliferation of long term estrogen deprived human breast cancer cells. Breast cancer research and treatment *62*, 167-175.

Jeon, T.I., Esquejo, R.M., Roqueta-Rivera, M., Phelan, P.E., Moon, Y.A., Govindarajan, S.S., Esau, C.C., and Osborne, T.F. (2013). An SREBP-responsive microRNA operon contributes to a regulatory loop for intracellular lipid homeostasis. Cell metabolism *18*, 51-61.

Jeon, T.I., and Osborne, T.F. (2016). miRNA and cholesterol homeostasis. Biochimica et biophysica acta *1861*, 2041-2046.

Katzenellenbogen, B.S., Kendra, K.L., Norman, M.J., and Berthois, Y. (1987). Proliferation, Hormonal Responsiveness, and Estrogen Receptor Content of MCF-7 Human Breast Cancer Cells Grown in the Short-Term and Long-Term Absence of Estrogens. Cancer research *47*, 4355-4360.

Knowlden, J.M., Hutcheson, I.R., Jones, H.E., Madden, T., Gee, J.M.W., Harper, M.E., Barrow, D., Wakeling, A.E., and Nicholson, R.I. (2003). Elevated Levels of Epidermal Growth Factor Receptor/c-erbB2 Heterodimers Mediate an Autocrine Growth Regulatory Pathway in Tamoxifen-Resistant MCF-7 Cells. Endocrinology *144*, 1032-1044.

Kohler, B.A., Sherman, R.L., Howlader, N., Jemal, A., Ryerson, A.B., Henry, K.A., Boscoe, F.P., Cronin, K.A., Lake, A., Noone, A.-M., *et al.* (2015). Annual Report to the Nation on the Status of Cancer, 1975-2011, Featuring Incidence of Breast Cancer Subtypes by Race/Ethnicity, Poverty, and State. JNCI: Journal of the National Cancer Institute *107*, djv048-djv048.

Kondo, A., Yamamoto, S., Nakaki, R., Shimamura, T., Hamakubo, T., Sakai, J., Kodama, T., Yoshida, T., Aburatani, H., and Osawa, T. (2017). Extracellular Acidic pH Activates the Sterol Regulatory Element-Binding Protein 2 to Promote Tumor Progression. Cell reports *18*, 2228-2242.

Kralik, P., and Ricchi, M. (2017). A Basic Guide to Real Time PCR in Microbial Diagnostics: Definitions, Parameters, and Everything. Frontiers in Microbiology *8*.

Kubista, M., Aakerman, B., and Norden, B. (1987). Characterization of interaction between DNA and 4',6-diamidino-2-phenylindole by optical spectroscopy. Biochemistry *26*, 4545-4553.

Kumar, A.S., Benz, C.C., Shim, V., Minami, C.A., Moore, D.H., and Esserman, L.J. (2008). Estrogen receptor-negative breast cancer is less likely to arise among lipophilic statin users. Cancer epidemiology, biomarkers & prevention : a publication of the American Association for Cancer Research, cosponsored by the American Society of Preventive Oncology *17*, 1028-1033.

Kurashina, Y., Imashiro, C., Hirano, M., Kuribara, T., Totani, K., Ohnuma, K., Friend, J., and Takemura, K. (2019). Enzyme-free release of adhered cells from standard culture dishes using intermittent ultrasonic traveling waves. Communications Biology *2*, 393.

Kwizera, R., Akampurira, A., Kandole, T.K., Nielsen, K., Kambugu, A., Meya, D.B., Boulware, D.R., Rhein, J., and Team, A.-C.S. (2017). Evaluation of trypan blue stain in a haemocytometer for rapid detection of cerebrospinal fluid sterility in HIV patients with cryptococcal meningitis. BMC Microbiol *17*, 182-182.

Lánczky, A., Nagy, Á., Bottai, G., Munkácsy, G., Szabó, A., Santarpia, L., and Győrffy, B. (2016). miRpower: a web-tool to validate survival-associated miRNAs utilizing expression data from 2178 breast cancer patients. Breast Cancer Res Treat *160*, 439-446.

Li, M., Fu, W., Wo, L., Shu, X., Liu, F., and Li, C. (2013a). miR-128 and its target genes in tumorigenesis and metastasis. Experimental Cell Research *319*, 3059-3064.

Li, P., Veldwijk, M.R., Zhang, Q., Li, Z.-b., Xu, W.-c., and Fu, S. (2013b). Co-inhibition of epidermal growth factor receptor and insulin-like growth factor receptor 1 enhances radiosensitivity in human breast cancer cells. BMC Cancer *13*, 297.

Li, Y.C., Park, M.J., Ye, S.-K., Kim, C.-W., and Kim, Y.-N. (2006). Elevated levels of cholesterol-rich lipid rafts in cancer cells are correlated with apoptosis sensitivity induced by cholesterol-depleting agents. Am J Pathol *168*, 1107-1405.

Liang, J., and Shang, Y. (2013). Estrogen and cancer. Annual review of physiology *75*, 225-240.

Lim, P.K., Bliss, S.A., Patel, S.A., Taborga, M., Dave, M.A., Gregory, L.A., Greco, S.J., Bryan, M., Patel, P.S., and Rameshwar, P. (2011). Gap Junction–Mediated Import of MicroRNA from Bone Marrow Stromal Cells Can Elicit Cell Cycle Quiescence in Breast Cancer Cells. Cancer research *71*, 1550-1560.

Lin, S., and Gregory, R.I. (2015). MicroRNA biogenesis pathways in cancer. Nat Rev Cancer *15*, 321-333.

Llaverias, G., Danilo, C., Mercier, I., Daumer, K., Capozza, F., Williams, T.M., Sotgia, F., Lisanti, M.P., and Frank, P.G. (2011). Role of cholesterol in the development and progression of breast cancer. Am J Pathol *178*.

Loh, H.Y., Norman, B.P., Lai, K.S., Rahman, N., Alitheen, N.B.M., and Osman, M.A. (2019). The Regulatory Role of MicroRNAs in Breast Cancer. Int J Mol Sci *20*.

Lou, G., Ma, N., Xu, Y., Jiang, L., Yang, J., Wang, C., Jiao, Y., Gao, X (2015). Differential distribution of U6 (RNU6-1) expression in human carcinoma tissues demonstrates the requirement for caution in the internal control gene selection for microRNA quantification. International Journal of Molecular Medicine *36*, 1400-1408.

Lowe, S.W., and Lin, A.W. (2000). Apoptosis in cancer. Carcinogenesis *21*, 485-495.

Lu, W.J., Desta, Z., and Flockhart, D.A. (2012). Tamoxifen metabolites as active inhibitors of aromatase in the treatment of breast cancer. Breast cancer research and treatment *131*, 473-481.

Lynch, J., and Wang, J. (2014). MicroRNA Regulation of Cancer Stem Cell Phenotypes. . SOJ Genet Sci *1*, 1-8.

Ma, H.P., Kong, W.X., Li, X.Y., Li, W., Zhang, Y., and Wu, Y. (2019). miRNA-223 is an anticancer gene in human non-small cell lung cancer through the PI3K/AKT pathway by targeting EGFR. Oncol Rep *41*, 1549-1559.

Mahammad, S., and Parmryd, I. (2015). Cholesterol depletion using methyl-β-cyclodextrin. Methods in molecular biology (Clifton, NJ) *1232*, 91-102.

Mandal, C.C., and Rahman, M.M. (2014). Targeting Intracellular Cholesterol is a Novel Therapeutic Strategy for Cancer Treatment. Journal of cancer science & therapy *6*, 510-513.

Mansoori, B., Mohammadi, A., Davudian, S., Shirjang, S., and Baradaran, B. (2017). The Different Mechanisms of Cancer Drug Resistance: A Brief Review. Adv Pharm Bull *7*, 339-348.

Martin, L.-A., Farmer, I., Johnston, S.R.D., Ali, S., Marshall, C., and Dowsett, M. (2003). Enhanced Estrogen Receptor (ER) α, ERBB2, and MAPK Signal Transduction Pathways Operate during the Adaptation of MCF-7 Cells to Long Term Estrogen Deprivation. J Biol Chem *278*, 30458-30468.

Martín, M.G., Pfrieger, F., and Dotti, C.G. (2014). Cholesterol in brain disease: sometimes determinant and frequently implicated. EMBO reports *15*, 1036-1052.

Masamura, S., Santner, S.J., Heitjan, D.F., and Santen, R.J. (1995). Estrogen deprivation causes estradiol hypersensitivity in human breast cancer cells. The Journal of Clinical Endocrinology & Metabolism *80*, 2918-2925.

Masri, S., Liu, Z., Phung, S., Wang, E., Yuan, Y.-C., and Chen, S. (2010). The role of microRNA-128a in regulating TGFbeta signaling in letrozole-resistant breast cancer cells. Breast cancer research and treatment *124*, 89-99.

Massarweh, S., Osborne, C.K., Creighton, C.J., Qin, L., Tsimelzon, A., Huang, S., Weiss, H., Rimawi, M., and Schiff, R. (2008). Tamoxifen Resistance in Breast Tumors Is Driven by Growth Factor Receptor Signaling with Repression of Classic Estrogen Receptor Genomic Function. *68*, 826-833.

Maxfield, F.R., and Wüstner, D. (2012). Analysis of cholesterol trafficking with fluorescent probes. Methods Cell Biol *108*, 367-393.

Miller, T.E., Ghoshal, K., Ramaswamy, B., Roy, S., Datta, J., Shapiro, C.L., Jacob, S., and Majumder, S. (2008). MicroRNA-221/222 confers tamoxifen resistance in breast cancer by targeting p27Kip1. The Journal of biological chemistry *283*, 29897-29903.

Miller, T.W., Balko, J.M., and Arteaga, C.L. (2011). Phosphatidylinositol 3-Kinase and Antiestrogen Resistance in Breast Cancer. Journal of Clinical Oncology *29*, 4452-4461.

Mohammad, N., Malvi, P., Meena, A.S., Singh, S.V., Chaube, B., Vannuruswamy, G., Kulkarni, M.J., and Bhat, M.K. (2014). Cholesterol depletion by methyl-β-cyclodextrin augments tamoxifen induced cell death by enhancing its uptake in melanoma. Molecular Cancer *13*, 204.

Monchusi, B., and Kaur, M. (2020). microRNAs targeting cellular cholesterol: implications for combating anticancer drug resistance. Genes & cancer *11*, 20-42.

Mostaghel, E.A., Solomon, K.R., Pelton, K., Freeman, M.R., and Montgomery, R.B. (2012). Impact of Circulating Cholesterol Levels on Growth and Intratumoral Androgen Concentration of Prostate Tumors. PloS one *7*, e30062.

Musgrove, E.A., and Sutherland, R.L. (2009). Biological determinants of endocrine resistance in breast cancer. Nature Reviews Cancer *9*, 631.

Nazih, H., and Bard, J.M. (2020). Cholesterol, Oxysterols and LXRs in Breast Cancer Pathophysiology. Int J Mol Sci *21*, 1356.

Nelson, E.R., Chang, C.-y., and McDonnell, D.P. (2014). Cholesterol and breast cancer pathophysiology. Trends in Endocrinology & Metabolism *25*, 649-655.

Park, S., Shimizu, C., Shimoyama, T., Takeda, M., Ando, M., Kohno, T., Katsumata, N., Kang, Y.K., Nishio, K., and Fujiwara, Y. (2006). Gene expression profiling of ATP-binding cassette (ABC) transporters as a predictor of the pathologic response to neoadjuvant chemotherapy in breast cancer patients. Breast Cancer Res Treat *99*, 9-17.

Payne, A.H., and Hales, D.B. (2004). Overview of Steroidogenic Enzymes in the Pathway from Cholesterol to Active Steroid Hormones. Endocrine Reviews *25*, 947-970.

Peck, B., and Schulze, A. (2014). Cholesteryl esters: fueling the fury of prostate cancer. Cell Metab *19*, 350-352.

Pinatel, E.M., Orso, F., Penna, E., Cimino, D., Elia, A.R., Circosta, P., Dentelli, P., Brizzi, M.F., Provero, P., and Taverna, D. (2014). miR-223 is a coordinator of breast cancer progression as revealed by bioinformatics predictions. PloS one *9*, e84859.

Proudfoot, N.J., Furger, A., and Dye, M.J. (2002). Integrating mRNA Processing with Transcription. Cell *108*, 501-512.

Putcha, G.V., Harris, C.A., Moulder, K.L., Easton, R.M., Thompson, C.B., and Johnson, E.M. (2002). Intrinsic and extrinsic pathway signaling during neuronal apoptosis: lessons from the analysis of mutant mice. The Journal of Cell Biology *157*, 441-453.

Raghu, H., Sodadasu, P.K., Malla, R.R., Gondi, C.S., Estes, N., and Rao, J.S. (2010). Localization of uPAR and MMP-9 in lipid rafts is critical for migration, invasion and angiogenesis in human breast cancer cells. BMC cancer *10*, 647-647.

Rao, P.K., Toyama, Y., Chiang, H.R., Gupta, S., Bauer, M., Medvid, R., Reinhardt, F., Liao, R., Krieger, M., Jaenisch, R., *et al.* (2009). Loss of cardiac microRNA-mediated regulation leads to dilated cardiomyopathy and heart failure. Circulation research *105*, 585-594.

Ravindranath, K.J., Mohaideen, N.S.M.H., and Srinivasan, H. (2022). Phytocompounds of Onion Target Heat Shock Proteins (HSP70s) to Control Breast Cancer Malignancy. Applied Biochemistry and Biotechnology *194*, 4836-4851.

Riggins, R.B., Schrecengost, R.S., Guerrero, M.S., and Bouton, A.H. (2007). Pathways to tamoxifen resistance. Cancer letters *256*, 1-24.

Roy, R., Chun, J., and Powell, S.N. (2011). BRCA1 and BRCA2: different roles in a common pathway of genome protection. Nat Rev Cancer *12*, 68-78.

Ryan, B.M., Robles, A.I., and Harris, C.C. (2010). Genetic variation in microRNA networks: the implications for cancer research. Nat Rev Cancer *10*, 389-402.

Ryu, A.H., Eckalbar, W.L., Kreimer, A., Yosef, N., and Ahituv, N. (2017). Use antibiotics in cell culture with caution: genome-wide identification of antibiotic-induced changes in gene expression and regulation. Scientific reports *7*, 7533-7533.

Sagar, S., Esau, L., Moosa, B., Khashab, N.M., Bajic, V.B., and Kaur, M. (2014). Cytotoxicity and Apoptosis Induced by a Plumbagin Derivative in Estrogen Positive MCF-7 Breast Cancer Cells. Anti-Cancer Agents in Medicinal Chemistry *14*, 170-180.

Santen, R.J., Song, R.X., Masamura, S., Yue, W., Fan, P., Sogon, T., Hayashi, S.-i., Nakachi, K., and Eguchi, H. (2008). Adaptation to Estradiol Deprivation Causes Up-Regulation of Growth Factor Pathways and Hypersensitivity to Estradiol in Breast Cancer Cells. Advances in experimental medicine and biology *630*, 19-34.

Santen, R.J., Song, R.X., Zhang, Z., Kumar, R., Jeng, M.-H., Masamura, S., Yue, W., and Berstein, L. (2003). Adaptive hypersensitivity to estrogen: mechanism for superiority of aromatase inhibitors over selective estrogen receptor modulators for breast cancer treatment and prevention. Endocrine-Related Cancer *10*, 111-130.

Santen, R.J., Song, R.X., Zhang, Z., Kumar, R., Jeng, M.H., Masamura, A., Lawrence, J., Jr., Berstein, L., and Yue, W. (2005). Long-term estradiol deprivation in breast cancer cells up-regulates growth factor signaling and enhances estrogen sensitivity. Endocr Relat Cancer *12 Suppl 1*, S61-73.

Schneider, C.A., Rasband, W.S., and Eliceiri, K.W. (2012). NIH Image to ImageJ: 25 years of image analysis. Nature Methods *9*, 671-675.

Schwarzenbach, H., da Silva, A.M., Calin, G., and Pantel, K. (2015). Data Normalization Strategies for MicroRNA Quantification. Clinical chemistry *61*, 1333-1342.

Shim, W.-S., Conaway, M., Masamura, S., Yue, W., Wang, J.-P., Kumar, R., and Santen, R.J. (2000). Estradiol Hypersensitivity and Mitogen-Activated Protein Kinase Expression in Long-Term Estrogen Deprived Human Breast Cancer Cells in Vivo1. Endocrinology *141*, 396-405.

Sikand, K., Singh, J., Ebron, J.S., and Shukla, G.C. (2012). Housekeeping gene selection advisory: glyceraldehyde-3-phosphate dehydrogenase (GAPDH) and β-actin are targets of miR-644a. PloS one *7*, e47510.

Sim, Y., Lim, C., Phyu, N., Tan, K.T.B., Chew, L.S.T., Wong, C.Y., Madhukumar, P., Yong, W.S., Lim, S.Z., Hamzah, J.L.B., *et al.* (2022). The Impact of Statin Use and Breast Cancer Recurrence - A Retrospective Study in Singapore. Frontiers in oncology *12*, 835320.

Simigdala, N., Gao, Q., Pancholi, S., Roberg-Larsen, H., Zvelebil, M., Ribas, R., Folkerd, E., Thompson, A., Bhamra, A., Dowsett, M., *et al.* (2016). Cholesterol biosynthesis pathway as a novel mechanism of resistance to estrogen deprivation in estrogen receptor-positive breast cancer. Breast Cancer Research *18*, 58.

Simões, A.E.S., Pereira, D.M., Amaral, J.D., Nunes, A.F., Gomes, S.E., Rodrigues, P.M., Lo, A.C., D'Hooge, R., Steer, C.J., Thibodeau, S.N., *et al.* (2013). Efficient recovery of proteins from multiple source samples after trizol® or trizol®LS RNA extraction and long-term storage. BMC Genomics *14*, 181.

Smith, P.K., Krohn, R.I., Hermanson, G.T., Mallia, A.K., Gartner, F.H., Provenzano, M.D., Fujimoto, E.K., Goeke, N.M., Olson, B.J., and Klenk, D.C. (1985). Measurement of protein using bicinchoninic acid. Analytical Biochemistry *150*, 76-85.

Snejdrlova, M., Altschmiedova, T., Vrablik, M., Stulc, T., Lastuvka, J., Lanska, V., and Ceska, R. (2020). Statin Intolerance in Clinical Practice. Current atherosclerosis reports *22*, 27.

Stancu, C., and Sima, A. (2001). Statins: mechanism of action and effects. Journal of cellular and molecular medicine *5*, 378-387.

Su, X., Xu, X., Li, G., Lin, B., Cao, J., and Teng, L. (2014). ER-α36: a novel biomarker and potential therapeutic target in breast cancer. OncoTargets and therapy *7*, 1525-1533.

Sun, X., Li, Y., Zheng, M., Zuo, W., and Zheng, W. (2016). MicroRNA-223 Increases the Sensitivity of Triple-Negative Breast Cancer Stem Cells to TRAIL-Induced Apoptosis by Targeting HAX-1. PloS one *11*, e0162754.

Tiwary, R., Yu, W., deGraffenried, L.A., Sanders, B.G., and Kline, K. (2011). Targeting cholesterol-rich microdomains to circumvent tamoxifen-resistant breast cancer. Breast cancer research : BCR *13*, R120.

Tosheska Trajkovska, K., and Topuzovska, S. (2017). High-density lipoprotein metabolism and reverse cholesterol transport: strategies for raising HDL cholesterol. Anatolian journal of cardiology *18*, 149-154.

Tosi, M.R., and Tugnoli, V. (2005). Cholesteryl esters in malignancy. Clinica Chimica Acta *359*, 27-45.

Tsuji, K., Ojima, M., Otabe, K., Horie, M., Koga, H., Sekiya, I., and Muneta, T. (2017). Effects of Different Cell-Detaching Methods on the Viability and Cell Surface Antigen Expression of Synovial Mesenchymal Stem Cells. Cell Transplant *26*, 1089-1102.

Vallianou, N.G., Kostantinou, K., Kougias, M., and Kazazis, C. (2014). Statins and Cancer. Anti-Cancer Agents in Medicinal Chemistry *14*, 706-712.

van der Veeken, J., Oliveira, S., Schiffelers, R.M., Storm, G., van Bergen En Henegouwen, P.M., and Roovers, R.C. (2009). Crosstalk between epidermal growth factor receptor- and insulin-like growth factor-1 receptor signaling: implications for cancer therapy. Current cancer drug targets *9*, 748-760.

van Tonder, A., Joubert, A.M., and Cromarty, A.D. (2015). Limitations of the 3-(4,5-dimethylthiazol-2-yl)-2,5-diphenyl-2H-tetrazolium bromide (MTT) assay when compared to three commonly used cell enumeration assays. BMC Res Notes *8*, 47-47.

Van Wyhe, R.D., Rahal, O.M., and Woodward, W.A. (2017). Effect of statins on breast cancer recurrence and mortality: a review. Breast Cancer (Dove Med Press) *9*, 559-565.

Vickers, K.C., Landstreet, S.R., Levin, M.G., Shoucri, B.M., Toth, C.L., Taylor, R.C., Palmisano, B.T., Tabet, F., Cui, H.L., Rye, K.A., *et al.* (2014). MicroRNA-223 coordinates cholesterol homeostasis. Proceedings of the National Academy of Sciences of the United States of America *111*, 14518-14523.

Viedma-Rodríguez, R., Baiza-Gutman, L., Salamanca-Gómez, F., Diaz-Zaragoza, M., Martínez-Hernández, G., Ruiz Esparza-Garrido, R., Velázquez-Flores, M.A., and Arenas-Aranda, D. (2014). Mechanisms associated with resistance to tamoxifen in estrogen receptor-positive breast cancer (Review). Oncology Reports *32*, 3-15.

Wagschal, A., Najafi-Shoushtari, S.H., Wang, L., Goedeke, L., Sinha, S., deLemos, A.S., Black, J.C., Ramírez, C.M., Li, Y., Tewhey, R., *et al.* (2015). Genome-wide identification of microRNAs regulating cholesterol and triglyceride homeostasis. Nat Med *21*, 1290-1297.

Wang, Q., Cheng, Y., Wang, Y., Fan, Y., Li, C., Zhang, Y., Wang, Y., Dong, Q., Ma, Y., Teng, Y.-E., *et al.* (2017). Tamoxifen reverses epithelial-mesenchymal transition by demethylating miR-200c in triple-negative breast cancer cells. BMC cancer *17*, 492-492.

Wang, Q., Jiang, J., Ying, G., Xie, X.-Q., Zhang, X., Xu, W., Zhang, X., Song, E., Bu, H., Ping, Y.-F., *et al.* (2018). Tamoxifen enhances stemness and promotes metastasis of ERα36(+) breast cancer by upregulating ALDH1A1 in cancer cells. Cell Research *28*, 336-358.

WHO (2020). Cancer Fact Sheets.

Wilson, R.C., Tambe, A., Kidwell, M.A., Noland, C.L., Schneider, C.P., and Doudna, J.A. (2015). Dicer-TRBP complex formation ensures accurate mammalian microRNA biogenesis. Mol Cell *57*, 397-407.

Winter, J., Jung, S., Keller, S., Gregory, R.I., and Diederichs, S. (2009). Many roads to maturity: microRNA biogenesis pathways and their regulation. Nature Cell Biology *11*, 228-234.

Wong, C., and Chen, S. (2012). The development, application and limitations of breast cancer cell lines to study tamoxifen and aromatase inhibitor resistance. The Journal of Steroid Biochemistry and Molecular Biology *131*, 83-92.

Xiao, M., Lou, C., Xiao, H., Yang, Y., Cai, X., Li, C., Jia, S., and Huang, Y. (2017). MiR-128 regulation of glucose metabolism and cell proliferation in triple-negative breast cancer. British Journal of Surgery *105*, 75-85.

Yamaguchi, R., Perkins, G., and Hirota, K. (2015). Targeting cholesterol with β-cyclodextrin sensitizes cancer cells for apoptosis. Federation of European Biochemical Societies *589*, 4097-4105.

Yang, M., Liu, W., Pellicane, C., Sahyoun, C., Joseph, B.K., Gallo-Ebert, C., Donigan, M., Pandya, D., Giordano, C., Bata, A., *et al.* (2014). Identification of miR-185 as a regulator of de novo cholesterol biosynthesis and low density lipoprotein uptake. Journal of lipid research *55*, 226-238.

Yang, Y., Jiang, Z., Ma, N., Wang, B., Liu, J., Zhang, L., and Gu, L. (2018). MicroRNA-223 Targeting STIM1 Inhibits the Biological Behavior of Breast Cancer. Cellular Physiology and Biochemistry *45*, 856-866.

Yoshikawa, M., Iinuma, H., Umemoto, Y., Yanagisawa, T., Matsumoto, A., and Jinno, H. (2018). Exosome-encapsulated microRNA-223-3p as a minimally invasive biomarker for the early detection of invasive breast cancer. Oncol Lett *15*, 9584-9592.

Yue, S., Li, J., Lee, S.-Y., Lee, H.J., Shao, T., Song, B., Cheng, L., Masterson, T.A., Liu, X., Ratliff, T.L., *et al.* (2014). Cholesteryl ester accumulation induced by PTEN loss and PI3K/AKT activation underlies human prostate cancer aggressiveness. Cell Metab *19*, 393-406.

Yue, W., Wang, J.-P., Conaway, M.R., Li, Y., and Santen, R.J. (2003). Adaptive hypersensitivity following long-term estrogen deprivation: involvement of multiple signal pathways. The Journal of Steroid Biochemistry and Molecular Biology *86*, 265-274.

Zhang, N., Chung, N., and Oldenburg, N. (1999). A Simple Statistical Parameter for Use in Evaluation and Validation of High Throughput Screening Assays. J Biomol Screen *4*, 67-73.

Zhao, Q., Lin, X., and Wang, G. (2022). Targeting SREBP-1-Mediated Lipogenesis as Potential Strategies for Cancer. Frontiers in oncology *12*, 952371.

Zheng, M., Kallio, A., and Harkonen, P. (2007). Tamoxifen-Induced Rapid Death of MCF-7 Breast Cancer Cells Is Mediated via Extracellularly Signal-Regulated Kinase Signaling and Can Be Abrogated by Estrogen. Endocrinology *148*, 2764-2777.

Zhu, Y., Yu, F., Jiao, Y., Feng, J., Tang, W., Yao, H., Gong, C., Chen, J., Su, F., and Zhang, Y. (2011). Reduced miR-128 in breast tumor–initiating cells induces chemotherapeutic resistance via Bmi-1 and ABCC5. Clinical Cancer Research *17*, 7105-7115.

Zipper, H., Brunner, H., Bernhagen, J., and Vitzthum, F. (2004). Investigations on DNA intercalation and surface binding by SYBR Green I, its structure determination and methodological implications. Nucleic Acids Res *32*, e103-e103.

11. SUPPLEMENTARY MATERIAL

Table S1: Primer sequences and pathways

Gene	Strand	Pathway	Annealing temperature (°C)	Primer sequence (5'-3')
ABCA1	Forward	Cholesterol efflux	63	ACCCACCCTATGAACAACATGA
ABCA1	Reverse	Cholesterol efflux	63	GAGTCGGGTAACGGAAACAGG
ABCG1	Forward	Cholesterol and drug efflux	55.7	ATTCAGGGACCTTTCCTATTCGG
ABCG1	Reverse	Cholesterol and drug efflux	55.7	CTCACCACTATTGAACTTCCCG
ABCC5	Forward	Drug efflux	56.2	GAACTCGACCGTTGGAATGC
ABCC5	Reverse	Drug efflux	56.2	TCATCCAGGATTCTGAGCTGAG
CETP	Forward	Cholesterol transport	54	GGCCAAGTCAAGTATGGGTTG
CETP	Reverse	Cholesterol transport	54	ACAGACACGTTCTGAATGGAGA
HMGCR	Forward	Cholesterol biosynthesis	55.7	TGATTGACCTTTCCAGAGCAAG
HMGCR	Reverse	Cholesterol biosynthesis	55.7	CTAAAATTGCCATTCCACGAGC
HMGCS1	Forward	Cholesterol biosynthesis	56	GATGTGGGAATTGTTGCCCTT
HMGCS1	Reverse	Cholesterol biosynthesis	56	ATTGTCTCTGTTCCAACTTCCAG
INISG2	Forward	Cholesterol biosynthesis	55	CTTGATGATTCGAGGAGTAGTGC
INSIG2	Reverse	Cholesterol biosynthesis	55	CAGGTGGAAAGAGCGTCACAT
LCAT	Forward	Cholesterol esterification and transport	56	ACCTGGTCAACAATGGCTACG
LCAT	Reverse	Cholesterol esterification and transport	56	TAGAGCAAGTGTAGACAGCCG

LDLR	Forward	Cholesterol uptake	58.7	TCTGCAACATGGCTAGAGACT
LDLR	Reverse	Cholesterol uptake	58.7	TCCAAGCATTCGTTGGTCCC
PCSK9	Forward	Cholesterol uptake	58	AGACCCACCTCTCGCAGTC
PCSK9	Reverse	Cholesterol uptake	58	GGAGTCCTCCTCGATGTAGTC
SREBF1	Forward	Cholesterol biosynthesis	58	ACAGTGACTTCCCTGGCCTAT
SREBF1	Reverse	Cholesterol biosynthesis	58	GCATGGACGGGTACATCTTCAA
SREBF2	Forward	Cholesterol biosynthesis	58	CCTGGGAGACATCGACGAGAT
SREBF2	Reverse	Cholesterol biosynthesis	58	TGAATGACCGTTGCACTGAAG
BRCA2	Forward	dsDNA break repair	55	CACCCACCCTTAGTTCTACTGT
BRCA2	Reverse	dsDNA break repair	55	CCAATGTGGTCTTTGCAGCTAT
EGFR	Forward	PI3K/Akt and MAPK signalling	57	AGGCACGAGTAACAAGCTCAC
EGFR	Reverse	PI3K/Akt and MAPK signalling	57	ATGAGGACATAACCAGCCACC
ESR1	Forward	Cellular proliferation	56.2	GGGAAGTATGGCTATGGAATCTG
ESR1	Reverse	Cellular proliferation	56.2	TGGCTGGACACATATAGTCGTT
IGF1R	Forward	PI3K/Akt and MAPK signalling	56.9	TCGACATCCGCAACGACTATC
IGF1R	Reverse	PI3K/Akt and MAPK signalling	56.9	CCAGGGCGTAGTTGTAGAAGAG
PTEN	Forward	PI3K/Akt/PKB and mTOR signalling	56	TGGATTCGACTTAGACTTGACCT
PTEN	Reverse	PI3K/Akt/PKB and mTOR signalling	56	GGTGGGTTATGGTCTTCAAAAGG

TP53	Forward	Tumour suppressor	55	AACTGCGGGACGAGACAGA
TP53	Reverse	Tumour suppressor	55	AGCTTCAAGAGCGACAAGTTTT
UGCG	Forward	GSL biosynthesis	55	GAATGGCCGTCTTCGGGTT
UGCG	Reverse	GSL biosynthesis	55	AGGTGTAATCGGGTGTAGATGAT

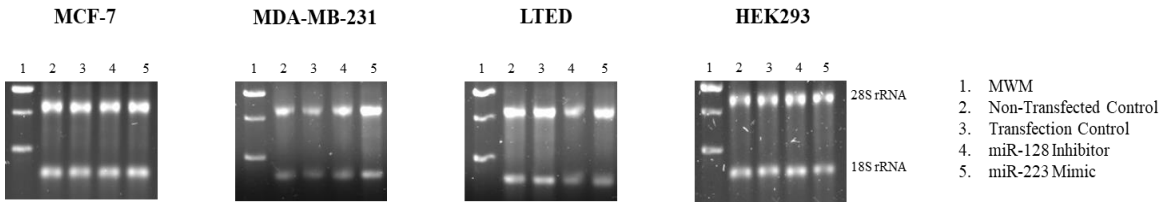

Figure S1: RNA integrity gels

Extracted RNA samples (500 ng) from MCF-7, MDA-MB-231, LTED, and HEK293 cells were run on a 1% agarose gel to check the integrity of samples by examining the rRNA bands. The intensity of the upper ribosomal band (28S) was twice that of the intensity of the lower band (18S), indicating good RNA integrity. ***Lane 1:*** *molecular weight marker,* ***Lane 2:*** *non-transfected control,* ***Lane 3:*** *transfection control,* ***Lane 4:*** *cells transfected with 5 nM miR-128-3p inhibitor,* ***Lane 5:*** *cells transfected with 5 nM miR-128-5p mimic. RNA concentrations, ratios, and integrity was observed in 3 biological replicates prior to downstream assays.*

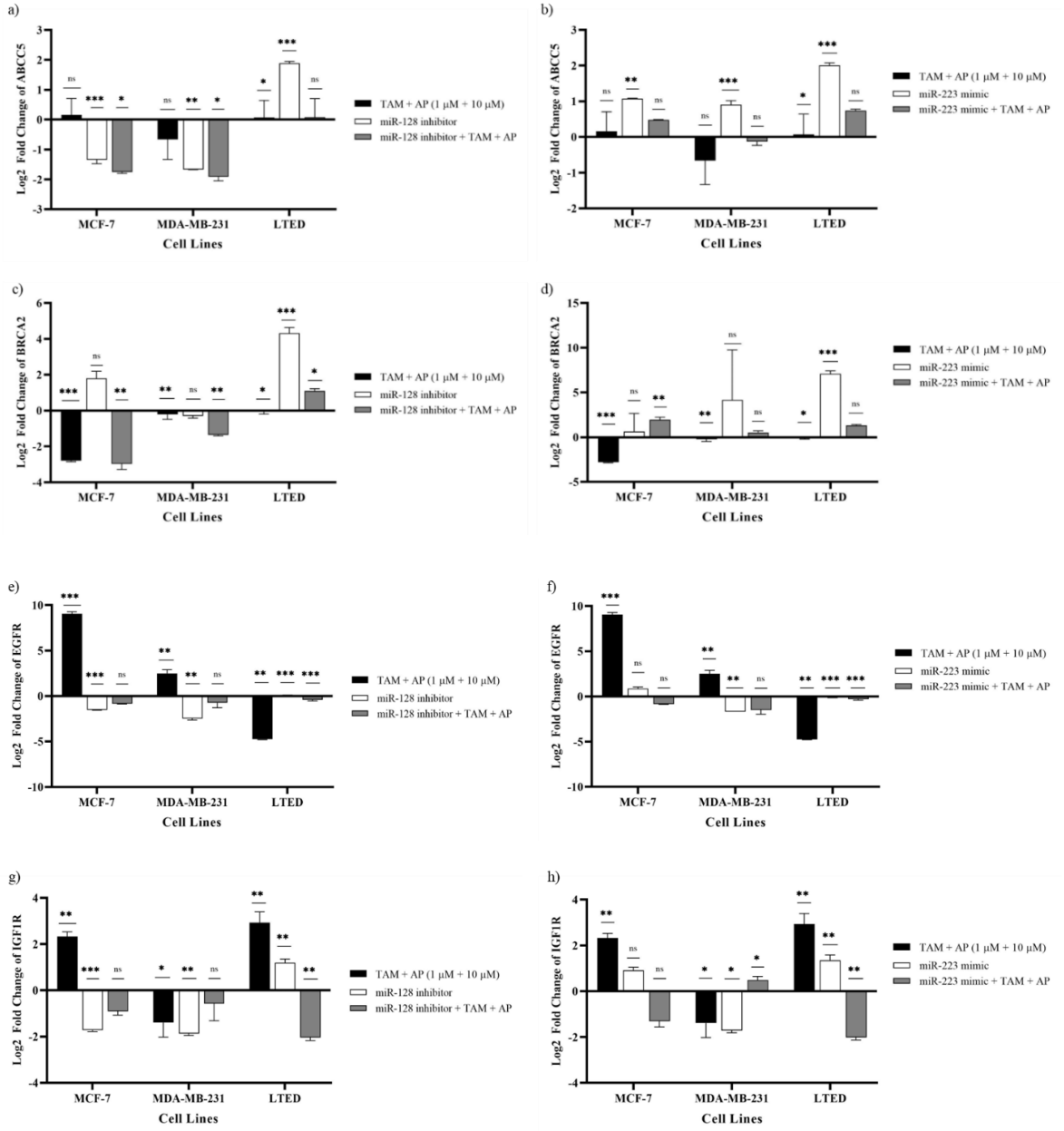
a)
Log2 Fold Change of ABCC5
MCF-7
MDA-MB-231
LTED
Cell Lines
TAM + AP (1 μM + 10 μM)
miR-128 inhibitor
miR-128 inhibitor + TAM + AP
b)
Log2 Fold Change of ABCC5
MCF-7
MDA-MB-231
LTED
Cell Lines
TAM + AP (1 μM + 10 μM)
miR-223 mimic
miR-223 mimic + TAM + AP
c)
Log2 Fold Change of BRCA2
MCF-7
MDA-MB-231
LTED
Cell Lines
TAM + AP (1 μM + 10 μM)
miR-128 inhibitor
miR-128 inhibitor + TAM + AP
d)
Log2 Fold Change of BRCA2
MCF-7
MDA-MB-231
LTED
Cell Lines
TAM + AP (1 μM + 10 μM)
miR-223 mimic
miR-223 mimic + TAM + AP
e)
Log2 Fold Change of EGFR
MCF-7
MDA-MB-231
LTED
Cell Lines
TAM + AP (1 μM + 10 μM)
miR-128 inhibitor
miR-128 inhibitor + TAM + AP
f)
Log2 Fold Change of EGFR
MCF-7
MDA-MB-231
LTED
Cell Lines
TAM + AP (1 μM + 10 μM)
miR-223 mimic
miR-223 mimic + TAM + AP
g)
Log2 Fold Change of IGF1R
MCF-7
MDA-MB-231
LTED
Cell Lines
TAM + AP (1 μM + 10 μM)
miR-128 inhibitor
miR-128 inhibitor + TAM + AP
h)
Log2 Fold Change of IGF1R
MCF-7
MDA-MB-231
LTED
Cell Lines
TAM + AP (1 μM + 10 μM)
miR-223 mimic
miR-223 mimic + TAM + AP

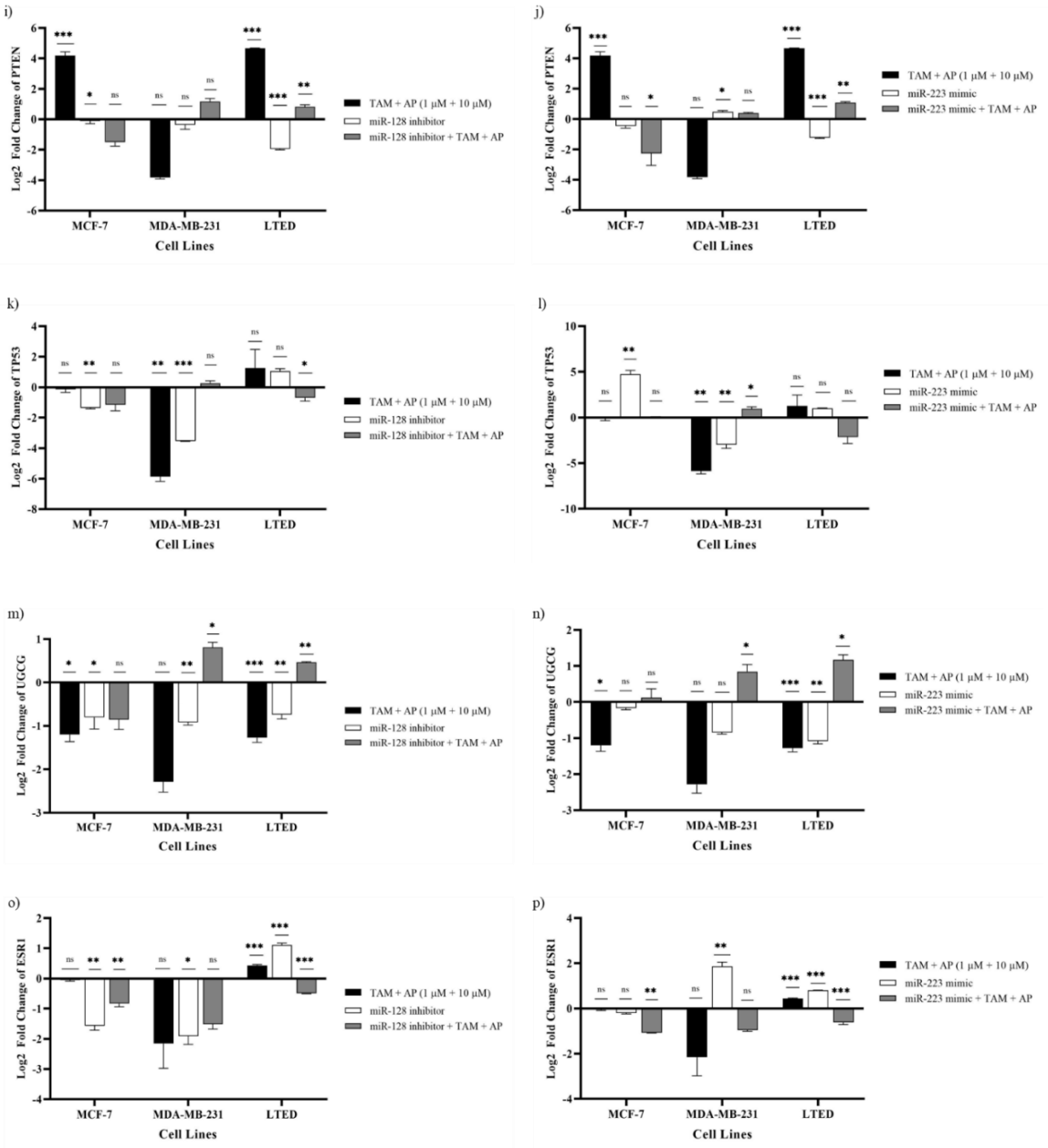

Figure S2: Changes in mRNA expression of genes involved in cancer drug resistance and BC pathways

Graphs indicating mRNA expression as log2 fold change. Endogenous expression of the GAPDH gene was used to normalise the data. Graphs on the left indicate BC cells solely treated with TAM + AP, BC cells solely transfected with a miR-128 inhibitor, and BC cells transfected with a miR-128 inhibitor and treated with TAM + AP. Graphs on the right indicate BC cells solely treated with TAM + AP, BC cells solely transfected with a miR-223 mimic, and BC cells transfected with a miR-223 mimic and treated with TAM + AP. Genes involved in cancer drug resistance pathways include: ABCC5 ***(a-b)****, EGFR* ***(e-f)****, IGF1R* ***(g-h)****, PTEN* ***(i-j)****, TP53* ***(k-l)****, and UGCG* ***(m-n)****. Genes involved in BC pathways include: BRCA2* ***(c-d)****, and*

ESR1 ***(o-p)***. *Statistical analysis was performed by using a student's t-test, where * P < 0.05, ** P < 0.01, *** P < 0.001, and ns = non-significant compared to untreated or non-transfection controls. Data represents the mean ± S.D; (n=3).*

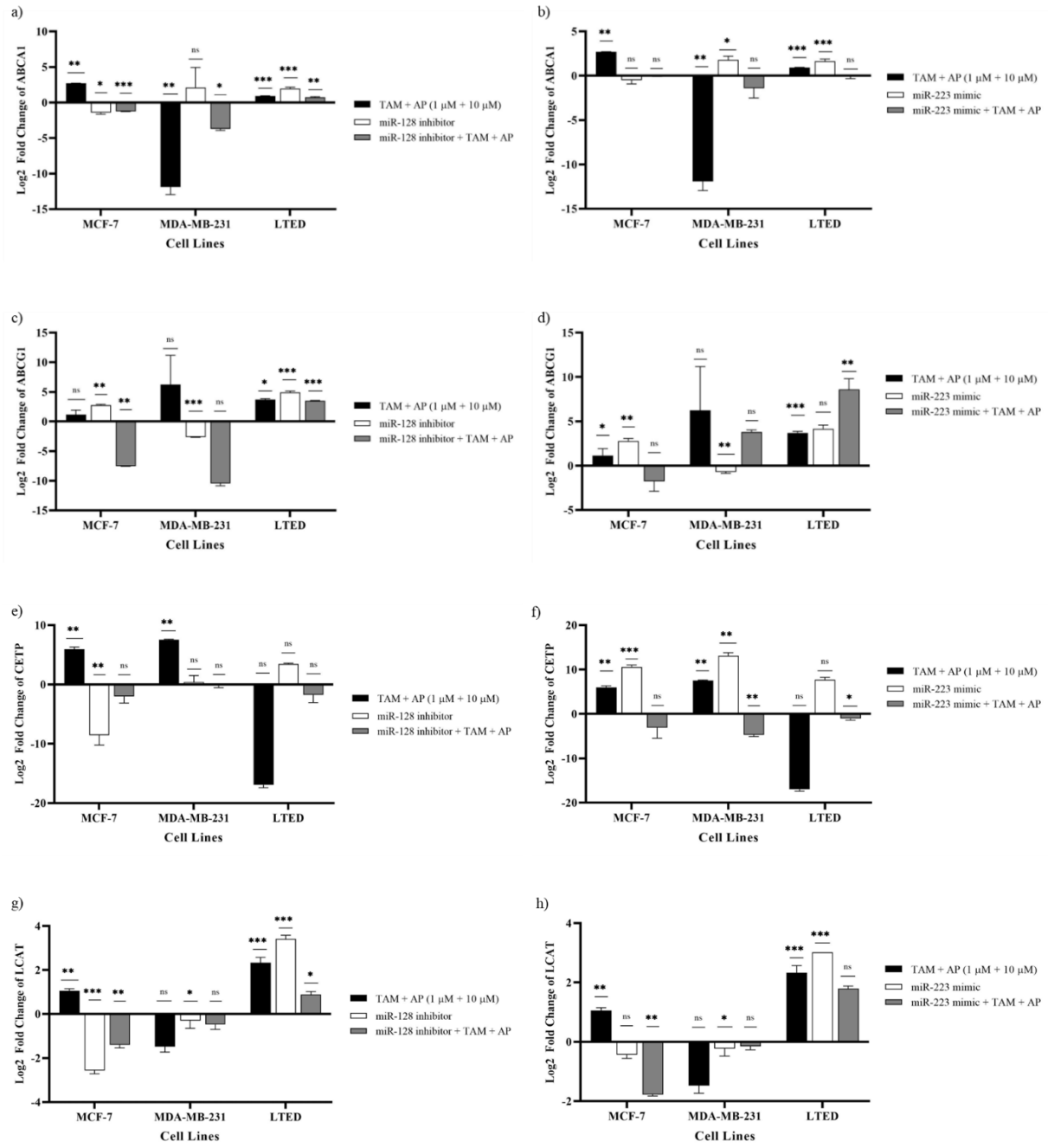

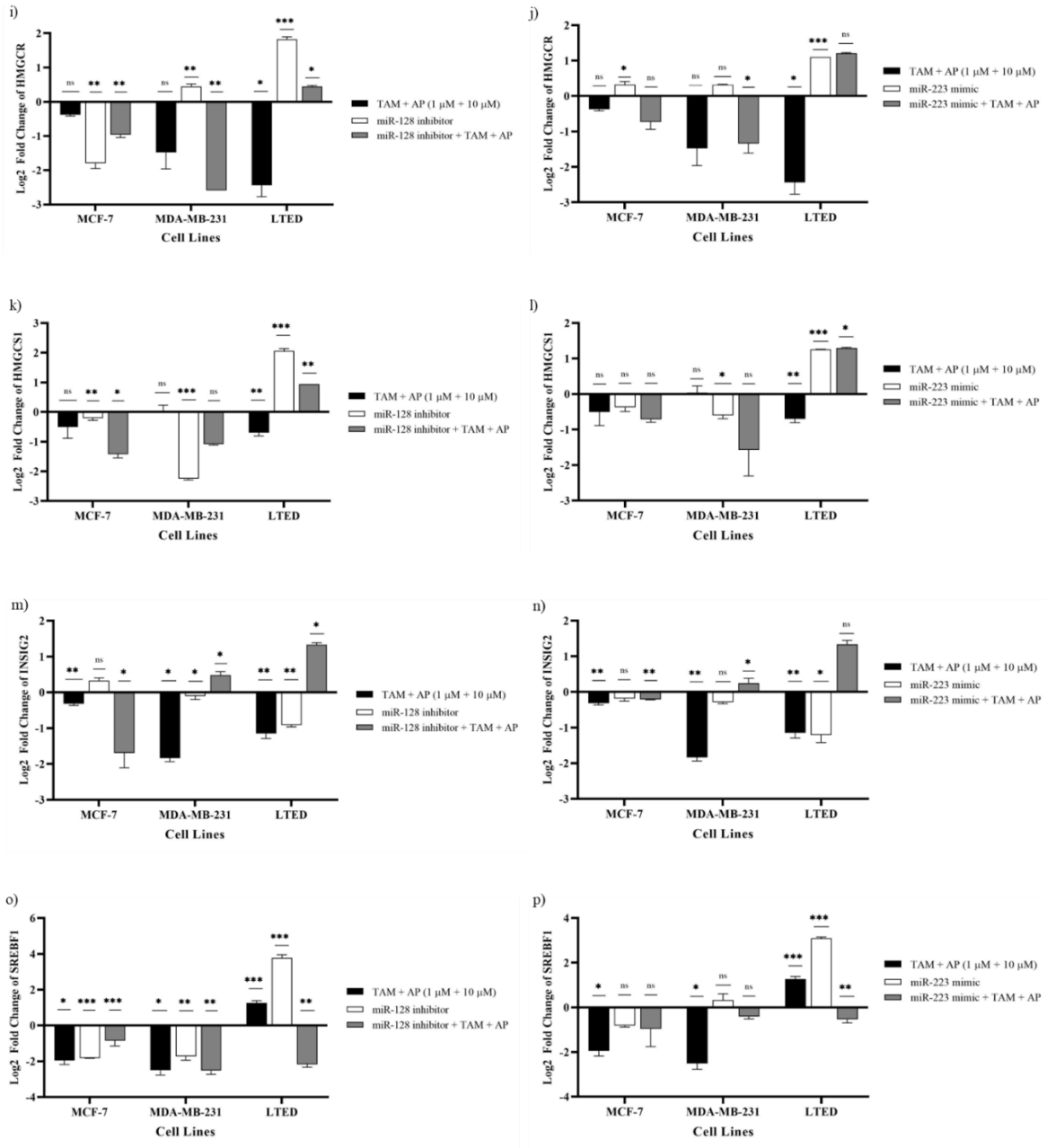
i)
Log2 Fold Change of HMGCR
TAM + AP (1 μM + 10 μM)
miR-128 inhibitor
miR-128 inhibitor + TAM + AP
MCF-7
MDA-MB-231
LTED
Cell Lines
j)
Log2 Fold Change of HMGCR
TAM + AP (1 μM + 10 μM)
miR-223 mimic
miR-223 mimic + TAM + AP
MCF-7
MDA-MB-231
LTED
Cell Lines
k)
Log2 Fold Change of HMGCS1
TAM + AP (1 μM + 10 μM)
miR-128 inhibitor
miR-128 inhibitor + TAM + AP
MCF-7
MDA-MB-231
LTED
Cell Lines
l)
Log2 Fold Change of HMGCS1
TAM + AP (1 μM + 10 μM)
miR-223 mimic
miR-223 mimic + TAM + AP
MCF-7
MDA-MB-231
LTED
Cell Lines
m)
Log2 Fold Change of INSIG2
TAM + AP (1 μM + 10 μM)
miR-128 inhibitor
miR-128 inhibitor + TAM + AP
MCF-7
MDA-MB-231
LTED
Cell Lines
n)
Log2 Fold Change of INSIG2
TAM + AP (1 μM + 10 μM)
miR-223 mimic
miR-223 mimic + TAM + AP
MCF-7
MDA-MB-231
LTED
Cell Lines
o)
Log2 Fold Change of SREBF1
TAM + AP (1 μM + 10 μM)
miR-128 inhibitor
miR-128 inhibitor + TAM + AP
MCF-7
MDA-MB-231
LTED
Cell Lines
p)
Log2 Fold Change of SREBF1
TAM + AP (1 μM + 10 μM)
miR-223 mimic
miR-223 mimic + TAM + AP
MCF-7
MDA-MB-231
LTED
Cell Lines

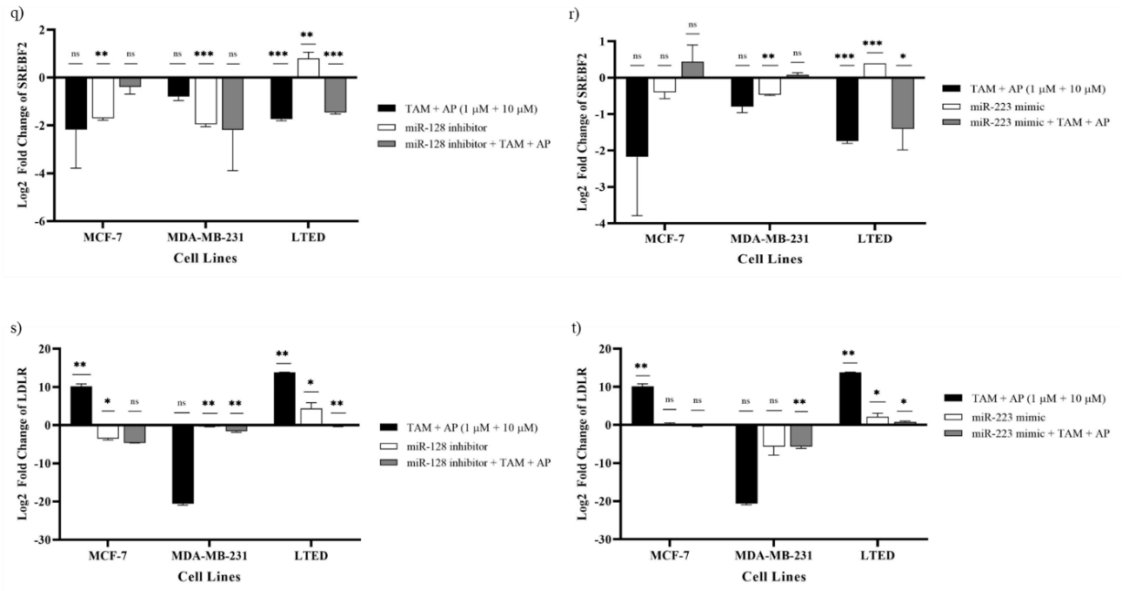

Figure S3: Changes in mRNA expression of genes involved in lipoprotein signalling and cholesterol metabolism pathways

Graphs indicating mRNA expression as log2 fold change. Endogenous expression of the GAPDH gene was used to normalise the data. Graphs on the left indicate BC cells solely treated with TAM + AP, BC cells solely transfected with a miR-128 inhibitor, and BC cells transfected with a miR-128 inhibitor and treated with TAM + AP. Graphs on the right indicate BC cells solely treated with TAM + AP, BC cells solely transfected with a miR-223 mimic, and BC cells transfected with a miR-223 mimic and treated with TAM + AP. Genes involved in cholesterol and drug efflux include: ABCA1 ***(a-b)*** *and ABCG1* ***(c-d)****; genes involved in cholesterol transport include: CETP* ***(e-f)*** *and LCAT* ***(g-h)****; genes involved in cholesterol biosynthesis include: HMGCR* ***(i-j)****, HMGCS1* ***(k-l)****, INSIG2* ***(m-n)****, SREBF1* ***(o-p)****, and SREBF2* ***(q-r)****; and genes involved in cholesterol uptake include: LDLR* ***(s-t)****. Statistical analysis was performed by using a student's t-test, where * P < 0.05, ** P < 0.01, *** P < 0.001, and ns = non-significant compared to untreated or non-transfection controls. Data represents the mean ± S.D; (n=3).*

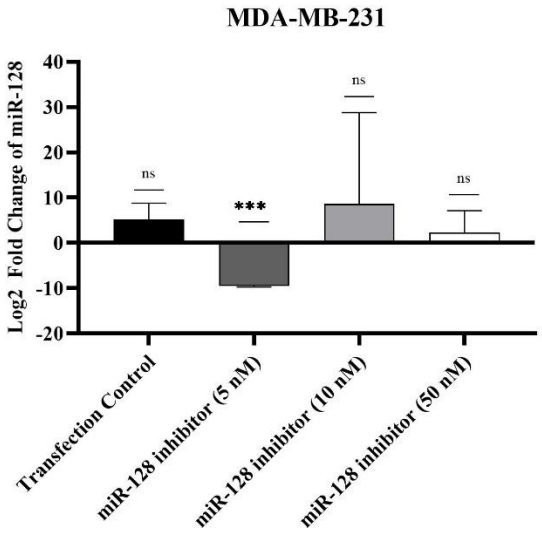

Figure S4: miR-128 expression in MDA-MB-231 cells

*Graph indicating miR-128 expression as log2 fold change. The miR-128 inhibitor at different concentrations (5 nM, 10 nm, and 50 nM, respectively) was encapsulated into lipid NPs and transfected into cells for 96 h. Endogenous expression of the RNU6 gene was used to normalise the data. Statistical analysis was performed by using a student's t-test, where * P < 0.05, ** P < 0.01, *** P < 0.001, and ns = non-significant compared to non-transfection control. Data represents the mean ± S.D; (n=2).*